5-2000

Structural requirements in calmodulin for n-methyltransferase recognition and NAD kinase activation

Jennifer Ann Cobb

To the Graduate Council:

I am submitting herewith a dissertation written by Jennifer Ann Cobb entitled "Structural requirements in calmodulin for n-methyltransferase recognition and NAD kinase activation." I have examined the final electronic copy of this dissertation for form and content and recommend that it be accepted in partial fulfillment of the requirements for the degree of Doctor of Philosophy, with a major in Biochemistry and Cellular and Molecular Biology.

Daniel M. Roberts, Major Professor

We have read this dissertation and recommend its acceptance:

Cynthia B. Peterson, Wesley D. Wicks, Frank D. Larimer

Accepted for the Council:

Carolyn R. Hodges

Vice Provost and Dean of the Graduate School

(Original signatures are on file with official student records.)

To the Graduate Council:

I am submitting herewith a dissertation written by Jennifer Ann Cobb entitled "Structural Requirements in Calmodulin for N-Methyltransferase Recognition and NAD Kinase Activation." I have examined the final copy of this dissertation for form and content and recommend that it be accepted in partial fulfillment of the requirements for the degree of Doctor of Philosophy, with a major in Biochemistry and Cellular and Molecular Biology.

Daniel M. Roberts, Major Professor

We have read this dissertation
and recommend its acceptance:

Accepted for the Council:

Associate Vice Chancellor and
Dean of The Graduate School

STRUCTURAL REQUIREMENTS IN CALMODULIN FOR N-METHYLTRANSFERASE RECOGNITION AND NAD KINASE ACTIVATION

A Dissertation
Presented for the
Doctor of Philosophy
Degree
The University of Tennessee, Knoxville

Jennifer Ann Cobb
May 2000

DEDICATION

For my husband John

ACKNOWLEDGEMENTS

I would like to express my appreciation to my advisor, Dr. Dan Roberts for his direction throughout my study. He has led me through these five years with a combination of rigor, enthusiasm, and wit. Thanks to my committee members, Drs. Wesley Wicks, Cynthia Peterson, and Frank Larimer for their guidance and insight. Thanks to Dr. Jill Trewhella at Los Alamos National Laboratory for doing the X-ray scattering experiments. Also, I would especially like to thank Dr. Elizabeth Howell for all the time she spent with me, suggestions regarding my project, and the use of her computer.

A special thanks to Drs. Chang-Hoon Han and Scott Harding for helping me with early work. I would also like to thank laboratory members, Robert Dean, James Guenther, Rana Ferrebee, and Nouth Chanmanivone for their friendship and endless funny stories.

I want to express my deepest thanks to my husband John Cobb who gave me love, support and encouragement when life seemed dark. His ability to seize the day and his love for life has taught me many invaluable lessons. I would like to thank my parents, Curtis W. Dodd and Sandra J. Dodd for their encouragement and love throughout this process.

Finally, I would like to thank my parent in-laws, James E. Cobb and Martha S. Cobb for support and help with everything.

ABSTRACT

Calmodulin is trimethylated at lysine 115 by a lysine N-methyltransferase that utilizes S-adenosyl methionine as a co-substrate. Lysine 115 is located within a six amino acid loop (LGE**K**LT) between EF hand III and EF hand IV in the carboxyl terminal lobe. Previous studies have shown that the methyltransferase is highly specific for calmodulin, and that minimal requirements for methylation are a folded carboxyl terminal lobe (Han, C.H., Richardson, J., Oh, S.H., and Roberts, D.M. (1993) *Biochemistry* 32, 13974-13980). In the present work a mutagenesis approach was used to investigate the structural features of the carboxyl terminal lobe that are required for calmodulin methylation.

Three approaches were taken. First, based on the symmetry between EF hands I and III, and EF hands II and IV, a series of domain (entire EF hand) and subdomain (individual helix or Ca^{2+}-binding loop) exchange mutants were generated in which symmetrical elements in the amino terminal lobe were substituted into the carboxyl terminal lobe. Secondly, a converse mutation was made in which the methylation loop sequence was introduced between EF hands I and II in the amino terminal lobe. Finally, a series of

site-directed mutations in the methylation loop and adjacent α-helices (helix 6 of EF hand III and helix 7 of EF hand IV) were generated and analyzed.

Substitutions at three conserved positions in the methylation loop (G113S, E114A, L116T) abolished the ability of calmodulin to be methylated. A fourth mutant, L112T showed normal methylation in the presence of calcium, but a 4.5 fold reduction in catalytic efficiency in the absence of calcium. These results suggest that conservation of the methylation loop sequence is essential for methylation. However, results with domain mutants CaM^{EKL}, CaM^{1214}, and CaM^{1232} suggest that the methylation loop sequence alone is not adequate for methylation. CaM^{EKL} has the methylation loop sequence placed at a symmetrical position between EF hands I and II in the amino terminal lobe. CaM^{1214} has EF hand III replaced with EF hand I and CaM^{1232} has EF hand IV replaced with EF hand II. None of the domain exchange mutants were methyltransferase substrates suggesting that structural features unique to both EF hands III and IV (and not found in EF hands I and II) are required.

To identify these unique regions in EF hands III and IV, a series of subdomain mutants were constructed. The

most substantial effects were observed with the substitution of helix 2 in EF hand I for helix 6 in EF hand III (CaM^{H6}) and helix 3 in EF hand II for helix 7 in EF hand IV (CaM^{H7}). CaM^{H6} was a poor methylation substrate in both the presence and absence of Ca^{2+}, and showed a 20-fold (apo) and 13-fold (Ca^{2+}-bound) reduction in catalytic efficiency compared to VU-1. CaM^{H7} was not a substrate in the absence of calcium, but showed normal methylation kinetics in the presence of calcium. Thus, the substitution of both helix 6 or 7 affected methyltransferase recognition but in a different fashion, since calcium binding restores the ability of the CaM^{H7} to be recognized by the methyltransferase.

Helix 7 shows a high number of surface exposed acidic side chains (6 out of 11 residues). To examine the role of these negative charges, a number of calmodulin mutants with substitutions for the various glutamate/aspartate residues were analyzed. Substitutions at residues 118,120,122,126,and 127 were found to affect the rates of methylation [with rates ranging from 5% (VU-12) to 60% (D122A) of wildtype]. Similar to CaM^{H7}, activity with most of these mutants was enhanced in the presence of calcium.

In contrast to helix 7, single amino acid substitutions in helix 6 showed no effect on the methylation rate. Thus, the loss of methylation in CaM^{H6} is not due to the substitution of any specific amino acid. Rather, it appears that the replacement of the entire sequence of helix 6 with helix 2 resulted in an unexpected change in the conformation that disrupts the binding site for the methyltransferase in both the apo- and calcium-bound states.

Overall, the highly conserved methylation loop and α-helices (6 & 7) flanking the loop appear to be important for methyltransferase recognition. However, the role these regions play in methyltransferase recognition appears to be very different. The most critical residues appear to be within the methylation loop (G113, E114, L116). These residues are very close to site of methylation on lysine-115, and might provide important points of contact with the active site of the enzyme or provide flexibility (e.g., G113) or stability (L116) for the conformation of the loop structure. Secondly, the conservation of negative charges on helix 7 appears to be important particularly in apo-calmodulin. After the binding of calcium, a hydrophobic surface is exposed and the substitutions on helix 7 appear

less important for interaction. This supports previous findings that suggest that ionic forces are important for interaction of apo-CaM with the methyltransferase whereas additional hydrophobic interaction occur with Ca^{2+}-CaM (Han, C.H., Richardson, J., Oh, S.H., and Roberts, D.M. (1993) *Biochemistry* 32, 13974-13980).

Lastly, it is clear that helix 6 is important for methyltransferase recognition but it is less certain whether specific interactions with the enzyme take place. It is likely that packing interactions of this helix with others in the carboxyl terminal lobe may be important for stabilizing the conformation of the residues that are recognized and bound by the methyltransferase. Additional structural work of the calmodulin mutants in question, as well as the methyltransferase, will be necessary to clarify further the specific role of these structural elements.

During the course of this study, the activator properties of each calmodulin mutant were also tested with two representative calmodulin-dependent enzymes, NAD kinase (NADK) and cyclic nucleotide phosphodiesterase (PDE). While most mutants activated these target proteins in a normal fashion, mutant calmodulins with substitutions in the loop-turn region of the amino terminal lobe and helix 6

of the carboxyl-terminal lobe showed defects in NAD kinase activation. CaM^{EKL} activated PDE normally, but did not activate NAD kinase and was actually a potent antagonist of the enzyme with a binding affinity similar to wild type calmodulin. X-ray scattering studies support this and showed that the conformation of CaM^{EKL} in complex with a target peptide is similar to wild type calmodulin.

While CaM^{EKL} was a complete NAD kinase antagonist, single substitutions within this region were "partial agonists", activating the enzyme to a fraction of the level observed with wild type. Similarly, it was found that both CaM^{1214} and CaM^{H6} were partial agonists, and that the defect of these two calmodulins was the result of a substitution at threonine 110. Overall, these results show that the binding and activation of NAD kinase can be distinguished, and that the residues required for the activation of PDE are distinct from those required for NAD kinase. Further, these regions on calmodulin are within or adjacent to a "latch domain" which is formed between the helix 2 of the amino terminal lobe and helix 6 of carboxyl terminal lobe upon enzyme binding (Meador, W., Means, A.R., and Quiocho, F.A. (1992) *Science* 257, 1251-1255). This domain has been proposed to be essential for achieving an activated state.

TABLE OF CONTENTS

LIST OF TABLES

LIST OF FIGURES

LIST OF ABBREVATIONS

AdoMet, S-adenosyl methionine; **^{3}H-AdoMet**, [^{3}H-methyl]-S-adenosyl methionine; **BCA**, bicinchoninic acid; **CHAPS**, 3-[(3-cholamidopropyl)-dimethylammonio]-1-propanesulfonate; **CaM^{EKL}**, mutant calmodulin with a arginine at position 115 and the substitution of EKL for QNP 41-43; **CaM^{1214}**, mutant calmodulin which has a substitution of EF hand I for EF hand III; **CaM^{1232}**, mutant calmodulin which has a substitution of EF hand II for EF hand IV; **CaM^{CL3}**, mutant calmodulin which has a substitution of calcium binding loop 1 for calcium binding loop 3; **CaM^{H6}**, mutant calmodulin which has a substitution helix 2 for helix 6; **CaM^{CL4}**, mutant calmodulin which has a substitution of calcium binding loop 2 for calcium binding loop 4 **CaM^{H7}**, mutant calmodulin which has a substitution helix 3 for helix 7;; **CaM^{H8}**, mutant calmodulin which has a substitution helix 4 for helix 8; **D122A**, calmodulin with an aspartic acid to alanine-122 mutation; **E114A**, calmodulin with a glutamate to alanine-114 mutation; **E119A**, calmodulin with a glutamate to alanine-119 mutation; **E120A**, calmodulin with a glutamate to alanine-120 mutation; **E123A**, calmodulin with a glutamate to alanine-123 mutation; **E127A**, calmodulin with a glutamate to alanine-127 mutation; **E139A**, calmodulin with a glutamate to alanine-139 mutation;

EDTA, Ethylenediamine Tetraacetic Acid; **G113S**, calmodulin with a glycine to serine-113 mutation; **HEPES**, N-(2-hydroxyethyl)piperazine-N'-(2-ethanesulfonic acid); **H107A**, calmodulin with a histidine to alanine-107 mutation; **IPTG**, isopropyl β-D-thiogalactopyranoside; **L112T**, calmodulin with a leucine to threonine-112 mutation; **L116T**, calmodulin with a leucine to threonine-116 mutation; **MLCK**, myosin light chain kinase; **N42K**, calmodulin with an asparagine to lysine-42 mutation; **NADK**, pea NAD kinase; **P43L**, calmodulin with a proline to leucine-43 mutation; **PDE**, calmodulin-dependent cyclic nucleotide phosphodiesterase; **Q41E**, calmodulin with a glutamine to glutamic acid-41 mutation; **R106A**, calmodulin with an arginine to alanine-106 mutation; **R106A/H107A**, calmodulin with arginine to alanine-106 and histidine to alanine-107 mutations; **R126A**, calmodulin with an arginine to alanine-126 mutation; **Tris**, tris(hydroxylmethyl)aminomethane; **T110A**, calmodulin with a threonine to alanine-110 mutation; **T110R**, calmodulin with a threonine to arginine-110 mutation; **T117A**, calmodulin with a threonine to alanine-117 mutation; **VU-1 calmodulin**, calmodulin derived from a cloned synthetic gene (Robert *et al.*, 1985); **VU-3 calmodulin**, calmodulin derived from VU-1

which has a lysine to arginine-115 mutation (Roberts et al., 1986).

CHAPTER I

INTRODUCTION

Calcium

Calcium is a universal signal molecule that regulates a wide variety of cellular processes, such as numerous metabolic processes, muscle and cell contractions, cell-cycle control, and differentiation (Clapham and Sneyd, 1995). The concentration of calcium in most resting eukaryotic cells is held between 10^{-7} and 10^{-8} M in the cytosol. Cells have developed complex interrelated systems of membrane ion gates, exchangers, and pumps that maintain the average intracellular levels of calcium at this extraordinary low concentration (Clapham and Sneyd, 1995; reviewed in Carafoli *et al.*, 1987). As a result of the vast concentration gradient cells have recruited calcium as an intracellular signal. They respond to various stimuli by triggering a transient rise in the concentration of free calcium (to approximately 10^{-6} M), a concentration at which calcium functions as a second messenger or a coupling factor (reviewed in Carafoli, 1987; Berridge, 1993; Clapman & Sneyd, 1995). The cytosolic targets of calcium signals are a family of calcium-modulated proteins with EF hand calcium-

binding domains (reviewed in Kretsinger, 1980; Strynadka and James, 1989; Moncrief *et al.*, 1990; Ikura 1996).

EF hand proteins: structural features

The EF-hand motif is a specialized calcium binding domain that was first described by Moews and Kretsinger (1975) based on the crystal structure of muscle parvalbumin. Since this discovery over 150 different calcium modulated proteins containing this motif have been described (Moncrief *et al.*, 1990; Nakayama and Kretsinger, 1994; Kawasaki *et al.*, 1998). The Ca^{2+}-binding motif consists of two amphipathic α-helices 10 to 12 residues long that flank a "loop" of 12 contiguous residues that contribute oxygen ligands for the coordination of calcium ions. The structure has been likened to an index finger (E-helix), a curled second finger (the loop), and a thumb (F-helix) of a right hand, so that the term "EF-hand" has been widely applied to describe the Ca^{2+}-binding site (Kretsinger and Nockolds, 1973).

The features of the coordination of Ca^{2+} ions in EF hand calcium-binding proteins have been highly refined by the solution of several crystal structures (reviewed in Strynadka and James, 1989). These structures show seven oxygen atoms located at the seven vertices of a pentagonal bipyramid that are ~2.4 Å from the central Ca^{2+} ion. The

seven ligands come from six residues located at positions 1,3,5,7,9, and 12 of the loop and interact either directly or indirectly with the calcium ion (Fig. 1). Not all of the seven ligands are from the amino acid side chains; many of the binding sites have one water molecule in the coordination sphere of the Ca^{2+} ion. These six residues are denoted as the +X, +Y, +Z, -Y, -X, -Z positions on the axes of the calcium coordination shell. The -Z ligand contributes two oxygen atoms to coordination.

The residue in position 1 of the Ca^{2+} -binding loop is an invariant aspartate. The carboxylate group of this side contributes an oxygen atom as a direct Ca^{2+} ion ligand (+**X**) (Fig.1). The other oxygen atom is the recipient of a strong hydrogen bond from the main-chain NH of the conserved glycine in position 6. The nature of the residue at position 2 is not conserved. However, in many (50%) of the Ca^{2+} binding loops this is a basic residue of either lysine or arginine (Fig.1)(Strynadka and James, 1989). The residue in position 3 is usually an aspartate or an asparagine, with a side chain oxygen that forms a direct coordination to the Ca^{2+} ion (+**Y**)(Fig.1). The most common residue in position 4 is a glycine, however other residues at this position include asparagine, alanine, and lysine. Position 5 is also a Ca^{2+} -binding ligand (+**Z**) with the side chain oxygen ,and

	+X		+Y		+Z		-Y	-X			-Z	
Helix E -	1	2	3	4	5	6	7	8	9	10	11	12-Helix F
	D	K/R	D/N	G	D/N	**G**	-	I/V	-	-	D/E	**E**

Figure 1. Organization of the calcium-binding loop in an EF hand domain. Positions of the 12 amino acids in the calcium binding loop are shown (Kretsinger, 1980; Strynadka and James, 1989). The X, Y, Z, -X, -Y, and -Z indicate the vertices of a pentagonal bipyramid that forms upon the binding of calcium, with -Z contributing two ligands. The line above the numbered positions indicate residues which are part of either the E or F helix. The residues at positions 1 (aspartate), 6 (glycine), and 12 (glutamate) are invariant and shown in bold. Highly conserved residues are shown at specific positions, and (-) represents less conserved positions.

the most common residue is an aspartate or asparagine, but serine and glycine have also been observed (Fig. 1). The main-chain NH of residue 5 hydrogen bonds with the oxygen atoms in positions 1 and 3 that coordinate the Ca^{2+} ion. There is an invariant glycine at position 6, and the main-chain NH forms an important hydrogen bond to the non-coordinating oxygen atom of the carboxylate of aspartate in position 1 (Fig. 1). This glycine allows the chain to make a 90° turn in direction so that the remaining Ca^{2+} ligands are in coordinating positions. The residue at position 7 initiates a small antiparallel β strand that extends for three residues (7-9), and forms contact with a similar β strand in an adjacent EF hand. Of all positions in the loop, position 7 is the most variable in terms of the nature of the amino acid (Fig. 1). The main-chain carbonyl oxygen atom of residue 7 is involved in the coordination sphere of the Ca^{2+} ion (- **Y**). Position 8 is the central residue of the short β strand. It is a hydrophobic amino acid and is almost always either an isoleucine or a valine. This side chain packs into the hydrophobic core and stabilizes the loop structure (Strynadka and James, 1989). The main-chain NH and CO groups of this residue face away from the central cavity toward a neighboring EF hand loop. The residue in position 9 has several functions including coordination to the Ca^{2+}

ion (**-X**). This residue initiates the exiting F helix , and requires formation of a hydrogen bond to the NH of the invariant glutamate at position 12 (Fig. 1). The residue in position 10 is the first one in the exiting helix, and in many cases it is an aromatic residue. The amino nitrogen of residue 10 is often hydrogen bonded to a conserved water molecule. The residue in position 11 is most commonly a negatively charged aspartate or glutamate. The carboxylate groups are not involved in calcium coordination but stabilize the amino-terminus of the exiting F helix. Position 12 is the last position in the Ca^{2+}-binding loop and it is in the third position of the exiting helix (Fig. 1). This residue is an invariant glutamate that has both oxygen atoms of its carboxylate group coordinating to the Ca^{2+} ion in a bidentate manner (**-Z**). Further, this residue could be the key residue for adapting the metal-binding loop toward the binding of either Mg^{2+} or Ca^{2+} ions. The coordination number for Mg^{2+} is six, and one of the main determinants of Ca^{2+} seven-fold coordination is the bidentate nature and the conformation of the glutamate carboxylate at position 12 (reviewed in Carafoli, 1987; Strynadka and James, 1989).

In many proteins, EF hands exist as a pair. The EF hand pairs form an anti-parallel four α-helix bundle

stabilized by hydrophobic interactions and a short anti-parallel β-strand between the calcium binding loops interaction between the two Ca^{2+} binding loops. There is concerted movement in the α-helices of EF hand pairs upon binding calcium that is described in greater detail below in the calmodulin structure section (Babu *et al.*, 1985; Zhang *et al.*, 1995).

Calcium binding to some EF hand proteins result in conformational changes while other proteins do not show these changes (Ikura *et al.*, 1996). EF hand proteins with regulatory roles are often termed calcium-sensor or calcium-modulated proteins, while those involved in calcium buffer or transport functions are termed calcium-buffer proteins (da Silva and Reinach, 1991). Examples of EF-hand proteins functioning as calcium-buffers include parvalbumin and calbindin D (Tanaka *et al.*, 1995). Usually calcium-buffer proteins show only small conformational changes upon binding calcium (Skelton, 1994; reviewed in Ikura *et al.*, 1996). For example, the single domain of calbindin D exhibits only small conformational changes in response to binding calcium. It retains a 'closed' conformation with its hydrophobic residues sequestered in the interior of the molecule even after binding calcium (Ikura *et al.*, 1996).

Proteins that function as calcium-sensors include calmodulin, troponin C, calcineurin B, recoverin, and S100 proteins. Calcium-sensor proteins usually bind calcium with a K_d between 10^{-5} and 10^{-7} M in the presence of cytosolic concentrations of (10^{-3}) Mg^{2+} (Kretsinger, 1977). As a result they are able to respond to increases in cytosolic calcium levels. These proteins tend to show large conformational changes upon binding calcium (Zhang *et al.*, 1995, Kuboniwa *et al.*, 1995, Finn *et al.*, 1995, Gagne *et al.*, 1995, and Tanaka *et al.*, 1995) which allow them to act as molecular switches. They can convert from an inactive calcium-free conformation to an active calcium-bound conformation in response to a stimulatory influx of Ca^{2+} in the cell (Ikura, 1996). The well-studied and prototypical calcium-sensor protein is calmodulin (reviewed in Cohen and Klee, 1988).

Calmodulin

Calmodulin (CaM) is a highly conserved calcium binding protein that is ubiquitous among eukaryotes (Klee & Vanaman, 1982; Means *et al.*, 1982). It is a small acidic protein of 148-162 residues with a molecular weight of 16.7 kDa (Fig.2). There is 100% identity in amino acid sequence among vertebrates (Friedberg, 1990). Higher plant calmodulin differs from vertebrate calmodulin by only 13 of

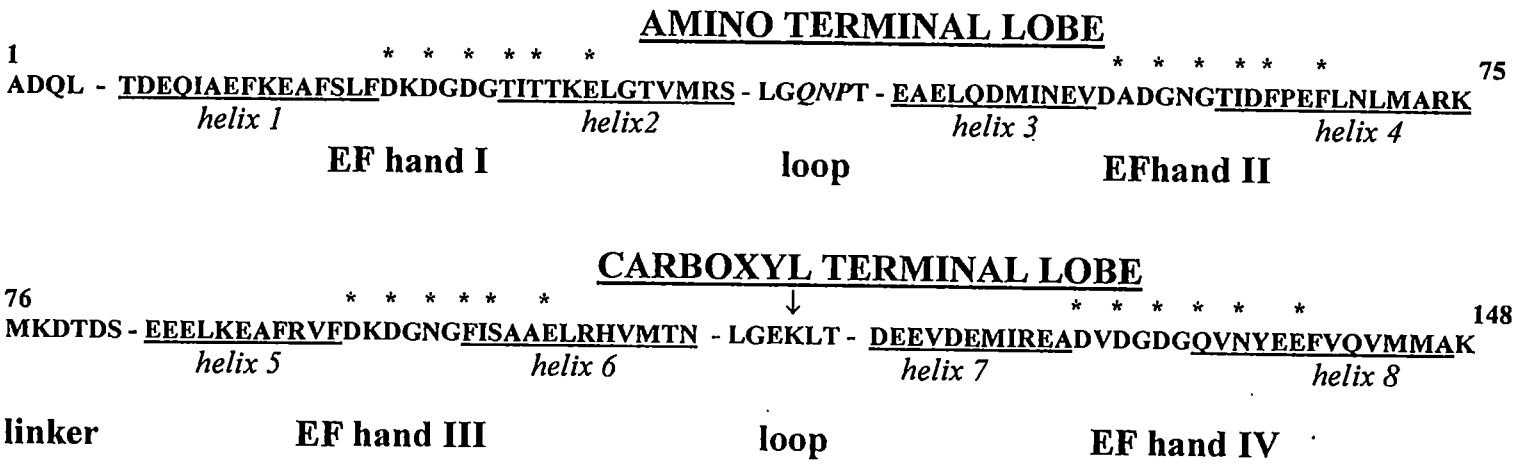

Figure 2. Sequence and domain organization of calmodulin. Sequence of VU-1 calmodulin derived from a synthetic gene (Roberts *et al.*, 1985) showing the location of EF hands I-IV, the central linker region, and the two loops between the EF hands. α-Helical regions are underlined and calcium ligands are indicated by an asterisk. The site of trimethylation is K115 between EF hand III and IV and is indicated by an arrow.

148 residues and they are functionally interchangeable (Roberts *et al.*, 1986a). Only in organisms as diverse as protozoans and mammals does the sequence divergence exceed 10%. Variability in calmodulin sequence occurs in the linker region (residues 70-85) between EF hands II and III, and within the carboxyl-terminal domain particularly within EF hand IV, where at least seven different amino acids are found at position 143 (Fig. 2, Wylie and Vanaman, 1998). The importance of calmodulin is evident by the observation that disruption of the calmodulin gene results in a recessive lethal mutation in yeast (Davis et al., 1986; Takeda and Yamamoto, 1987)

Calmodulin is involved in the regulation of many cellular processes (reviewed in Cohen and Klee, 1988), and was first discovered as an activator of cyclic nucleotide phosphodiesterase in brain and heart (Cheung, 1970; Kakiuchi and Yamazaki, 1970). In trying to understand how calmodulin works, it is important to become familiar with the interaction between calmodulin and Ca^{2+}. Calmodulin contains four EF hands numbered I, II, III, IV starting from the amino-terminus of the protein (Fig.2). EF hands I & II interact and form the amino-terminal lobe, and EF hands III & IV form the carboxy-terminal lobe (Fig.2).

Consistent with the presence of four EF hands, calmodulin has four calcium binding sites that bind calcium reversibly (Klee, 1988). Calmodulin has low affinity calcium binding sites as well as high affinity binding sites. Studies showed that binding of the first two equivalents of calcium resulted in a large increase in the fluorescence yield of tyrosine 138 of calmodulin (Kilhoffer *et al.*, 1981), and that there was no increase in fluorescence upon the binding of the next two equivalents of calcium. This suggests that the higher calcium affinity sites reside in the carboxyl-terminal lobe of calmodulin (Kilhoffer *et al.*, 1981).

Additional experiments using isolated tryptic fragments supported the fluorescence data, and showed that the higher affinity sites reside in the carboxyl-terminal lobe (residues 78-148) and lower calcium affinity sites reside in the amino-terminal lobe (residues 1-77) (Minowa and Yagi, 1984; Linse et al., 1991). Isolated fragments from the tryptic digest of calmodulin showed that the amino and carboxyl-terminal lobes do not interact, but retain their secondary structure, ability to bind Ca^{2+}, and their ability to undergo Ca^{2+}-dependent structural transitions similar to the intact molecule (Linse *et al.* 1991). One way to measure the affinity of calcium to calmodulin has been to

determine the kinetic constants of the rates of dissociation (off-rates). The amino-terminal domain (residues 1-77) contains two low affinity calcium- binding sites (off-rates $280s^{-1}$), and the carboxyl-terminal domain (residues 78-148) contains two high affinity calcium- binding sites ($37s^{-1}$) (Martin *et al.*, 1986).

Although the two lobes do not interact, the two calcium binding sites within each lobe of calmodulin do interact, and the binding of calcium ions to each globular domain shows positive cooperativity (Klee, 1988; Linse *et al.*, 1991; Minowa and Yagi, 1984; Yazawa *et al.*, 1987). Further, the calcium affinity of isolated fragments containing a single EF hand is much lower than that of the intact calmodulin (Kretsinger, 1980; Klee, 1988). This suggests that the interaction between the two calcium binding loops in each domain is important for cooperative, high affinity calcium binding.

Calmodulin structure: Ca^{2+}-bound and apo-CaM

The structure of Ca^{2+}-bound calmodulin as determined by X-ray crystallography revealed a dumbbell shaped molecule, with a flexible central helix connecting two independent globular domains (Babu *et al.*, 1985, 1988; Kretsinger *et al.*, 1986; Chattopadhyaya *et al.*, 1992) (Fig. 3). Overall, 66% of the residues in CaM are in helical conformation

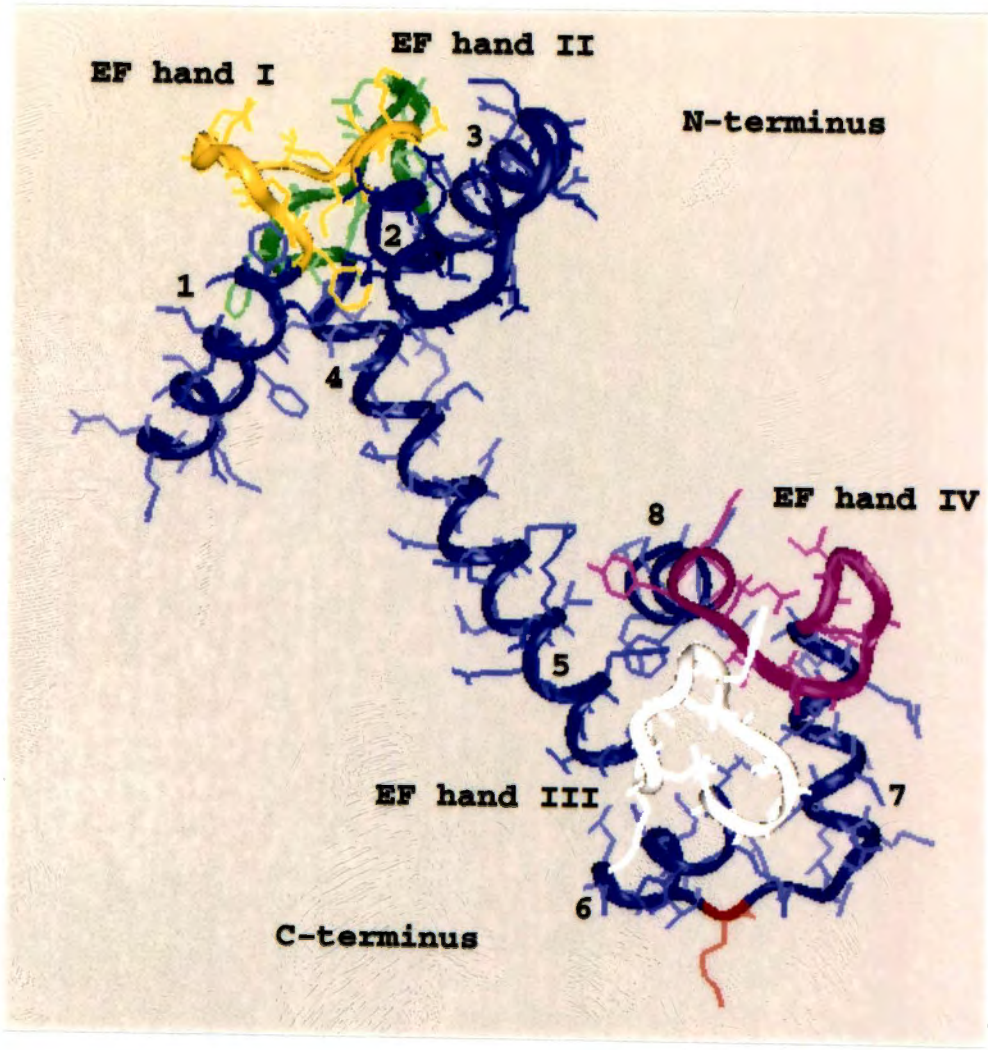

Figure 3. Structure of calcium bound calmodulin. The X-ray crystal structure (Babu *et al.*, 1988) with the α-helices numbered 1-8 is shown. As discussed in the text, although one central helix is observed in the crystal structure, NMR measurements (Ikura *et al.*, 1991; Barbato *et al.*, 1992) show that the center of this helix is disordered. Therefore, helical regions 4 and 5 are listed separately. The calcium binding loops of the four EF hands are colored yellow for EF hand I and green for EF hand II in the amino-terminal lobe, and white for EF hand III and pink for EF hand IV in the carboxyl-terminal lobe. Lysine 115, colored in red, is the site of posttranslational trimethylation.

giving a total of eight α-helices contributing to the make up of the four EF hands (Fig. 3). Helix 1 (residues 6-18, see Fig.2) and
helix 2 (residues 29-38) are found in EF hand I, helix 3 (residues 45-54) and helix 4 (residues 65-74) are found in EF hand II, helix 5 (residues 83-91) and helix 6 (residues 102-111) are found in EF hand III, and helix 7 (residues 118-127) and helix 8 (residues 139-145) are found in EF hand IV.

Ca^{2+}-bound calmodulin is 65 Å long, and each globular lobe has the dimensions 25 X 20 X 20 Å. The two halves of the molecule are similar, and superpositions of residues 5 to 74 of the amino-terminal lobe with residues 78 to 147 of the carboxyl-terminal show an rms deviation of 1.04 Å for all main-chain atoms (Babu et al., 1988). The two Ca^{2+}-binding domains in each half of the molecule are related to each other by a 2-fold axis of symmetry. The Ca^{2+} ions in the amino-terminal lobe are 11.9 Å apart, and in the carboxyl-terminal lobe they are 11.5 Å apart (Babu et al., 1985).

Although the crystal structure shows a central α-helix (Fig. 3) the solution structure of CaM shows that the middle portion (residues 76-82) is non-helical and flexible in solution (Ikura et al., 1991; Barbato et al., 1992).

Residues in this linker region have the highest temperature factors in the molecule (Babu et al., 1988; Chattopadhyaya *et al.*, 1992), and Persechini and Kretsinger (1988) proposed that the central helix is more like a flexible tether, enabling the two independent lobes to come together when binding target proteins (Ikura et al., 1992; Meador et al., 1992, 1993).

Similar to other EF-hand containing proteins, each lobe of the molecule is stabilized by multiple hydrophobic interactions between the helices and by hydrogen bonds between adjacent Ca^{2+}-binding loops. In the amino-terminal lobe, residues 25-29 in Ca^{2+}-binding loop 1 form a short β-sheet that runs antiparallel to a β-sheet formed by residues 61-65 in Ca^{2+}-binding loop 2 (Babu *et al.*, 1985). Similarly, in the carboxyl-terminal lobe, residues 99-101 in Ca^{2+}-binding loop 3 and residues 135-137 in Ca^{2+}-binding loop 4 also form a similar β-sheet that run antiparallel to each other (Babu *et al.*, 1985; 1988). In addition, there are two turns in calmodulin that are not EF hand turns consisting of residues 39-44 in the amino-terminal lobe, and residues 112-117 in the carboxy-terminal lobe which are also stabilized by hydrogen bonds (Chattopadhyaya *et al.*, 1992). The loop region in the carboxyl-terminal is solvent-exposed and

contains lysine 115, the site of post-translational trimethylation in CaM (Fig. 3).

Ca^{2+}-bound calmodulin contains a large hydrophobic cleft in each half of the molecule (Fig.4). Each cleft is approximately 10 X 12.5 Å and has a depth of 9.5 Å (Babu et al., 1988). Each hydrophobic core is composed of 14 amino acid side chains, 11 from the α-helices, 1 from each calcium-binding loop, and 1 from each non-EF-hand loop-turn region. The hydrophobic clefts are very similar in amino acid composition (71% identity), and both clefts are surrounded by a polar rim that is rich in negatively charged residues (Babu *et al.*, 1988; Chattopadhyaya *et al.*, 1992).

The solution structure of apo-calmodulin (Ca^{2+}- free calmodulin) as determined by NMR (Kuboniwa *et al.*, 1995; Zhang *et al.*, 1995) is shown in Fig. 4. It is a more compact structure (< 65A°) than Ca^{2+}-bound calmodulin (Fig. 4), but it possesses a very similar secondary structure (Zhang *et al.*, 1995). Like Ca^{2+}-bound calmodulin there is no interaction between the amino and carboxyl terminal lobes. The Ca^{2+}-binding loops are flexible and partially unstructured in apo-CaM. For example, the first Ca^{2+}-binding loop in the amino-terminal lobe is twisted in the β-sheet region. In addition, NMR analyses showed that the first six amino acids in each Ca^{2+}-binding loop are not well

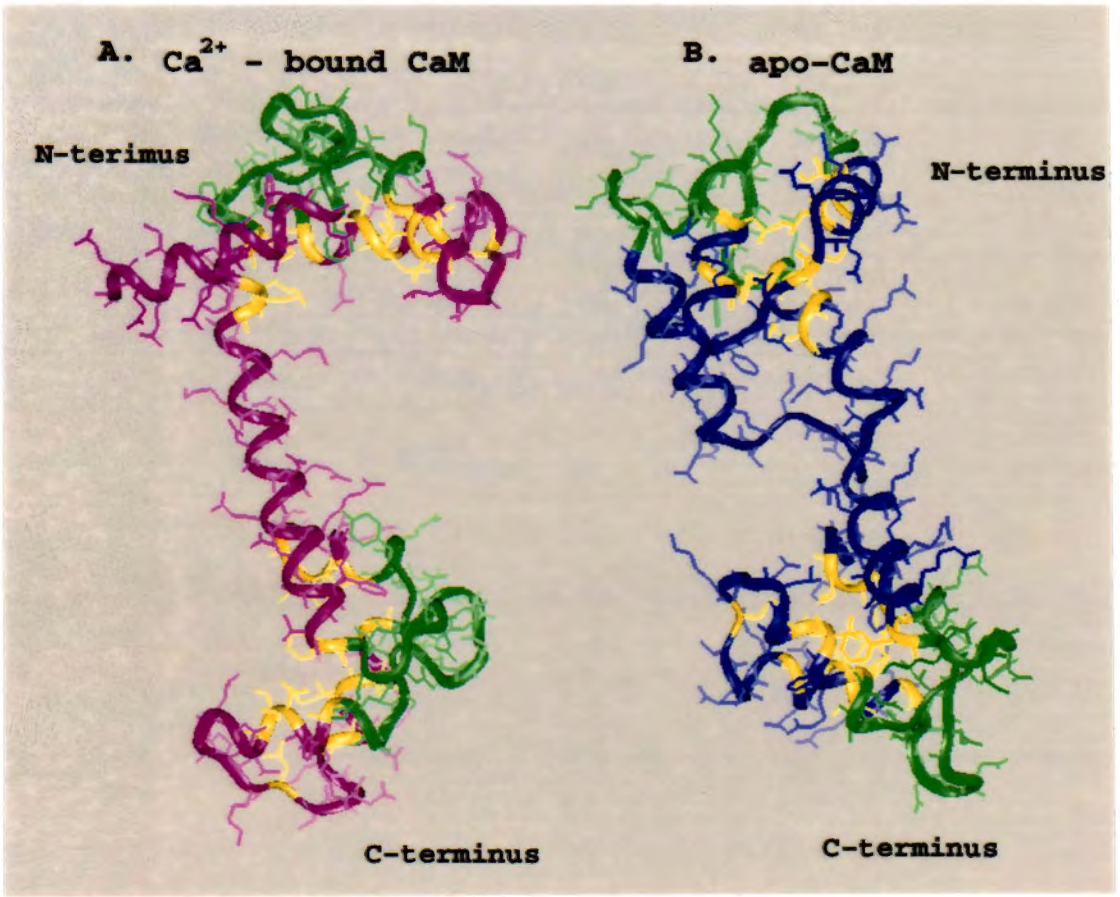

Figure 4. Structures of calcium-bound and apo-calmodulin. In each structure the calcium binding loops are shown in green. Residues forming the hydrophobic cleft are shown in yellow. **A.** X-ray crystal of calcium-saturated CaM (Babu *et al.*, 1988); **B.** NMR structure of calcium-depleted (apo) CaM (Kuboniwa *et al.*,1995)

defined, most likely because of the high flexibility (Kuboniwa *et al.*, 1995; Zhang *et al.*, 1995). The binding of Ca^{2+} to each loop dramatically reduces their flexibility (Zhang *et al.*, 1995) by initiating structural rearrangements around the binding sites allowing negatively charged side chains and back-bone carbonyl oxygens to form the pseudo bipyramidal coordination sphere suitable for calcium ligation (Babu *et al.*, 1985; Kretsinger *et al.*, 1986).

Apo-CaM does not have large hydrophobic clefts that are present on the exterior of the molecule in Ca^{2+}-calmodulin (Fig. 4). Instead these residues in apo-CaM are sequestered within a hydrophobic core. However, there are two smaller clusters of hydrophobic residues, one in each globular lobe of the protein, that are surrounded by many charged acidic residues (Kuboniwa *et al.*, 1995; reviewed in Ikura *et al.*, 1996). These resulting negatively charged but partially hydrophobic patches have been proposed to be involved in the interaction of apo-CaM with certain target proteins.

One of the most significant differences between the two forms of CaM, and the key to the conformational changes that result in calcium activation, is how the helices within each lobe pack with each other. In apo-CaM the interhelical angles within each EF hand (between helices 1&2, 3&4, 5&6, 7&8) are antiparallel (128°-137°). The binding of Ca^{2+}

induces an opening of the EF hands, resulting in almost perpendicular angles between these helices (Zhang *et al.*, 1995; Kuboniwa *et al.*, 1995; Finn *et al.*, 1995). The distance between the two helices of each EF hand in the apo-form (11.9-12.3 Å) increases upon binding calcium (14.4-18.5 Å). However, in contrast to the drastic helical changes within each EF hand, much smaller alterations are seen in the inter-helical distances of adjacent helices in EF hand pairs. For example, helices 1/4 and 2/3 in the amino terminal lobe and helices 5/8 and 6/7 in the carboxy-terminal are closely associated, and upon binding calcium the relative distances remain almost unchanged (Kuboniwa et al., 1995). The movement of helices 2 and 3 relative to 1 and 4 (amino-terminal lobe), and the movement of helices 6 and 7 relative to helices 5 and 8 (carboxyl-terminal lobe) results in the opening of the hydrophobic cleft.

Calmodulin function: different modes of interaction between calmodulin and target proteins.

After calcium binding, the next step in the mechanism of calmodulin signal transduction is the association of Ca^{2+}-CaM with a target protein resulting in its activation. CaM is a multifunctional protein, and Table I lists some of the Ca^{2+}-calmodulin target proteins. Calmodulin-binding domains on target proteins generally reside near "autoinhibitor" sequences where CaM binding allows the

Table I. Ca^{2+}-calmodulin-binding proteins and their cellular functions.

Target	Putative Function	Ref.
Cyclic nucleotide phosphodiesterase	Cyclic nucleotide homeostasis	a
Myosin light Chain kinase (MLCK)	Smooth muscle contraction	b
Phosphorylase *b* kinase	Glycogen metabolism regulation	c
CaM kinase I	Multifunctional;neuronal function	d
CaM kinase II	Multifunctional; learning and memory	e
CaM kinase III	Translation	f
CaM kinase IV	Multifunctional; transcriptional regulation	g
CaM kinase kinase	Activation of CaM kinase IV	h
NO synthase	NO signal production	i
NAD kinase	Nicotinamide co-enzyme homeostasis	j
Adenylate cyclase	cAMP production from ATP	k
Inositol 3-kinase	IP_4 production	l
Calcineurin (2b)	Multifunctional; cell cycle metabolic regulation.	m
Ca^{2+}-ATPase	calcium export from cytosol calcium homeostasis	n

a. Beavo, 1995; b. Stull *et al.*, 1997; c. Brushia and Walsh, 1999; d. Nairn & Greengard, 1987; e. Dupont and Goldbeter, 1998; f. Nairn *et al.*, 1985; g. Enslen *et al.*, 1994; h. Tokumitsu *et al.*, 1995; i. Masters, 1996; j. Roberts & Harmon, 1992; k. Tesmer and Sprang, 1998; l. Woodring and Garrison,1997; m. Klee *et al.*, 1998; n. Grover & Khan,1992).

activation of the enzyme by removing the autoinhibitor (reviewed by Soderling, 1990; Kemp and Pearson, 1991; Kemp *et al.*, 1996; Kobe *et al.*, 1997). The region of the target protein that interacts with calmodulin is small and linear. As a result much of the information about the interaction between Ca^{2+}-CaM and its targets comes from using synthetic peptides corresponding to the CaM-binding domain of target proteins (Ikura *et al.*, 1992; Meador *et al.*, 1992; Meador *et al.*, 1993; Osawa et al., 1999, Elshorst et al., 1999).

One of the most intensely studied CaM-dependent enzymes is myosin light chain kinase (Gallagher *et al.*, 1997; Stull *et al.*, 1997). Two forms of myosin light chain kinase from smooth muscle (smMLCK) and skeletal muscle (skMLCK) have been the principle focus of study (Ikura *et al.*, 1992; Meador *et al.*, 1992;). Both enzymes are inactive in the absence of calcium and become fully activated in the presence of Ca^{2+}-CaM. Phosphorylation of myosin light chains by MLCK is the basis of control for myosin contraction in these tissues (Allen and Walsh, 1994). Dissection of the structure of smMLCK (Lukas *et al.*, 1986) and skMLCK (Blumenthal *et al.*, 1985) showed that the site of interaction with calmodulin resides on a small linear sequence of 20-27 residues.

The structure of calmodulin bound to a 26-residue peptide (RS20) including the smMLCK sequence has been solved by NMR (Fig. 5, Ikura et al., 1992). A similar crystal structure has also been determined using calmodulin bound to a peptide (M13) containing the sequence of the CaM-binding region of skMLCK (Meador et al., 1992). In addition, a similar structure has been solved with the peptide from CaM kinase II (CaMKII) (Meador et al., 1993). The structures of CaM complexed with either MLCK or CaMKII show the complex as compact and ellipsoidal with overall dimensions of 47 X 32 X 30 Å (Ikura et al., 1992; Meador *et al.*, 1992; 1993).

The reason for this compact structure is that a major conformational change in Ca^{2+}-calmodulin occurs upon binding these peptides. The linker connecting the two globular lobes becomes very flexible resulting in a bend and twist of ~100° and 120° respectively. The two CaM domains come together and surround the peptide in a hydrophobic channel formed by the exposed hydrophobic clefts on each lobe of CaM (Ikura *et al.*, 1992, see Fig. 5). The CaM-binding peptides which are mainly random coil in solution adopt an amphipathic α-helical structure when complexed with calmodulin, and interact with CaM in an antiparallel manner. The amino-terminal domain of calmodulin mainly contacts hydrophobic residues in the carboxyl-terminal half of the

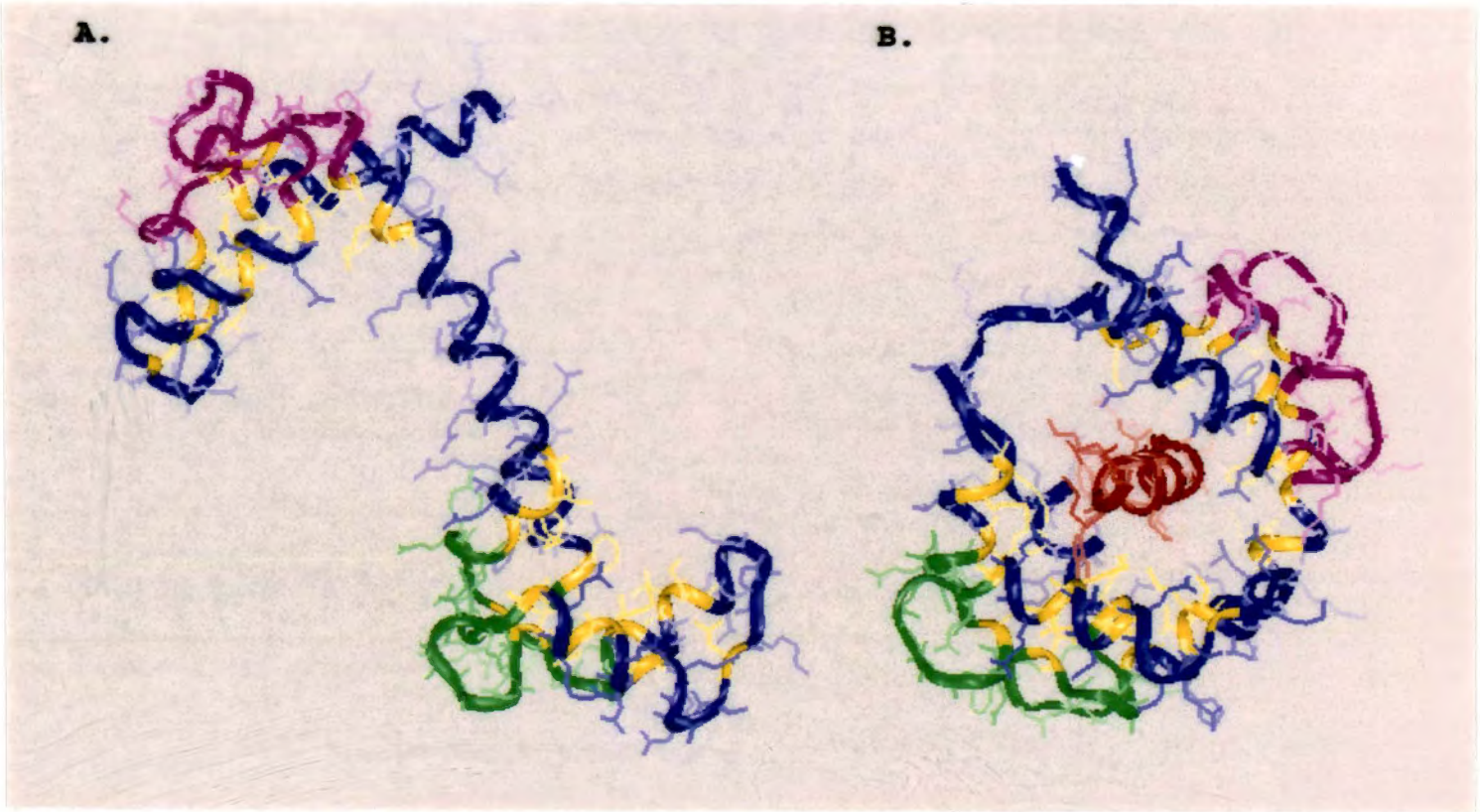

Figure 5. Structures of calcium-bound and calcium-peptide bound calmodulin. In each structure, the calcium binding loops are shown in pink (amino-terminal lobe) or in green (carboxy-terminal lobe). Residues forming the hydrophobic cleft in both lobes are colored in yellow, and the bound peptide in red. **A.** X-ray crystal structure calcium-saturated calmodulin (Babu *et al.*, 1988); **B.** NMR structure of peptide bound form of calcium-saturated calmodulin (Ikura *et al.*, 1992).

peptide, and the carboxyl-terminal domain principally interacts with hydrophobic residues in the amino-terminal half of the peptide (Ikura *et al.*, 1992; Meador *et al.*, 1992).

More recently additional structures of Ca^{2+}-calmodulin in complex with other target proteins have been determined. These structures show similarity to the archetype MLCK, but also differences that underscore the diversity and flexibility of calmodulin-target protein interactions. The NMR structure of calmodulin complexed with a peptide containing the target sequence from Ca^{2+}-calmodulin-dependent protein kinase kinase (CaMKK) has been determined (Osawa et al., 1999). CaMKK (Table I) is involved in a calcium-dependent signal transduction cascade which phosphorylates CaM kinase I and CaM kinase IV. The CaM-CaMKK structure also shows that the linker region drastically changes upon peptide binding, allowing the amino and carboxyl-terminal lobes to clamp the peptide. However, upon CaM binding the 26-residue peptide from CaMKK consists of two distinct structural segments. One segment of 11-residues (corresponding to 444-454 in CaMKK) forms an α helix, and the other segment is comprised of 5-residues (corresponding to 455-459) that forms a hairpin-like loop structure. The N-terminal lobe of calmodulin interacts

with the N-terminal portion of the CaMKK peptide, and the C-terminal portion of the helix and the hairpin loop mainly interact with the hydrophobic pocket in the C-terminal lobe of CaM (Osawa *et al.*, 1999). This orientation is opposite of CaM complexed with smMLCK and CaMKII where the orientation is antiparallel (Ikura *et al.*, 1992; Meador *et al.*, 1992; 1993)

The NMR structure of calmodulin complexed with a peptide (C20W) containing the CaM-binding domain of the plasma membrane calcium-pump has also recently been determined (Elshorst *et al.*, 1999). The global structure of the Ca^{2+}-CaM-C20W complex is quite different from other peptide-calmodulin complexes. There is no collapsed structure after peptide binding, and only the C-terminal half of calmodulin interacts with the peptide (Elshorst *et al.*, 1999). This supports biochemical observations that the calcium pump can be activated by the C-terminal half of CaM alone (Guerini *et al.*, 1984). Similar to other calmodulin binding peptides, C20W which has a random coil structure in solution, adopts an α-helical structure upon binding to the C-terminal domain of CaM. The complex resembles an intermediate state of the CaM-M13 complex, in which both domains of CaM are bound to the peptide (Elshorst et al., 1999).

In all CaM-peptide complexes mentioned above the backbone rms deviations between the amino- (residues 6 to 73) and carboxyl- (residues 83 to 146) terminal domains of the Ca^{2+}-CaM-peptide complex and the corresponding residues in Ca^{2+}-CaM alone (Babu *et al.*, 1998) are <1.8 Å and <1.5 Å respectively (Ikura *et al.*, 1992; Meador *et al.*, 1992; Meador *et al.*, 1993; Osawa et al., 1999, Elshorst *et al.*, 1999). This suggests that there is no significant conformational change within each lobe in the complexed and uncomplexed states, and that the principal change is in the flexible linker region between the lobes.

The high flexibility of the domain linker in CaM is clearly important in allowing CaM to adopt various binding configurations, and this allows Ca^{2+}-calmodulin to bind to multiple, divergent target sequences. The CaM-peptide complex is also stabilized by numerous electrostatic and hydrophobic interactions. Another reason for the ability of CaM to bind a wide variety of peptides is related to the high abundance of flexible methionine residues in the hydrophobic cleft (Zhang et al., 1998). The fine adjustments in conformation of the methionine residues provide optimal interactions between CaM an specific target peptides (Osawa *et al.*, 1998).

A key requirement in the target peptide for CaM binding is the presence of two branched hydrophobic or aromatic residues separated by a specific number of residues. The residues are important for anchoring the peptide to the hydrophobic pockets in the two domains of calmodulin (Meador *et al.*, 1992). The distance between the residues varies from 8 to 14 residues for various calmodulin binding peptides (Fig. 6). The flexibility of the central linker allows CaM to adapt to different distances between key hydrophobics. The C20W peptide lacks the second hydrophobic anchor residue (Fig. 6), and the complexed structure shows flexibility between the two CaM domains which is typical of CaM in solution (Kataoka *et al.*, 1991; Trewhella *et al.*, 1994). Further, in the CaM-C20W complex only methionine residues in the carboxyl-terminal domain of CaM showed a large chemical shift upon binding to the peptide, and all methionine residues in the N-terminal domain remained similar to free CaM (Elshorst *et al.*, 1999).

The distance between the two key hydrophobic residues in the peptide appears to be important for CaM binding orientation. An examination of structures (Ikura *et al.*, 1992; Meador *et al.*, 1992; Meador *et al.*, 1993; Osawa *et al.*, 1999) by Osawa *et al* (1999) identified two important features for peptide binding by calmodulin. As the two

skMLCK (577-602)[a]	KRR**W**KKNFIAVSAANR **F**KKI
smMLCK (796-815)	RRK**W**QKTGHAVRAIGR**L**SSM
calcineurin (406-425)	RRA **I** KNK ILAIG RLS R**V**FQV
CaMKIV (319-338)	RRK **L**KAAVKAVVASSR**L**GSA
CaMKI (300-317)	KSK**W**KQAFNATA**V**VRHMR
CaMKII (293-310)	RRK **L**KGAIL TTM **L**ATRNF
CaMKK (438-463)	I PS **W** TT VILVKSMLRKRS**F**GNPF
Myosin ninaC (1040-1059)	VIK **V** QSMMRALLARKR**V**KGG
GNRP (206-225)	IKK **V** QFSLRGWL CRRK **W**KNI
Ca^{2+}-pump (1102-1122)	LRRGQIL**W** FRGLNRIQTQIK

Figure 6: Peptide sequences from the CaM-binding domains of target proteins. [a]Amino acid sequences in the calmodulin-binding region of target proteins: skMLCK (Ikura *et al.*, 1992), smMLCK (Meador *et al.*, 1992), CaMKI (Picciotto *et al.*, 1993), CaMKII (Meador *et al.*, 1993), CaMKIV (Jones *et al.*, 1991), calcineurin (Higuchi *et al.*, 1991), CaMKK (Osawa et al., 1999), *Drosophila* unconventional myosin (Myosin nina C) (Montell *et al.*, 1988), rat guanine nucleotide-releasing protein (GNPR) (Shou *et al.*, 1992), and Ca^{2+} pump (Elshorst *et al.*, 1999) are aligned based on key hydrophobic residues which anchor the peptide to calmodulin (bold). Peptide C20W contains the CaM-binding domain of the Ca^{2+}-pump with the sequence shown above. The proteins with peptides whose structure in complex with Ca^{2+}-CaM has been determined are underlined.

domains of calmodulin engulf the peptide a channel is formed around the peptide. In the peptide complex there are two channel outlets which Osawa *et al.,* (1999) termed channel outlet 1 (CO-1) and channel outlet two (CO-2). CO-1 is created by helices 2, 3, and 4 from the N-terminus and helix 5 from the C-terminus, and CO-2 is created by helix 1 from the N-terminus and helices 6, 7, and 8 from the C-terminus. There is electrostatic polarity in the channel created by non-uniform distribution of acidic and basic residues at the two channel outlets. CO-2 is more negatively charged than CO-1, and the central linker region in calmodulin partially covers CO-1 resulting in CO-1 being smaller than CO-2 (Osawa *et al.*, 1999). Steric and electrostatic effects contribute to the orientation that calmodulin binds to target peptides. For example, smMLCK and CaMKII contain a basic cluster at their amino-terminus suggesting that these portions of the peptides will interact with CO-2 (Fig.6). Based on these particular characteristics, CaM-dependent kinase I and IV, and calcineurin would be predicted to bind calmodulin similar to MLCK and CaMKII because they possess a basic cluster located at the N-terminal portion of their CaM-binding domains (Fig. 6). In contrast, CaMKK contains a bulky hairpin loop and basic cluster at its carboxyl-terminus (Fig. 6) which would interact with CO-2.

Drosophila unconventional myosin, and rat guanine nucleotide-releasing protein also possess a basic cluster at the C-terminal portion of their CaM-binding domain and would be predicted to bind in the same orientation as CaMKK (Fig. 6)(Osawa *et al.*, 1999).

As an additional complexity in calmodulin signaling, it has been observed that some proteins interact with apo-CaM and not Ca^{2+}-CaM (Apel & Storm, 1992; reviewed in Jurado et al., 1999). Table II lists some of the proteins that calmodulin can bind to and activate in a Ca^{2+}-independent manner. The binding of CaM to proteins in the presence of Ca^{2+} chelators (e.g., EGTA or EDTA) is referred to as apo-CaM binding (Rhoads, A.R., and Friedberg, F. 1997). Apo-CaM binding sites fall into two classes: 1. IQ binding motifs found in myosins, neuromodulin, neurogranin, and other proteins; and 2. Concerted binding exemplified by CaM binding to the catalytic (γ) subunit of glycogen phosphorylase b kinase (reviewed in Jurado *et al.*, 1999). The sequence IQXXXRGXXXR defines a calmodulin-binding IQ motif, however the motif is rather loosely adhered to in many cases. The IQ motif is repeated one to six times in muscle and non-muscle myosins (Cheney and Mooseker, 1992). In many cases, the IQ motifs are located adjacent to or overlapping phosphorylation sites in proteins phosphorylated

Table II. Apo-calmodulin-binding proteins and their cellular functions.

Target	Putative Function	Ref.
Brush-border myosin I	Actin-activated ATPase	a
Myr4	ATP-dependent binding to F-actin	b
Neuromodulin	Reversible CaM storage, and regulation of phosphotidylinositol metabolism	C,d
Neurogranin	Neonatal synaptogenesis	e
Inositol 1,4,5-triphosphate receptor	Inositol 1,4,5-triphosphate binding	f
SR Ca^{2+} channel protein	Release of Ca^{2+} from the SR	g

a. Cheney & Mooseker, 1992; b. Bahler *et al.*, 1994; c. Alexander *et al.*, 1987; d. Van Hooff *et al.*, 1988; e. Baudier et al., 1991; f. Patel *et al.*, 1997; g. Yang *et al.*, 1994.

by protein kinase C (PKC), and dephosphorylated by calcineurin. (Apel *et al.*, 1990). Apo-CaM interactions allow for the activation of target proteins by calmodulin in the absence of calcium. The structural determinants for apo-CaM binding to targets are unknown, however Houdusse and Cohen (1995) have presented a model for apo-CaM binding to targets through IQ domain interaction. The model shows a more open CaM structure compared to Ca^{2+}-CaM-peptide complex, with interaction between CaM and target protein spread over a longer length of the target. Their model suggests that apo-CaM binds to the IQ motif, but also additional sites both amino and carboxyl terminal to it. In addition, others have shown that ionic interactions are important and that the calmodulin structure does not change much upon binding IQ domains (Urbauer *et al.*,1995).

Protein methyltransferases

Another feature of calmodulin from a wide variety of species from higher plants to vertebrate organisms is the specific trimethylation of lysine 115 (Fig.2). This modification is catalyzed by a specific N-lysine methyltransferase (reviewed in Siegel *et al.*, 1990). The general features of protein methyltransferases are reviewed below as well as specific features of the calmodulin methyltransferase.

A large group of post-translational modification reactions involve the addition of a methyl group to a polypeptide chain. These kinds of reactions can occur during or immediately after protein synthesis, or at later points in the lifetime of a protein molecule (Paik and Kim, 1990). Enzymes that catalyze these reactions are termed protein methyltransferases. They utilize S-adenosylmethionine as the methyl donor and can modify a variety of nucleophilic oxygen, nitrogen, and sulfur atoms on the polypeptide chain (Paik and Kim, 1990; Clarke 1993). The most well defined are the roles of protein methylation in carnitine biosynthesis where trimethyllysine serves as a precursor for carnitine (La Badie *et al.*, 1976); in bacterial chemotaxis desensitization (Kleene *et al.*, 1997; Van Der Werf and Koshland, 1977), in protein repair (Clarke, 1985), and in protein transport (Park *et al.*, 1987).

Protein methyltransferases can be classified in two major groups. The first group modifies carboxyl groups to form methyl esters (carboxyl methylation). These reactions are generally reversible and can function to regulate the activities of the target protein. For example, carboxyl methyltransferases have been shown to modify glutamate residues on several membrane-bound bacterial chemoreceptors to regulate their signal output (Springer *et*

al., 1979) and to modify aspartate residues in enzymes involved in the metabolism of protein damaged in the biological aging process (Najbauer *et al.*, 1996). Carboxyl methyltransferase reactions can be seen as analogous to those reactions catalyzed by protein kinases/phosphatases (Clarke, 1993; Aletta *et al.*, 1998).

The second group of protein methyltransferases (N-methyltransferases) result in the irreversible methyl transfer to the side-chain nitrogens of the amino acids lysine, arginine, and histidine (Paik and Kim, 1990). In addition, this group is also responsible for the methylation of sulfur atoms in the pathway converting homocysteine to methionine (Selhub 1999). Unlike carboxyl-methyltransferases, N-methyltransferases have extremely high specificity for particular amino acid residues on specific proteins (Paik and Kim, 1980; 1985; 1990). Also, in contrast to carboxyl-methylation, N-methylation is an irreversible post-translational modification (Clarke, 1985; Paik and Kim, 1985; Najbauer and Aswad, 1990).

Both mono- and di-methylated arginine residues have been found in myelin, myosin, nuclear proteins, and ribosomal proteins (Paik and Kim, 1980; 1990). Several of these proteins bind nucleic acids, and it has been suggested that arginine methylation may disrupt specific hydrogen-

bonds required for the interaction between the protein and nucleic acids (Najbauer *et al.*, 1993). The methylation of histidine residues has been observed in actin, myosin, histones, and rhodopsin (Paik and Kim, 1980; 1990). However, the function of methylhistidine in these proteins still remains unclear.

A number of proteins contain internal mono-, di-, and trimethylysine residues. Lysine-N-methyltransferases from various sources have narrow substrate specifity for histones (Paik and Kim, 1990), rubisco (Klein and Houtz 1995; Ying et al., 1999), cytochrome C (Durban *et al.*, 1978), and calmodulin (Sitaramayya *et al.*, 1980; Rowe et al., 1986; Morino et al., 1987). The physiological roles for most of these methylation reactions have not been well established, however, it is speculated that the quaternary nitrogen of trimethyllysines may function by providing a fixed positive charge (Paik and Kim, 1980; 1990). The potential role of calmodulin methylation is discussed further below.

Most sequence information available for methyltransferases comes primarily from carboxyl-methyltransferases (Clarke 1985; 1993). There is only one lysine N-methyltransferase sequence from the rubisco methyltransferase (Klein and Houtz 1995; Ying et al., 1996), and only one arginine N-methyltransferase sequence

(Niewmierzycka and Clarke, 1999) that have been determined. Currently no sequences are available for histidine methyltransferases. Alignment of the known sequences shows only three motifs (I, II, and III) conserved in diverse protein methyl-transferases. These motifs are thought to form the S-adenosylmethionine (AdoMet) binding pocket. With the exception of this conserved AdoMet binding pocket, diverse protein methyltransferases are not predicted to have a similar structure (Kagan and Clarke, 1994). In addition, only motif I is conserved in some DNA methyltransferases, and they are not predicted to be similar in structure to the protein methyltransferases.

The structures of only seven methyltransferases are presently available. Six of the seven structures are DNA or RNA methyltransferases, and only one crystal structure is available for a protein methyltransferase. The structure for glycine N-methyltransferase (GNMT) has been determined (Pattanayek et al., 1998). GNMT is abundant in liver and is a tetrameric enzyme that catalyzes the transfer of a methyl group from S-adenosylmethionine to glycine to produce S-adenosylhomocysteine and sarcosine (Pattanayek et al., 1998). Sarcosine has no known physiological role and it has been suggested that the function of GNMT is not to synthesize sarcosine, but rather to control the ratio of S-

adenosylmethionine to S-adensylhomocysteine (Ogawa and Fujioka, 1982). The tetramer resembles a square with a central channel where the amino-terminal domains are intertwined (Pattanayek *et al.*, 1998).

Calmodulin methylation

Calmodulin has been shown to be a substrate for both carboxyl- and N-methylation reactions (Gagnon *et al.*, 1981; Sitaramayya *et al.*, 1980). Carboxyl methylation of calmodulin was first observed by incubating bovine brain calmodulin with partially purified protein carboxylmethyltransferase and S-adenosyl-L-methionine (Gagnon et al., 1981). The carboxylmethylation reaction in calmodulin is reversible, and the levels of methylation are substoichiometric and unstable at pH values greater than 6 (Clarke 1985). It is unclear what residues in calmodulin are carboxyl-methylated *in vivo*, however, Aswad and Johnson (1987) and Clarke (1985) suggested that calmodulin is only methylated following deamidation of asparagine, and that the resulting isoaspartate residues are the site of methylation with little regard to the surrounding sequence. The carboxyl methylation reaction of calmodulin is principally an *in vitro* reaction, and is a function of the purification protocol used (which resulted in deamination). It is not clear whether calmodulin is carboxyl-methylated *in vivo*, but

it could have a role in repair or degradation pathways of deamination-damaged proteins (Aswad and Johnson, 1987).

It is more certain that N-methylation of calmodulin is a bona fide in vivo post-translational modification. It was first discovered by amino acid composition analyses of isolated rat testis calmodulin which revealed one mole of trimethyllysine per mole of calmodulin (Jackson *et al.*, 1977), and subsequent amino acid analysis of bovine brain calmodulin identified the position of trimethyllysine as residue 115 (Watterson *et al.*, 1980). An analysis of multiple vertebrate tissues (Rowe *et al.*, 1986) shows that calmodulin from most vertebrate tissues is stoichiometrically methylated. Other amino acid sequence analyses showed that many, if not most calmodulins, ranging from higher plants to protists and vertebrate organisms, are trimethylated at lysine 115 (reviewed in Roberts *et al.*, 1986b; Siegel *et al.*, 1990). However, it is also clear that some organisms, such as *Chlamydomonas* (Schleicher *et al.*, 1984), *Dictyostelium* (Marshak *et al.*, 1984) and certain invertebrate organisms (Molla *et al.*, 1981; Hergenhahn *et al.*, 1984; Morishima and Bodnaryk, 1985) do not trimethylate this position in calmodulin. Interestingly, *Paramecium* methylates two lysines in its calmodulin, with an additional dimethyllysine residue found at residue 13 in the first EF

hand (Schaefer *et al.*, 1987). *Euglena gracilis* calmodulin has been reported to have two moles of trimethyllysine per mole of calmodulin (Toda *et al.*, 1992).

Calmodulin-N-methyltransferase activity was first shown by incubating rat brain cytosol with [methyl-^{3}H]-S-adenosyl-L-methionine, and visualizing the methylated peptides by fluorography (Sitaramayya *et al.*, 1980). The methyltransferase has been purified from several sources including brain and testis and shows a high specificity for calmodulin (Rowe *et al.*, 1986; Morino *et al.*, 1987; Han *et al.*, 1993; Pech and Nelson, 1994; and Wright *et al.*, 1996; reviewed in Siegel *et al.*, 1990). Only calmodulins with an unmethylated lysine at residue 115 are substrates for the N-methyltransferase. When testing calmodulin N-methyltransferase, undetectable level of activity were observed when either myosin light chains, S-100 protein, histones, or cytochrome c were used as substrates, all of which are known to be methylated by other N-methyltransferases (Morino *et al.*, 1987; Siegel *et al.*, 1990). This suggests that a highly specific calmodulin methyltransferase co-evolved with calmodulin with the dedicated function of trimethylating lysine 115. Lysine-115 is a solvent-exposed residue (Babu *et al.*, 1988; Chattopadhyaya *et al.*, 1992; Zhang *et al.*, 1995) that is

found on a highly conserved six amino acid loop-turn region (LGEKLT) located between the helix 6 of the EF hand III and the helix 7 of the EF hand IV (Figs. 2 and 3).

Although post-translational N-methylation of lysine 115 occurs on calmodulin from several species, its biological significance remains undetermined. Previous work showed that trimethylation affects certain *in vitro* activities of calmodulin, such as the ability to activate plant NAD kinase (Roberts *et al.*, 1986b; Roberts et al., 1992). Calmodulin that is not methylated at lysine 115 shows a four fold higher activation of NAD kinase compared to calmodulins that possess trimethyllysine-115 (Roberts *et al.*, 1984; Marshak *et al.*, 1984; Roberts *et al.*, 1985). The trimethylation of recombinant wild-type (VU-1) CaM reduces its level of NAD kinase activation (Roberts *et al*, 1986b) while other calmodulin activities are unaffected (Roberts *et al.*, 1984; Marshak *et al.*, 1984; Roberts *et al.*, 1985; Putkey *et al*, 1986). This suggests that trimethylation may be a mechanism for selectively attenuating NAD kinase activation. Further, a mutant calmodulin containing arginine instead of lysine at position 115 (VU-3) is not methylated *in vitro*. This mutant calmodulin still retains the ability to fully activate NAD kinase similar to unmethylated VU-1 calmodulin, indicating that the reduction in the level of NAD kinase activation is

the direct result of trimethylation of lysine 115 of calmodulin (Roberts *et al.*, 1986b).

This feature of VU-3 CaM (i.e. high NAD kinase activation, and the inability to be methylated) was used to probe for the biological significance of methylation by the use of transgenic plant technology. Transgenic tobacco plants expressing VU-3 calmodulin were produced and showed decreased stem internode growth, reduced seed production, and reduced seed and pollen viability (Roberts *et al.*, 1992). These abnormal phenotypes suggest that the presence of an unmethylated calmodulin affects plant growth and development. Further, transgenic tobacco lines expressing VU-3 calmodulin exhibit an enhanced elicitor-stimulated oxidative-burst and a 3-fold increase in the rate of cell death (Harding *et al.*, 1997; Harding and Roberts, 1998). The expression of VU-3 *in vivo* likely causes these effects by hyperactivating the endogenous NAD kinase (Harding *et al.*, 1997). One interpretation of these results is that methylation serves to attenuate the ability of calmodulin to activate NAD kinase, and that the loss of the ability to perform this function results in enhanced NADPH production. This in turn causes an exaggerated oxidative burst plant defense response, presumably through NADPH oxidase (Harding et al., 1997). It has been noted that calmodulin

methylation levels are subject to developmental control (Oh and Roberts, 1990; Oh et al., 1992) and this could be an additional level of control of calmodulin signaling.

In addition to a potential role in enzyme modulation, methylation of lysine 115 may play a role in protein stability. A phenylalanine substitution at position 115 in *Schizosaccharomyces pombe* calmodulin resulted in reduced stability of the protein and growth arrest (Takeda *et al.*, 1989). In addition, it has been proposed that unmethylated lysine 115 of calmodulin is a site for ubiquitination (Gregori *et al.*, 1985; 1987), and that the methylation of lysine 115 is important for protecting calmodulin from the ubiquitin-dependent proteolytic pathway. However, Ziegenhagen et al. (1990) observed that even when calmodulin possessed a mono-ubiquitin conjugate there was 1 mole of trimethyllysine per mole of calmodulin. This suggests that the proposed ubiquitination does not necessarily occur at lysine 115, and it is not clear whether trimethylation affects calmodulin ubiquitination nor whether calmodulin ubiquitination occurs *in vivo*.

As discussed above, the high specificity of the N-methyltransferase for calmodulin suggests this is a dedicated enzyme that uses calmodulin solely as a substrate. The reason for this high specifity, and the structural

features of calmodulin and the methyltransferase that confer specific recognition, are not yet defined. Previous kinetic studies have shown the carboxyl terminal lobe (residues 78-148) is identical to intact calmodulin as a substrate for the N-methyltransferase, suggesting that the determinants for binding reside solely in the COOH-terminal lobe (Han *et al.*, 1993).

Several observations suggest that a folded functional carboxyl terminal lobe is required for methylation. For example, mutations or oxidation of residues in the hydrophobic core of the carboxyl terminal lobe destroy or reduce the ability of calmodulin to be methylated (Lukas et al., 1987; Han et al., 1993; Han and Roberts, 1997). Thus, it is likely that the structural requirements for calmodulin methylation are more complex than the simple availability of a solvent exposed lysine residue. However, beyond these preliminary studies, the specific features of the calmodulin carboxyl terminal lobe that lead to methyltransferase recognition and specificity remain unresolved. The goal of the present study is to further define which regions in the carboxyl terminal lobe of calmodulin are important for interaction with calmodulin N-methyltransferase.

CHAPTER II

MATERIALS AND METHODS

Materials

^{3}H-AdoMet was purchased from Du Pont-New England Nuclear. Phenyl-Sepharose CL-4B, and cyanogen bromide-activated Sepharose 4B were purchased from Pharmacia Fine Chemicals. Phosphocellulose P-11 and diethylaminoethyl cellulose DE53 were obtained from Whatman Biochemical Co. Sephadex G-10 was purchased from Sigma. Chelex 100 resin and Bradford protein assay reagent were purchased from Bio-Rad. BCA protein assay reagent and bovine serum albumin standard were purchased from Pierce Chemical Co. Synthetic oligonucleotides were purchased from Oligos Etc., Gibco/BRL, or Genosys Biotechnologies, Inc. The QuikChange™ Site-Directed Mutagenesis Kit was purchased from Stratagene. Restriction enzymes were purchased from New England Biolabs. Fura-2 was purchased from Molecular Probes. Dialysis membranes were purchased from Spectrum Medical Industries Inc. Centricon-30 units were purchased from Amicon. For all solutions and buffers NANO pure (SYBRON/Barnstead) treated water was used. Rat testes were purchased from Pel-Freeze. Sheep brains were obtained from the Food Technology Department of the University of Tennessee. Other reagents

were purchased from standard commercial sources and were of reagent grade or better.

Preparation of calmodulins

All calmodulins derived from the recombinant synthetic gene were expressed in *E. coli* and purified by a modification of the procedure of Roberts et al. (1985). JM101 cells were grown at 37°C in NZCYM media (1L) to an A_{550} of between 0.8 and 1.0. IPTG was added to a final concentration of 1 mM and cells were grown with shaking at 37°C overnight. Cells were lysed by lysozyme treatment as previously described (Roberts *et al.*, 1985; 1987) and calmodulin was purified by calcium-dependent hydrophobic chromatography on Phenyl-Sepharose (1.5 cm X 4 cm column) (Gopalakrishna and Anderson, 1982). Fractions containing calmodulin were pooled, were dialyzed overnight at 4°C against 4 liters of 20 mM ammonium bicarbonate, and then were dialyzed extensively against deionized water. The sample was lyophilized and resuspended in 50 mM MOPS-NaOH buffer pH 7.5, and stored at -80°C.

Generation of calmodulin mutants

Domain mutants - CaM^{EKL} was generated by cassette mutagenesis of the K115R (VU-3) mutant calmodulin gene (Roberts *et al.*, 1986b). The VU-3 gene was digested with

*Msc*I and *Pst*I to remove a 27 bp region including the coding region for residues 41-43. The synthetic oligonucleotide cassette shown below was ligated into the *Msc*I/*Pst*I-digested plasmid.

5' C GAA AAG CTT ACT GAA GCT GAA CTG CA 3'
3' G CTT TTC GAA TGA CTT CGA CTT G 5'

The product introduces a *Hind*III site, and the modified codons that encode EKL 41-43 are underlined.

To generate CaM^{1214} and CaM^{1232}, cassettes containing EF hand I or II were generated from the CaM^{EKL} construct by a PCR approach. The region of the CaM^{EKL} sequence (nucleotides 47 to 234) which contains the coding regions for EF hands I and II was amplified (25 cycles at 94° for 1 min, 42° for 2 min, and 72° for 3 min) using *Taq* polymerase.

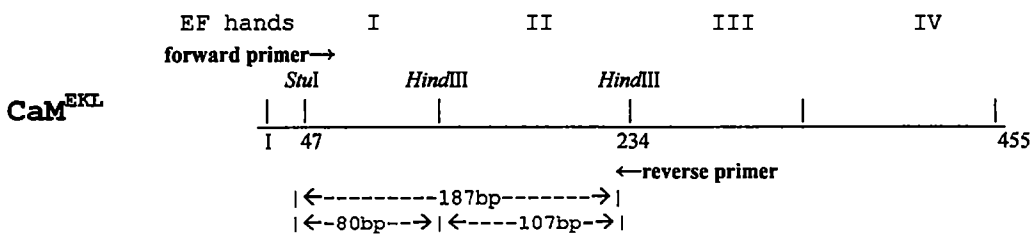

The forward primer (AA GAG GCC TCC TCT TCG TTT GAC AAA G) creates a new *Stu*I site at the 5′ end of the fragment, and the reverse primer (GA CTT GGA CTA CCG CGC GTT CAT CTT CGA ACC CGG GAA) creates a new *Hind*III and introduces a stop

codon after residue 75 of EF hand II. This amplified region (187 bp) also contains an additional *Hind*III restriction site within the loop-turn region between EF hands I and II. The PCR fragment was digested with *Stu*I and *Hind*III to generate a 80 bp fragment containing the coding region for EF hand I, and a 107 bp fragment containing the coding region for EF hand domain II. Each fragment was isolated by electrophoresis on 6.5% (w/v) polyacrylamide gels in Tris-Borate-EDTA (Sambrook *et al.*, 1989). To generate CaM^{1214}, the 80 bp fragment was cloned into the *Hind*III/*Stu*I sites of the VU-1 calmodulin gene (Roberts *et al.*, 1985). To generate CaM^{1232}, the 107 bp fragment was ligated into the *Hind*III site of the VU-1 gene. In both calmodulins, the methylation loop-turn sequence (residues 112-117) is regenerated and the only difference from wild type is the presence of the new EF hand sequences. Domain exchange mutants were identified by restriction mapping: a loss of an *Msc*I site for CaM^{EKL}, and the introduction of a new *Kpn*I site for CaM^{1214}, and the introduction of a new *Pst*I site for CaM^{1232}.

Subdomain mutants- CaM^{CL3} was generated by cassette mutagenesis. The VU-1 gene was digested with *Stu*I and *Eag*I to remove a 40 bp region including the coding region for

residues 90-101. The synthetic oligonucleotide cassette shown below was ligated into the *StuI*/*EagI*- digested plasmid.

5' CC TTC TCT CTG TTT GAC AAA GAC GGT GAC GGT ACC ATC AC 3'
3' GG AAG AGA GAC AAA CTG TTT CTG CCA CTG CCA TGG TAG TGC CGG 5'

The product contains a replacement of most of the amino acid sequence in calcium binding loop 3 (EF hand III) with the amino acid sequence in calcium binding loop 1 (EF hand I)(Fig.7). The third calcium-binding loop in EF hand III includes residues 93-104, and the resulting mutant includes the substitution of three amino acids within the C-terminal end of helix 5 (90-92/RVF) with sequence from helix 1 (17-19/SLF)(Fig.7). Further, three amino acids (102-104/AAE) at the end of calcium binding loop 3 are not replaced with sequence from calcium binding loop 1 (29-31/TKE)(Fig.7). CaM^{H6} was also generated by cassette mutagenesis by digestion of the VU-1 gene with *EagI* and *HindIII* to remove a 41 bp region including the coding region for helix 6 (residues 105-111). The synthetic oligonucleotide cassette shown below, which includes the coding sequence for helix 2 was ligated into the *EagI*/*HindIII* - digested VU-1 gene.

5' G GCC GCT GAA CTC GGC ACC GTT ATG CGC AGC CTT GGT GAA A 3'
3' CGA CTT GAG CCG TGG CAA TAC GCG TCG GAA CCA CTT TTC GA 5

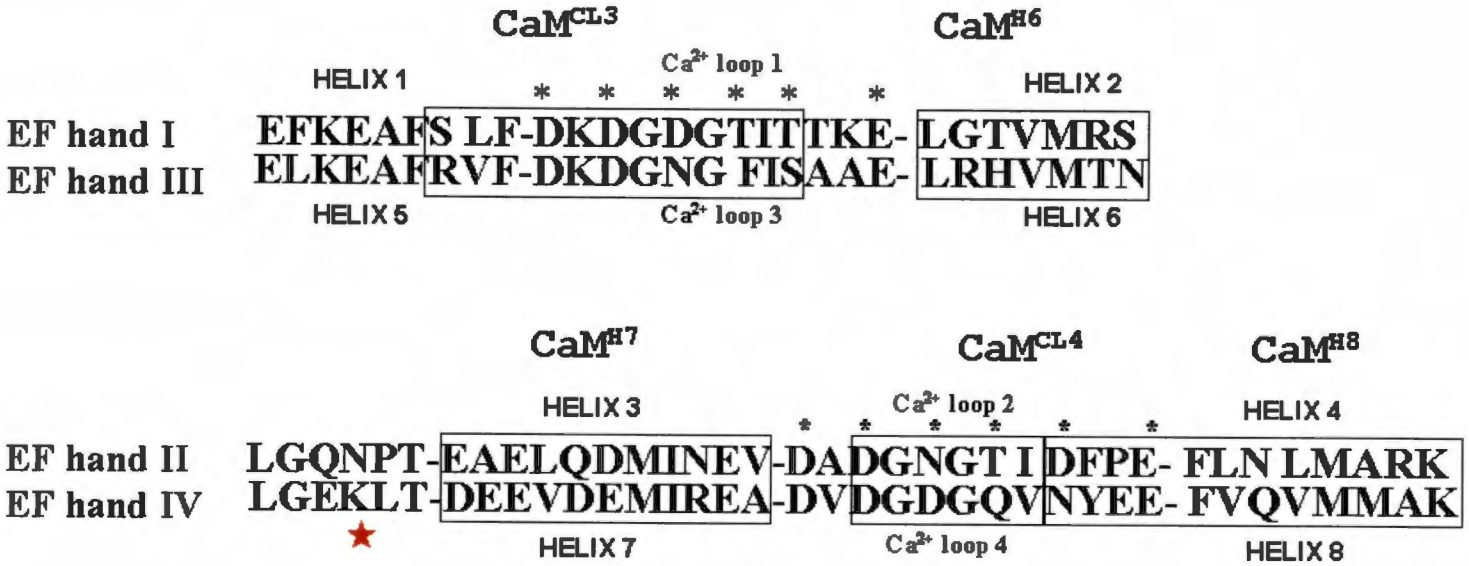

Figure 7. Organization of subdomain mutant calmodulins. Alignment of the amino acid sequence in the carboxyl-terminal lobe (EF hands III and IV) with homologous sequences from the amino-terminal lobe (EF hands I and II) is shown. The boxed areas represent amino acid sequence in the carboxyl-terminal lobe that was replaced by cassette mutagenesis with symmetry related sequence from the amino-terminal lobe for the generation of subdomain mutants: CaM^{CL3}, CaM^{H6}, CaM^{H7}, CaM^{CL4}, CaM^{H8}.

The product contains a replacement of helix 6(EF hand III) with helix 2 (EF hand I)(Fig.7).

For the generation of CaM^{H7}, an *Aat*II site at 2617 in the vector sequence was removed in pVUCH-1 by using the QuikChange™ Site-Directed Mutagenesis Kit with the following primers:

5' GTG CCA CCT GAC GAC TAA GAA ACC ATT ATT 3'
3' CAC GGT GGA CTG CTG ATT CTT TGG TAA TAA 5'

The resulting plasmid was digested with *Hind*III and *Aat*II to remove a 46 bp region including the coding region for helix 7 (residues 118-128). The synthetic oligonucleotide cassette shown below includes the coding sequence for helix 3, and was ligated into the *Hind*III/*Aat*II - digested plasmid, generating CaM^{H7}.

5' AG CTT ACT GAA GCT GAA CTG CAG GAC ATG ATT AAC GAA GTC GAC GT 3'
3' A TGA CTT CGA CTT GAC GTC CTG TAC TAA TTG CTT CAG C 5'

The product contains a replacement of helix 7(EF hand IV) with helix 3 (EF hand II)(Fig.7).

For the generation of CaM^{CL4} the pVUCH-1 plasmid (-*Aat*II site as described above) was digested with *Aat*II and *Hpa*I to remove a 23 bp fragment including the coding region for residues 131-136. The synthetic oligonucleotide cassette

shown below was ligated into the *Aat*II/*Hpa*I- digested plasmid, generating CaM^{CL4}.

5' C GAC GGT AAC GGC ACC ATC 3'
3' TG CAG CTG CCA TTG CCG TGG TAG 5'

The protein product encoded by the mutant has a substitution of residues 131 to 136 in calcium binding loop four with the sequence found between residues 58 to 63 in calcium binding loop 2 (Fig.7). Calcium-binding loop 4 includes residues 129-140, and calcium-binding loop 2 includes residues 56-67, therefore the resulting mutant does not replace residues 129(D) or 130(A) at the beginning of calcium binding loop 4 with 56(D) or 57(V) from calcium binding loop 2 (Fig.7). In addition, the four amino acids (137-140/NYEE) at the end of calcium-binding loop 4 are not replaced with sequence from calcium-binding loop 2 (64-67/DFPE).

For the generation of CaM^{H8}, the *BamHI* site in the pTAC promoter of pVUCH-1 (Lukas *et al.*, 1987) was changed to Bgl*II* by PCR. A segment (715 bp) of pVUCH-1 containing the pTAC promoter region and the CaM gene was amplified using the following primers:

5' CGC GGA TCC TAC TTA GCC ATC ATA ACC 3'

5' GGA AGA TCT GGC GTC AGG CAG CCA TCG G 5'

The amplified fragment has a BglII site introduced at start of the pTaC promoter and the BamHI site remaining at the end of the CaM gene. BglII and BamHI have complementary ends, and the fragment was ligated into BaMHI cut pVUCH-1. The resulting plasmid was digested with *HpaI* and *BamHI* to remove a 43 bp region including the coding region for helix 8 (residues 141-148). The synthetic oligonucleotide cassette shown below includes the coding sequence for helix 4, and was ligated into the *HpaI/BamHI* - digested plasmid.

```
5' GAT TTT CCG GAA TTT CTG AAC CTG ATG GCG CGC AAG TAG      3'
3' CTA AAA GGC CTT AAA GAC TTG GAC TAC CGC GCG TTC ATC CTA G  5'
```

The protein product of the mutant gene has the substitution of residues 137-148 with residues 64-75 from EF hand II. Thus, all of helix 8 is replaced with helix 4 as well as four residues (137-140/NYEE) within calcium-binding loop four being replaced with sequence from calcium-binding loop 2 (64-67/DFPE).

Alanine/threonine scanning mutants - Calmodulin mutants R106A, H107A, T110A, T110R, L112T, G113S, E114A, L116T, T117A, E119A, D122A, E123A, R126A, E127A, E139A, and double mutant R106A/H107A (Fig.8) were generated by QuikChange™ Site-Directed Mutagenesis Kit (Stratagene). Calmodulin

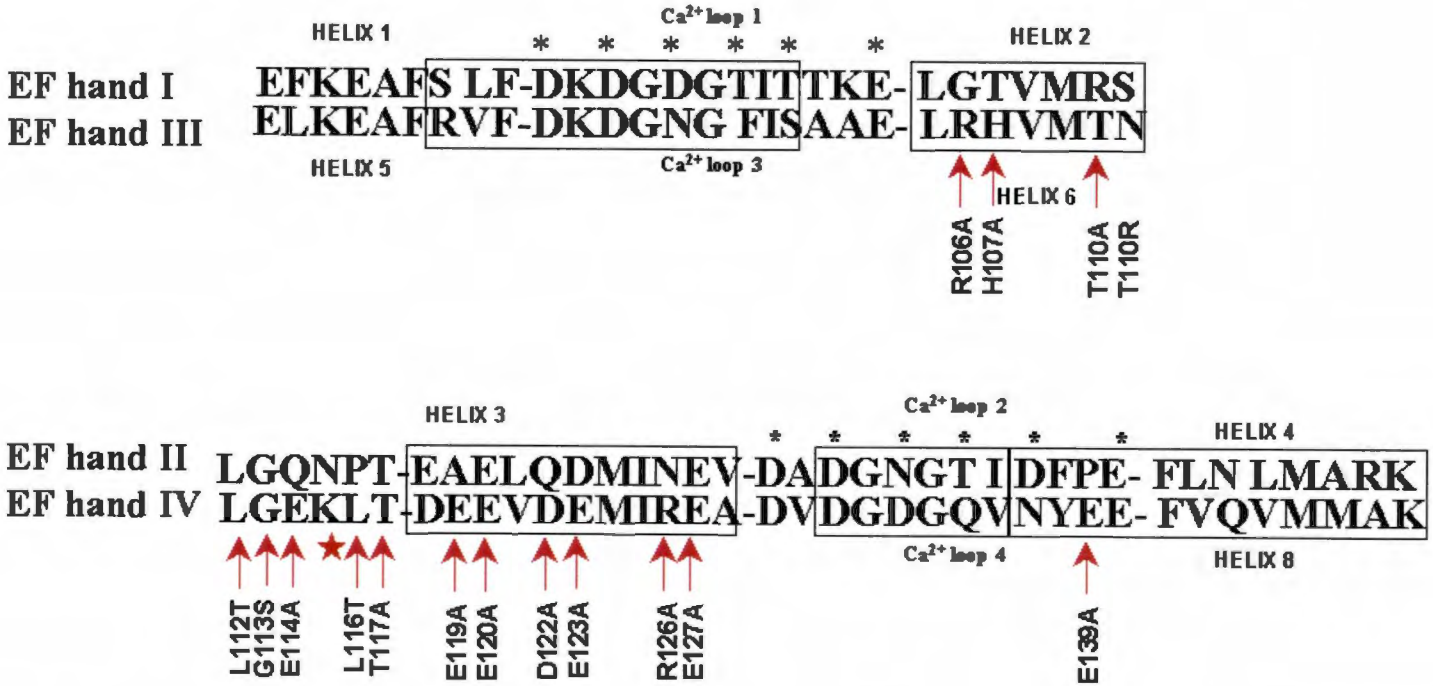

Figure 8. Site-specific alanine/threonine substitutions of residues in the carboxyl-terminal lobe. Alignment of the amino acid sequence in the carboxyl-terminal lobe (EF hands III and IV) with homologous sequence in the amino-terminal lobe (EF hands I and II) is shown. The arrows represent amino acid substitutions in the carboxyl-terminal lobe generated by the QuikChange Site-Directed Mutagenesis Kit. The star represents lysine 115 the site of methylation.

mutant R106A/E139A was generated by a *EcoRI/Hind*III digest of pVUCH-1/R106A. The 355bp fragment including the residue 106 was ligated into *EcoRI/Hind*III cut pVUCH-1/E139A. All domain, subdomain and scanning mutants were confirmed by automated DNA sequencing on a Perkin Elmer Applied Biosystems 373 DNA sequencer at the University of Tennessee Molecular Biology Research Facility. Sequencing reactions were done with a Prism Dye Terminator Cycle sequencing kit (Perkin Elmer Applied Biosystems).

Purification of calmodulin N-methyltransferase from sheep brain and rat testes.

Calmodulin N-methyltransferase from sheep brain was purified through the calmodulin-Sepharose step by using a modification of previously described procedures (Rowe *et al.*, 1986; Han *et al.*, 1993). Five sheep brains (456 g) were homogenized with 3.5 volumes of cold 25 mM Hepes-NaOH, pH 7.4, 4 mM β-mercaptoethanol, 0.25 M sucrose, 5 mM EGTA, 0.1 mM PMSF. The homogenate was centrifuged at 11,000 X g at 4°C for 30 min. The supernatant fraction was removed and placed on ice while the pellets were reextracted in 1 volume of homogenization buffer and centrifuged as described above. The supernatant fractions were combined and brought to 35%

saturation with solid ammonium sulfate added slowly with stirring at 4°C. The mixture was stirred for 45 min, and was centrifuged at 15,000 X g for 30 min at 4°C. The supernatant fraction was saved and brought to 70% saturation with solid ammonium sulfate, stirred for 45 min, and was centrifuged at 15,000 X g for 30 min. The pellet from the 35 to 70% saturation precipitation step was resuspended in 25 mM Hepes-NaOH, pH 6.8, 0.1 mM EGTA, 4 mM β-mercaptoethanol, 0.1 mM PMSF, and was dialyzed against 8 liters of the same buffer overnight at 4°C. The dialyzed sample was centrifuged at 15,000 X g for 30 min at 4°C. The supernatant fraction was applied to a phosphocellulose column (6 X 10 cm) which was equilibrated in 25 mM Hepes-NaOH, pH 6.8, 4 mM β-mercaptoethanol, 0.01% [w/v] triton x-100, 0.1 mM PMSF (phosphocellulose column buffer). The resin was washed with phosphocellulose column buffer until the A_{280} of the effluent was zero. The enzyme was eluted with phosphocellulose column buffer containing 0.5 M NaCl. $CaCl_2$ was added to a final concentration of 1 mM, and the eluted sample was applied to a calmodulin-Sepharose column (1.5 X 3 cm) equilibrated with 20 mM Tris-HCl, pH 7.4, 0.1 M NaCl, 0.1 mM $CaCl_2$, 0.05% (w/v) CHAPS, 4 mM β-mercaptoethanol, 0.1 mM

PMSF. The column was washed with 100 ml of the same buffer, followed by 200 ml of 20 mM Tris-HCl, pH 7.4, 0.6 M NaCl, 0.1 mM $CaCl_2$, 0.05% (w/v) CHAPS, 2 mM DTT, and 0.1 mM PMSF. The sample was eluted with 20 mM Tris-HCl, pH 7.4, 1 M NaCl, 1 mM EGTA, 0.05% (w/v) CHAPS, 2 mM DTT. The fractions with calmodulin methyltransferase activity were pooled and concentrated by ultrafiltration on a Centricon-30 unit (Amicon).

Calmodulin N-methyltransferase from rat testes was purified by a modified procedure of Rowe et al., (1986) and Han et al., (1993). Rat testes (40 g) were homogenized with 3 volumes of cold 10 mM Hepes-NaOH, pH 7.4, 4 mM β-mercaptoethanol, 0.25 M sucrose, 5 mM EGTA, 0.1 mM PMSF. The homogenate was centrifuged at 8,500 X g for 30 min. The supernatant fraction was removed and placed on ice while the pellets were re-extracted in 2 volumes of homogenization buffer and centrifuged as described above. The supernatant fractions were combined and subjected to differential ammonium sulfate fraction as described above. After dialysis, the ammonium sulfate fraction (35-70%) was centrifuged at 100,000 X g for 30 min at 4°C. Triton X-100 was added to a final concentration of 0.01% (w/v) and the

sample was applied to a Sephadex G-10 (6 X 5 cm) column equilibrated in 10 mM Hepes-NaOH, pH 7.4, 4 mM β-mercaptoethanol, 0.01% (w/v) triton X-100, and 0.1 mM PMSF. The absorbance of the effluent was continuously monitored at 280 nm. The fractions containing protein were combined and the resulting sample was applied to a 2.5 X 16 cm column of DEAE-cellulose (Whatman DE-53) equlibrated in the same buffer. The absorbance of the effluent was continuously monitored at 280 nm, and the non-binding protein fraction, which contains the calmodulin-N-methyltransferase was collected (120ml). Calcium was added to 2 mM and calmodulin-Sepharose was performed as described above. The fractions with calmodulin methyltransferase activity were pooled and concentrated by ultrafiltration on a Centricon-30 unit (Amicon).

Purification of calmodulin-dependent enzymes

Plant NAD kinase was purified through the polyethyleneglycol (PEG) step by using the procedure of Roberts et al. (1985). After PEG precipitation, the pellet was resuspended in (1/50 of homogenate volume) 50 mM Tris-HCl, pH 7.0, 100 mM KCl, 3 mM $MgCl_2$, 0.2 mM $CaCl_2$, 20% (v/v) glycerol, 0.5 mM NAD, and 0.5 mg/ml leupeptin (DEAE wash

buffer), and was centrifuged for 15 min at 27,000 X g at 4°C. The supernatant was then applied to a DEAE-Sephadex A-50 column (2.5 X 5 cm), and the column was washed with DEAE wash buffer until the absorbance at 280 nm was less than 0.02. Calmodulin-dependent NAD kinase was eluted with 50 mM Tris-HCl, pH 7.0, 100 mM KCl, 3 mM $MgCl_2$, 1 mM EGTA, 20% (v/v) glycerol, 0.5 mM NAD, and 0.5 mg/ml leupeptin.

Calmodulin-dependent cyclic nucleotide phosphodiesterase (PDE) was prepared from sheep brain by a modification of the protocol of Sharma et al. (1981). Sheep brains (460g) were partially thawed at room temperature, and homogenized with 100 mM Tris-HCl, pH 7.5, 2 mM EDTA (homogenization buffer). The homogenate was squeezed through cheesecloth and the filtrate was centrifuged at 10,000 X g for 20 min at 4°C. Pellets were re-extracted in 2 volumes of homogenization buffer and the filtrate was centrifuged as described above. The supernatant fractions were combined, and β-mercaptoethanol and EGTA were added to a final concentration of 10 mM and 0.1 mM respectively. The sample was applied to a DEAE cellulose column (3 X 20 cm) which was equilibrated with 20 mM Tris-HCl, pH 7.0, 1 mM imidazole, 1 mM Mg acetate, 0.1 mM EGTA, 10 mM β-

mercaptoethanol, and 0.05 M NaCl (DEAE column buffer). The column was washed with 200 ml of DEAE column buffer, and then was eluted with a linear (0.05 to 0.5 M) NaCl gradient. Fractions were assayed for calmodulin-stimulated cyclic nucleotide PDE activity. Fractions containing high activities of calmodulin-dependent cyclic nucleotide phosphodiesterase were pooled and were dialyzed overnight at 4°C against 10 mM Tris-HCl, pH 7.5, 0.1 mM β-mercaptoethanol, 0.1 mM $CaCl_2$, and 0.1 mM $MgCl_2$. The dialyzed sample was lyophilized, and stored at -80°C. The lyophilized powder was reconstituted in nanopure water prior to assay.

Enzyme assays

Calmodulin methyltransferase activity was assayed as described by Han et al. (1993). The standard assay mixture contained 0.1 M glycylglycine-NaOH (pH 8.0), 0.15 M KCl, 2 mM $MgCl_2$, 5 mM dithiothreitol, 0.01% (w/v) triton X-100, 12 μM [^{3}H]-AdoMet (1.6 μCi), 1 mM $CaCl_2$, and various amounts of calmodulin. The reaction was initiated by the addition of enzyme and the incubation was typically run for 20 min at 37°C. The reaction was terminated by heating at 90°C for 3 minutes. The samples were centrifuged in an Marathon 16 KM Fischer brand microfuge for 6 min and the supernatant

fractions were combined with 200 µl of a 1:1 phenyl-Sepharose slurry equilibrated in 50 mM Tris-HCl, pH 8.0, 0.3 M NaCl, 0.1 mM $CaCl_2$. The mixture was vortexed and centrifuged in Marathon 16 KM Fischer brand microfuge for 3 minutes. The supernatant fraction was decanted and the collected resin was washed twice with 800 µl of the same buffer. Calmodulin was eluted with 0.1 M NH_4HCO_3, pH 8.0, 2 mM EDTA and tritium incorporation was measured by liquid scintillation counting in a Beckman LS 3801 scintillation counter. The determination of kinetic parameters for the methyltransferase were derived under pseudo-first order conditions using calmodulin as the varied substrate and maintaining AdoMet at a constant concentration of 12 µM as previously described (Han *et al.*, 1993). Apparent K_m and V_{max} parameters were determined by fitting the data to the Michalis Menten equation using double reciprocal plots. k_{cat} was determined by using 38,000 as the molecular weight of the methyltransferase as previously described (Han *et al.*, 1993).

Pea NADK activity was assayed as described previously (Roberts *et al.*, 1985). PDE assays were done as described previously (Sharma *et al.*, 1981). The NADK and PDE

activation curves were generated by best fits to the data using the following equation for calmodulin activation:

$$\frac{v}{V_{max}} = \frac{[CaM]^n}{K_{0.5} + [CaM]^n}$$

Where v is the initial enzyme rate, $K_{0.5}$ is the concentration of calmodulin for half-maximal activation. V_{max} is the enzymatic rate at maximal activation, [CaM] is the concentration of calmodulin, and n represents the Hill coefficient.

Assays for the inhibition of NADK activation by CaM^{EKL} were done under standard assay conditions in 1 mM $CaCl_2$ with various amounts of CaM^{EKL} at several fixed concentrations of VU-1 calmodulin. The data were analyzed by constructing a Dixon plot and the K_i was determined using the following equation:

$$\frac{1}{v} = \frac{K_{0.5}}{V_{max} K_i [CaM]} \cdot [CaM^{EKL}] + \frac{1}{V_{max}} \left(1 + \frac{K_{0.5}}{[CaM]}\right)$$

Where v is the initial enzyme rate, $K_{0.5}$ is the concentration of VU-1 for half maximal activation. V_{max} is the enzyme rate at maximal activation, [CaM] is the concentration of VU-1

calmodulin, [CaM^{EKL}] is the concentration of CaM^{EKL}, and K_i is the inhibition constant.

Assays for the calcium dependence of NADK activation were done in 50 mM Hepes-NaOH (pH 7.5), 3 mM $MgCl_2$, 3 mM EGTA, 3 mM ATP, 2 mM NAD, 0.1 mM calmodulin, and various $CaCl_2$ concentrations that yielded a free calcium concentration ranging from 10^{-8} to 10^{-3} M calculated by using the Comic program as described previously (Han and Roberts 1997). Calculated free calcium concentrations in the reactions were verified by quantitation with fura-2 (Molecular Probes) as described in Grynkiewicz et al. (1985). All buffers and reagents were decalcified by chelex-100 (BioRad) resin treatment as described in Crouch et al. (1980).

X-ray scattering

Small angle X-ray scattering experiments were done in collaboration with Dr. Jill Trewhella at the Los Alamos National Laboratory by using the general approaches as previously described (Heidorn *et al.*, 1988; Krueger *et al.*, 1997; Krueger *et al.*, 1998). VU-1 and CaM^{EKL} were prepared as described above. Calmodulin samples were concentrated in a centricon-10 to 10 mM and were dialyzed against 50 mM HEPES-NaOH pH 7.5. The CaM samples and buffer from dialysis

were sent to the facility at Los Alamos. X-ray scattering data were collected on VU-1 and CaM^{EKL} with Ca^{2+}-CaM alone and Ca^{2+}-CaM in complex with the MLCK (M13) peptide (Krueger *et al.*, 1998). The Los Alamos facility uses a line source from a sealed X-ray tube that is driven by an Enraf Nonius generator. Data were recorded on an IBM-PC installed with a Nucleus PCA-8000 multichannel analyzer board. The scattering data from the protein molecules was calculated by subtracting a normalized buffer spectrum measured in the same cell. The scattering of X-rays from a homogeneous solution of monodisperse particles such as proteins can be expressed as:

$$I(Q) = \left| \int [\rho(\mathbf{r}) - \rho_s] \exp(-i\mathbf{Q}\bullet\mathbf{r}) d\mathbf{r} \right|^2$$

where $Q=(4\pi\sin\theta)/\lambda$ is the amplitude of the scattering vector (2θ is the scattering angle and λ is the wavelength of the X-rays or neutrons), $\rho(\mathbf{r})$ and ρ_s are the scattering density for the protein and the solvent respectively, and the integration is taken over the volume of the particle. The scattering data were analyzed to determine the radius of gyration (R_g) and the P(r) function as previously described (Heidorn and Trewhella, 1988; Olah and Trewhella, 1994).

Other analytical methods

Protein concentrations were determined by the BCA assay (Pierce Biochemicals) using bovine serum albumin as a standard. SDS-polyacrylamide gel electrophoresis was done by using the method of Laemmli (1970). Proteins were stained with Coomassie Brilliant Blue G-250. Protein concentrations were determined by the method of Bradford (1976) or by the bicinchoninic acid method of Smith et al. (1985) using bovine serum albumin as the standard.

CHAPTER III

RESULTS

Analyses of the calmodulin methyltransferase were conducted on two separate enzymes, from sheep brain (Han *et al.*, 1993) and rat testes (Rowe *et al.*, 1986). Initial studies were done with the sheep brain enzyme, but during the course of these studies enzyme from testes was used because of the lack of availability of suitable sheep brain tissues as well as difficulties with previous purification protocols. A new procedure was devised (Table III) to obtain a highly purified preparation of the testes enzyme. Compared to previous procedures (Han *et al.*, 1993), the new protocol introduced a gel filtration step and an anion exchange chromatography step on DEAE cellulose, prior to affinity chromatography on calmodulin-Sepharose. This modified procedure yielded an enzyme of comparable purity with superior yield (47% vs 1%). Kinetic analyses of both enzyme preparations showed comparable results with the various calmodulin proteins examined in this study.

Effect of mutations in the methylation loop on methyltransferase recognition.

The six amino acid LGEKLT (residues 112-117) loop-turn region between EF hands III and IV contains the site of

Table III. Recovery table for the purification of rat testes calmodulin N-methyltransferase.

Step	Total[a] Protein	Total Activity	% Recovery	Specific Activity	Fold Purification
Crude Extract	5560	3.88	100	0.7	1
30-60% $(NH_4)_2SO_4$ ppt.	1360	2.83	73	2.1	3
Sephadex G-10	553	2.94	75	5.32	7.6
DEAE cellulose DE-53	48	1.86	48	38.7	55.3
Calmodulin Sepharose	0.36	1.84	47	5110	7300

[a] Units are; total protein, mg; total activity, nmole/min; and specific activity, pmole/min/mg.

methylation, lysine 115 (Fig. 9). This loop sequence is highly conserved in all calmodulins (Roberts *et al.*, 1986b). To test whether this conserved six amino acid motif is required for calmodulin methyltransferase recognition, a series of mutations were performed as shown in Figure 9B. The leucines at position 112 and 116 were replaced by threonines resulting in polar substitutions at these positions. The charged glutamate at position 114 and the threonine at position 117 were replaced with an alanine (Fig. 9B). To test the role of the conserved flexible glycine at position 113 this residue was replaced by a small polar serine (Fig. 9B). This substitution will likely disrupt the bend of the loop that is facilitated by the phi psi angles (ϕ/ψ = 93°/10°) that can only be adopted by a flexible glycine residue (Ramachandran and Sasisekharan, 1968).

The desired effect is to introduce subtle mutations that do not result in global changes in the calmodulin structure, but rather to probe for specific sites involved in methyltransferase recognition. To test whether calmodulin function was affected, the mutants were tested for their ability to activate two calmodulin dependent

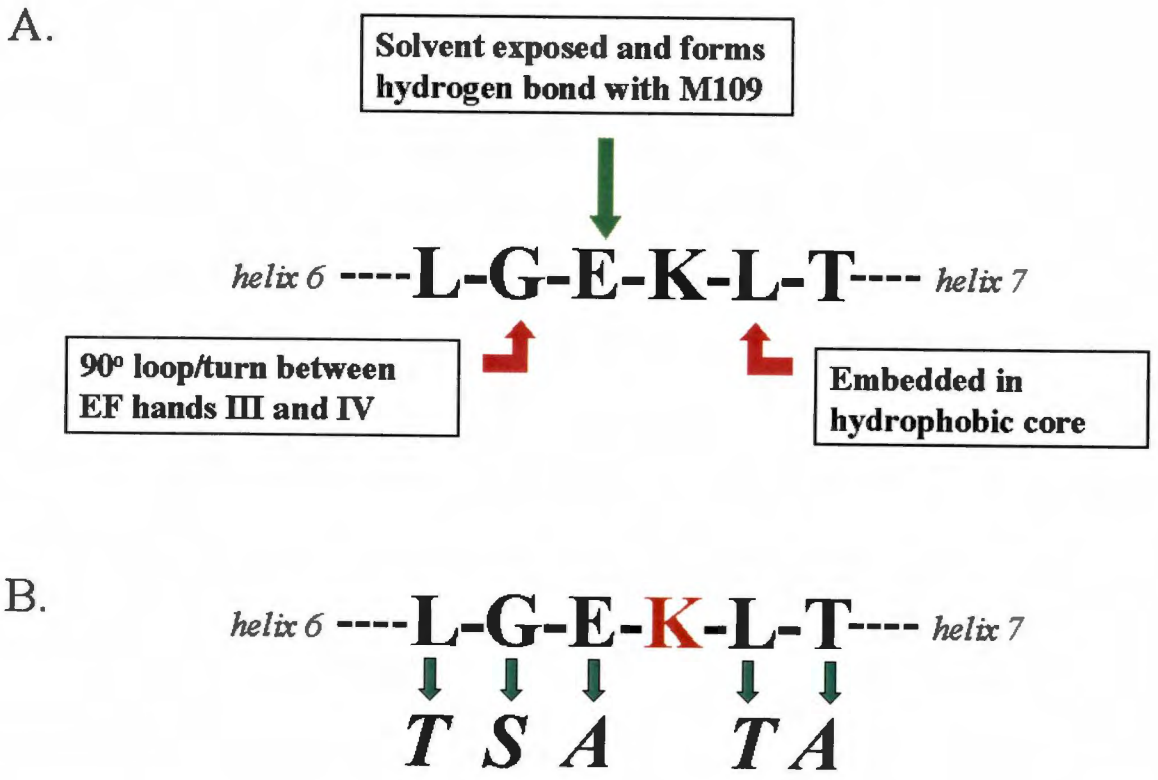

Figure 9. Amino acid sequence in the methylation loop. The six amino acid LGEKLT (residues 112-117).loop turn region between helix 6 (EF hand III) and helix 7 (EF hand IV). **A.** Describes the environment of the individual residues in the methylation loop and **B.** Indicates the mutations that were made in the conserved residues: L112T, G113S, E114A, L116T, and T117A.

enzymes, NAD kinase and cyclic nucleotide PDE. Dose dependent activation curves were generated for each calmodulin and from these two parameters were determined: the maximal level of activation and the $K_{0.5}$ (concentration required for half-maximal activation). All methylation loop mutants fully activated cyclic nucleotide PDE with similar $K_{0.5}$ values, with the exception of L116T, which showed a two-fold lower $K_{0.5}$ (Fig. 10, Table IV). Similarly L112T, G113S, and E114A showed essentially indistinguishable NAD kinase activation curves compared to from VU-1 calmodulin (Fig. 11, Table IV). L116T and T117A actually showed an enhanced activation of NADK, activating the enzyme to 130% (SE ±5.20) and 154% (SE ±14.2) of the level obtained with VU-1 calmodulin (Fig. 11, Table IV). Similar to PDE, L116T showed a 3-fold lower $K_{0.5}$ value for the activation of NAD kinase (Table IV). The data suggest that substitutions for these highly conserved residues in the methylation loop do not significantly alter their ability to activate calmodulin-dependent enzymes.

The mutations in the methylation loop showed varied effects on lysine 115 methylation. Mutations in residues flanking the site of methylation (E114A and L116T) showed a drastic effect on methylation and neither could serve as

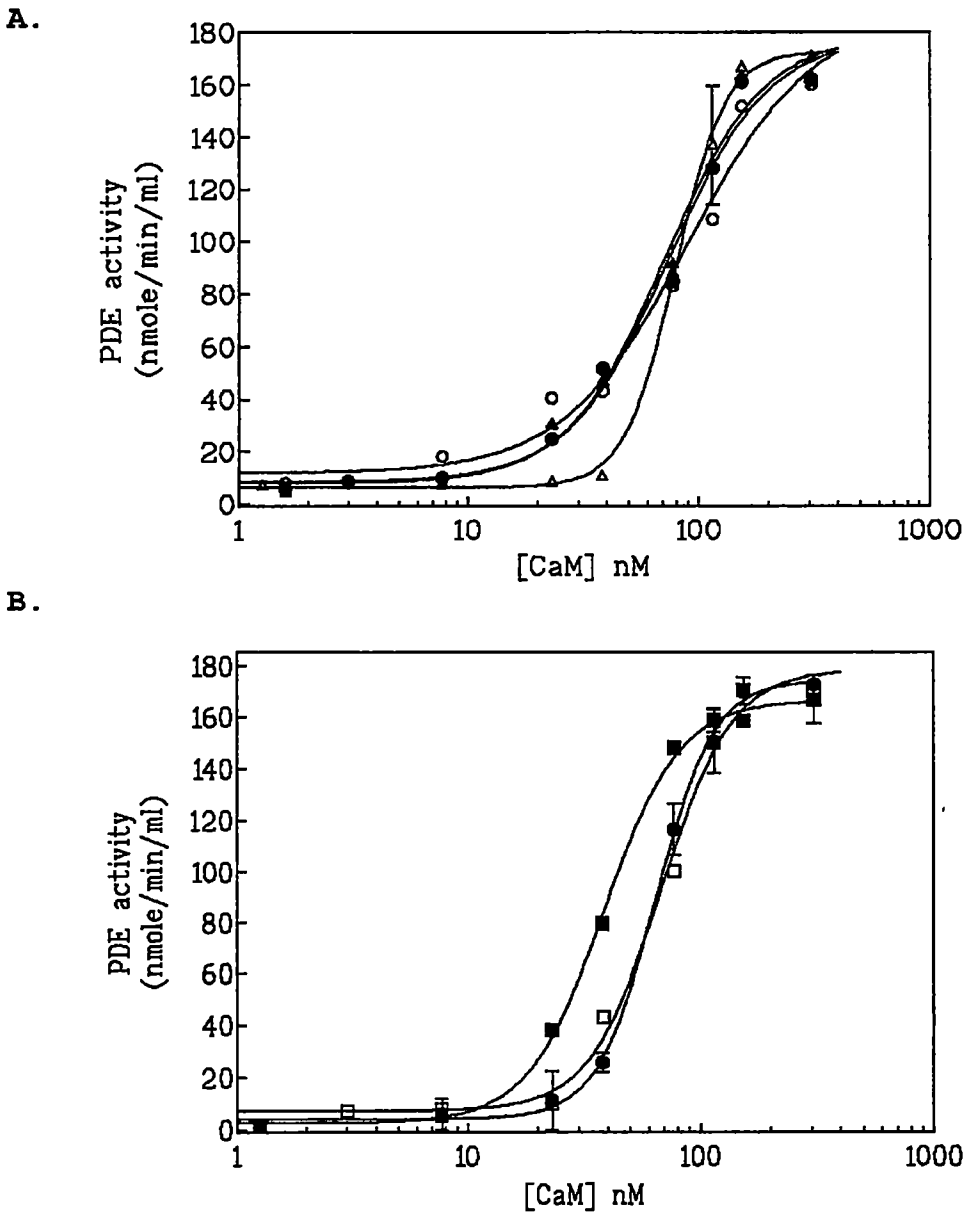

Figure 10. Activation of PDE by mutant calmodulins L112T, G113S, E114A, L116T, and T117A. Activation of PDE by VU-1 (●) compared with **A.** L112T (O), G113S (▲), E114A (Δ),and **B.** L116T (■) and T117A (□). All assays were done in 1 mM $CaCl_2$. Error bars show the S.E. and the absence of error bars indicates the error is smaller than the symbols.

Table IV. Activation parameters of calmodulin-dependent enzymes by calmodulins with mutations in the methylation loop.

CaM	PDE % maximal rate[a]	$K_{0.5}^{(CaM)}$ [b]	NADK % maximal rate	$K_{0.5}^{(CaM)}$
VU-1	100	69 (±1)	100	2.6 (±.2)
L112T	105	89 (±1)	94	2.0 (±.1)
G113S	100	71 (±1)	99	2.6 (±.2)
E114A	99	75 (±11)	97	3.0 (±.1)
L116T	96	38 (±7)	130	1.0 (±.2)
T117A	105	63 (±1)	154	3.0 (±.2)

[a] % maximal rate: maximal activation of enzymes (PDE or NAD kinase) by calmodulins standardized to VU-1 calmodulin (100%).

[b] $K_{0.5}^{(CaM)}$ Concentration of calmodulins (nM) giving half maximal activation. The S.E. value is shown in parentheses.

A.

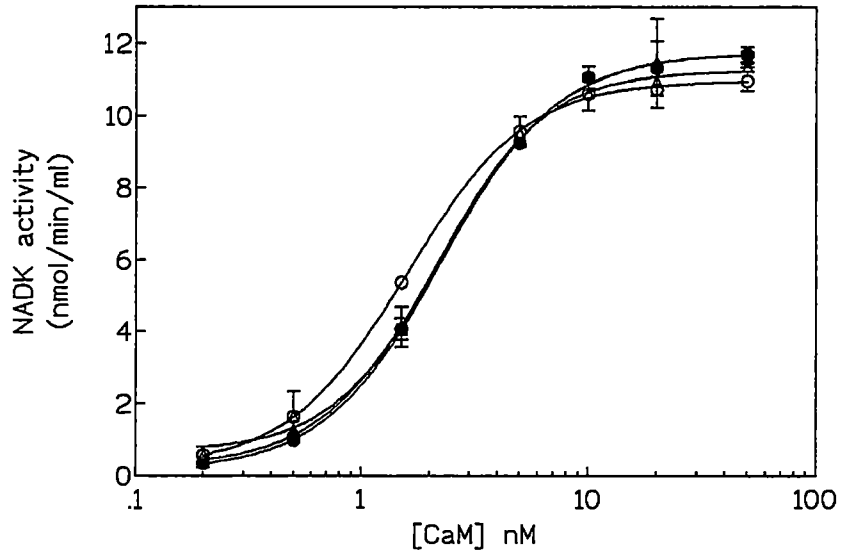

B.

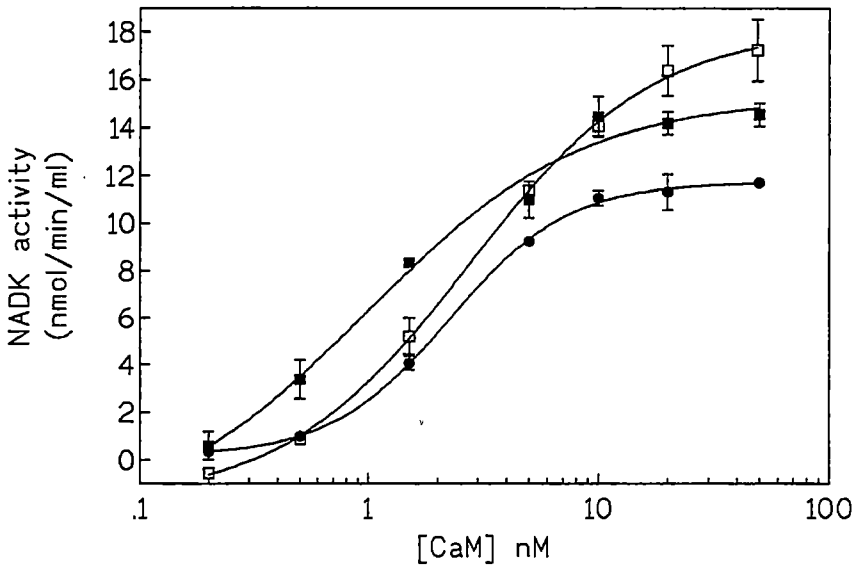

Figure 11. Activation of NAD kinase by mutant calmodulins L112T, G113S, E114A, L116T, and T117A. Activation of NAD kinase by VU-1 (●) compared with **A.** L112T (O), G113S (▲), E114A (Δ),and **B.** L116T (■) and T117A (□). All assays were done in 1 mM $CaCl_2$. Error bars show the S.E. and the absence of error bars indicates the error is smaller than the symbols.

a substrate for the methyltransferase either in the presence (Fig.12, Table V) or absence of calcium (Table VI). A similar result was observed with G113S which could not serve as a substrate for the methyltransferase under any condition (Figs. 13B & 14B, Tables V & VI). Overall, the data suggest that the highly conserved residues on either side of lysine 115, and the invariant glycine at position 113 are necessary for methyltransferase recognition and methylation.

In contrast, L112T showed substrate activity that was influenced by the binding of calcium. In the presence of calcium, L112T was very similar to VU-1 with respect to methyltransferase kinetics (Fig. 14A, Table V). However, apo-L112T CaM shows a 4.5 fold reduction in catalytic efficiency (k_{cat}/K_m=1.74 X 10^4) compared to VU-1 calmodulin (k_{cat}/K_m=8.18 X 10^4) (Fig. 13A, Table VI). This difference suggests that the binding of calcium restores the ability of this mutant to be recognized by the methyltransferase. The threonine to alanine mutation at position 117 (T117A) showed little effect on methyltransferase activity either in the presence or absence of calcium compared to VU-1 (Figs. 13C & 14C, Tables V & VI).

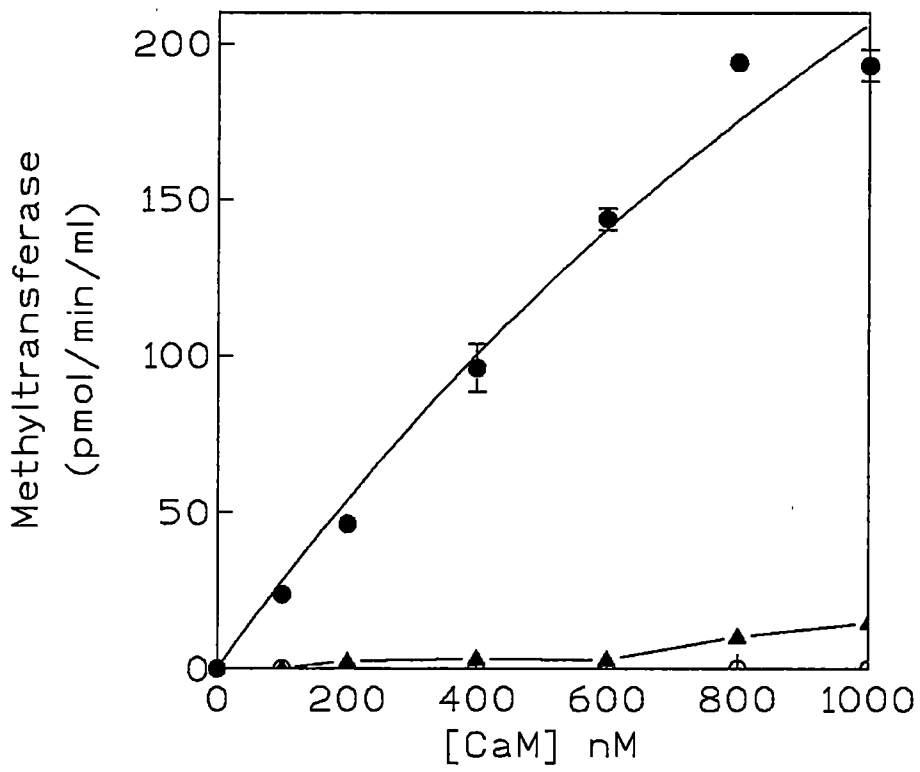

Figure 12. Methylation of E114A and L116T. Pseudo-first-order methyltransferase kinetics comparing VU-1 (●), E114A(O), and L116T (▲) at a constant concentration of S-adenosylmethionine(12 μM). Calmodulin is the varied substrate as described in the materials and methods, and the assay was carried out under standard conditions in 1 mM $CaCl_2$. Means ± S.E. are shown.

Table V. Kinetic parameters[a] of the methylation of loop mutant calmodulins in the presence of calcium.

CaM	K_m[b] (nM)	V_{max}[b] (nmol/min/mg)	k_{cat}[c] (s^{-1})	k_{cat}/K_m (s^{-1} M^{-1})
VU-1	144 (±28.3)	32.6 (±1.7)	.0205	14.2×10^4
L112T	232 (±29.8)	34.4 (±1.6)	.0217	9.35×10^4
G113S	-------	-------	-------	-------
E114A	-------	-------	-------	-------
L116T	-------	-------	-------	-------
T117A	148 (±35.2)	33.0 (±2.3)	.0208	14.1×10^4

[a] Assays were performed under standard conditions in the presence of 1 mM calcium and 0.15 M KCl.

[b] Data for the calculation of K_m and V_{max} were derived from double reciprocal plots of $1/[CaM]$ vs $1/V_{max}$ under a constant saturating concentration of [AdoMet].

[c] k_{cat} was calculated using 38 000 as the molecular weight of the enzyme.

Table VI. Kinetic parameters[a] of the methylation of loop mutant calmodulins in the presence of EDTA.

CaM	K_m[b] (nM)	V_{max}[b] (nmol/min/mg)	k_{cat}[c] (s^{-1})	k_{cat}/K_m (s^{-1} M^{-1})
VU-1	231 (±74.7)	30.0 (±3.2)	.0189	8.18 X 10^4
L112T	523 (±81.4)	14.4 (±1.6)	.0091	1.74 X 10^4
G113S	-------	-------	-------	-------
E114A	-------	-------	-------	-------
L116T	-------	-------	-------	-------
T117A	314 (±59.1)	30.1 (±2.1)	.0190	6.12 X 10^4

[a] Assays were performed under standard conditions in the presence of 1 mM EDTA and 0.15 M KCl.

[b] Data for the calculation of K_m and V_{max} were derived from double reciprocal plots of 1/[CaM] vs 1/V_{max} under a constant saturating concentration of [AdoMet].

[c] k_{cat} was calculated using 38,000 as the molecular weight of the enzyme.

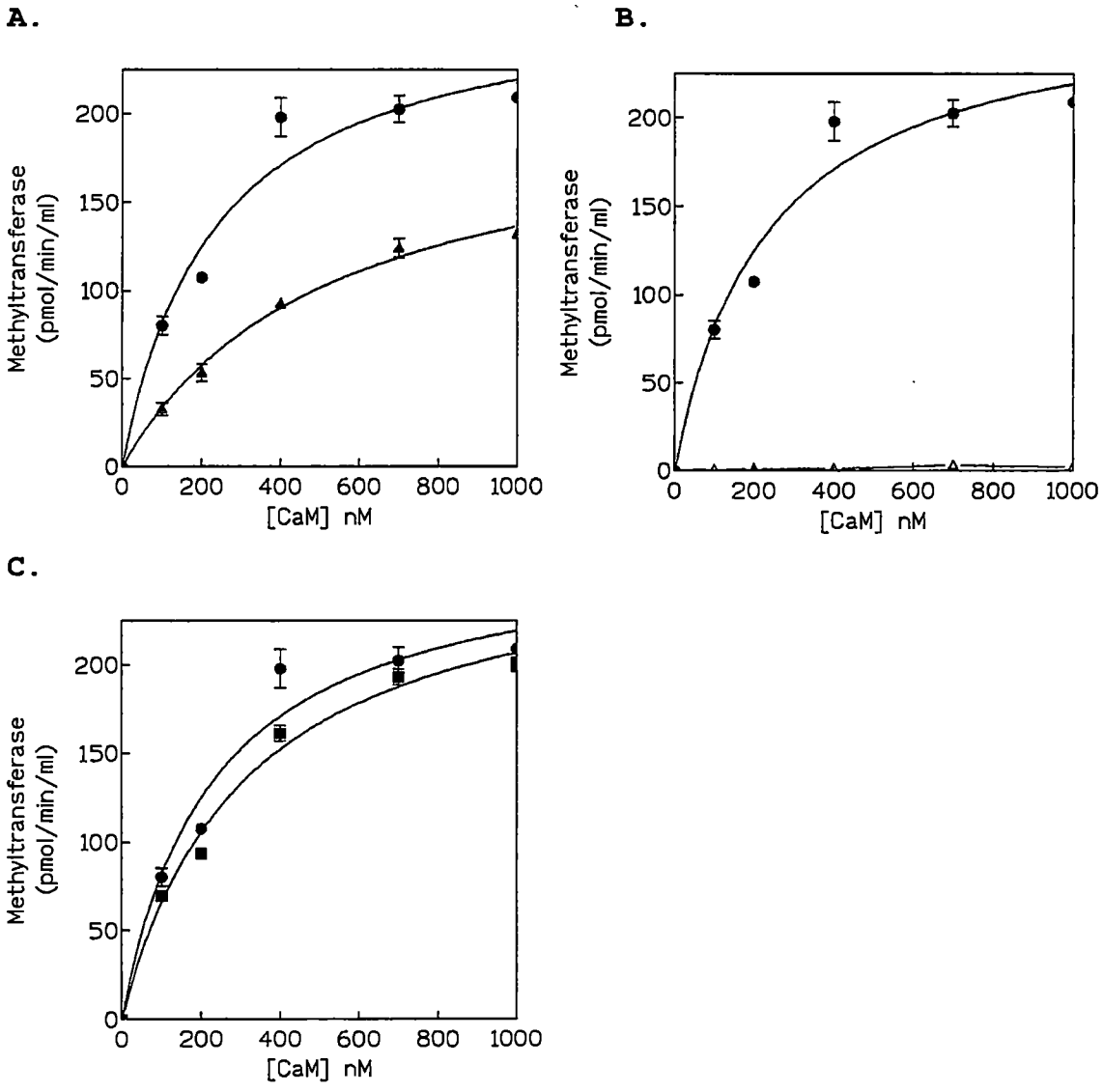

Figure 13. Methylation of L112T, G113S, and T117A in EDTA. Pseudo-first-order methyltransferase kinetics comparing VU-1 (●), L112T (▲), G113S(Δ) and T117A (■) at a constant saturating concentration of S-adenosylmethionine (12 μM). Calmodulin is the varied substrate, and the assay was performed under standard conditions in 1 mM EDTA. Means ± S.E. are shown.

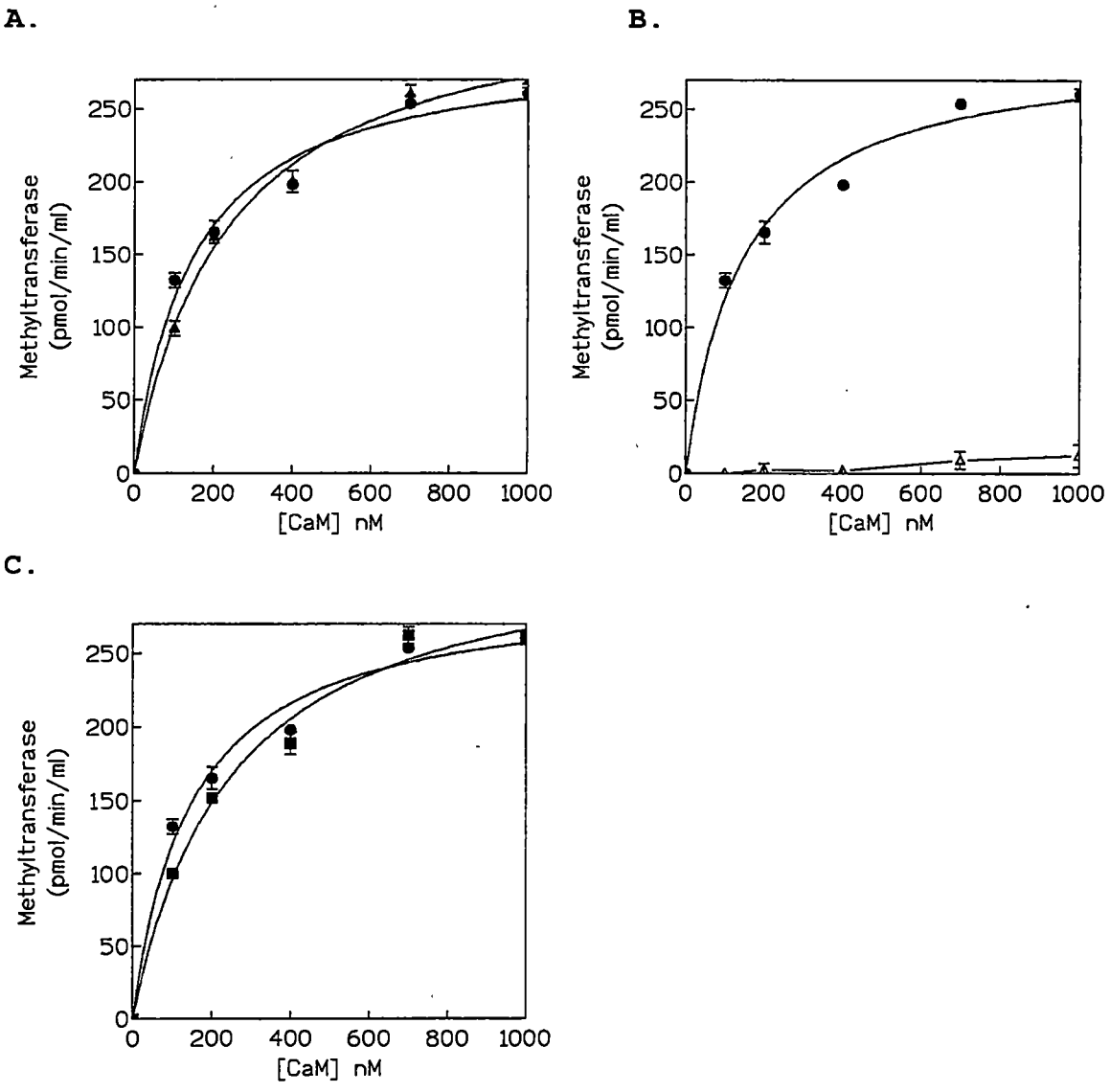

Figure 14. Methylation of L112T, G113S, and T117A in $CaCl_2$. Pseudo-first-order methyltransferase kinetics comparing VU-1 (●), L112T(▲), G113S(Δ) and T117A (■) at a constant saturating concentration of S-adenosylmethionine(12 μM). Calmodulin is the varied substrate, and the assay was carried out under standard conditions in 1 mM $CaCl_2$. Means ± S.E. are shown.

Domain exchange mutations in calmodulin and their effect on methyltransferase recognition.

The previous section showed that the conservation of certain residues in the six amino acid loop are important for methyltransferase recognition. Previous work has shown that the carboxyl terminal lobe alone is sufficient for methyltransferase recognition and methylation (Han *et al.*, 1993) and it remains unknown whether structural elements outside of the methylation loop unique to the carboxyl terminal lobe are essential for recognition. Calmodulin has internal symmetry between the amino terminal and carboxyl terminal lobes, including the presence of a six amino acid loop (LGQNPT) in the amino terminal lobe that is located at a position similar to the methylation loop in the carboxyl terminal lobe (Fig. 15). A comparison of the backbone structure of the two loop regions (residues 39-44 and 112-117) shows that they are superimposable with a root-mean-square difference of 0.33 Å (Fig. 16). Taking advantage of the symmetry and structural similarity between the two lobes, the methylation loop sequence was engineered into the loop region between EF hands I and II in the amino terminal lobe.

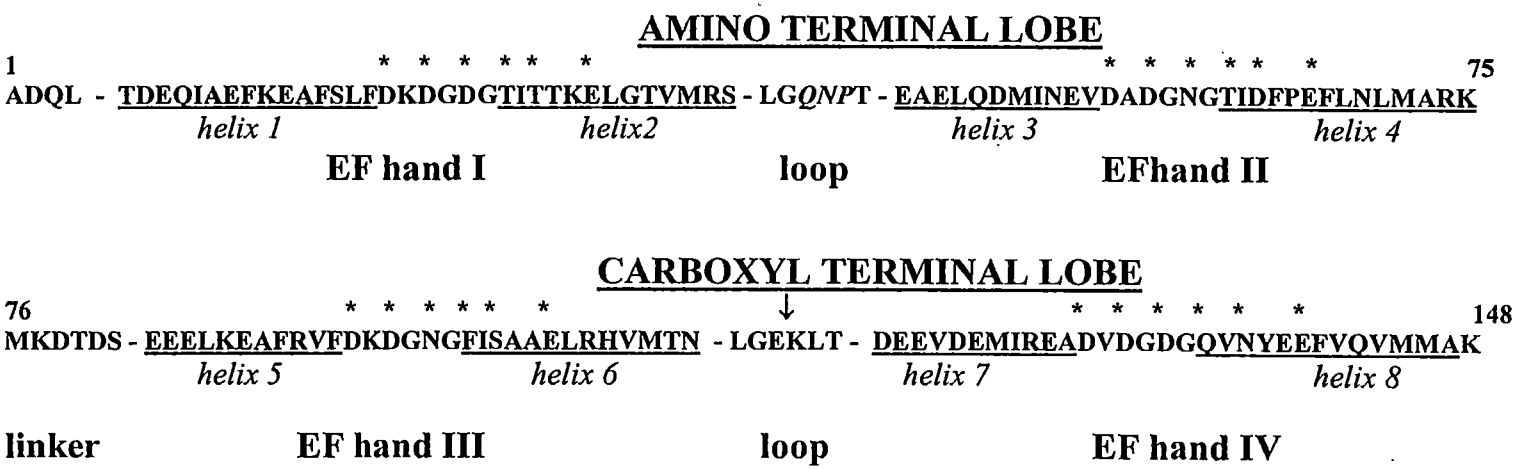

Figure 15. Sequence and domain organization of calmodulin . Sequence of VU-1 calmodulin showing the location of EF hands I-IV, the central linker region, and the two loops between the EF hands. α-Helical regions are underlined and calcium ligands based on X-ray crystallography (Babu *et al.*, 1988; Chattopadhyaya *et al.*, 1992) are indicated by an asterisk. The three amino acid region (residues 41-43) replaced by EKL in CaM^{EKL} is italicized. The site of lysine methylation is indicated by an arrow.

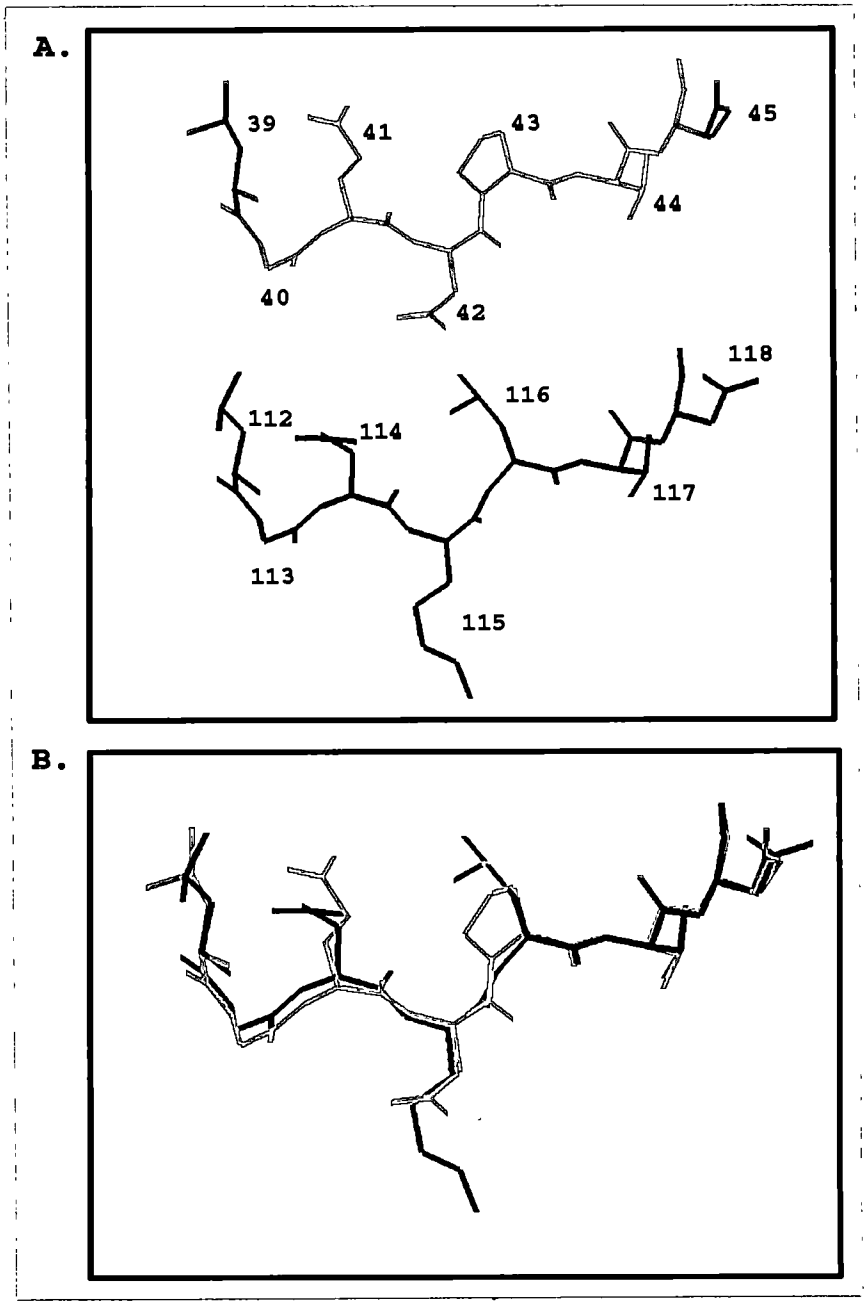

Figure 16. Comparison of the backbone structures of the loop-turn regions in the N- and C-terminal lobes. The methylation-site loop (LGEKLT, residues 112-117 shown in black) of the C-terminal lobe and its symmetrical loop region (LGQNPT, residues 39-44 shown in gray) of the N-terminal lobe are shown apart (**A**) and superimposed (**B**). The two structures superimposed with a root-means square difference of 0.33Å. The images were generated using Silicon Graphics Indigo system and Insight II software.

VU-3 calmodulin (Roberts *et al.*, 1986, Roberts et al., 1992) was used as the starting point for the generation of the mutant CaM^{EKL}. Since it has arginine instead of lysine at residue 115, it is not methylated by the calmodulin methyltransferase (Roberts *et al.*, 1986, Oh & Roberts, 1990). The sequence of the methylation loop (LGEKLT) of the carboxyl terminal was placed in the loop of the amino terminal lobe by substitution of coding region for QNP (residues 41-43) with EKL by cassette-based mutagenesis. The effects of this mutation on calmodulin function were tested. The EKL substitution showed a complex effect on calmodulin activator activity. Both VU-1 and CaM^{EKL} activated PDE to the same extent, with CaM^{EKL} showing only a slight shift in the concentration required for half-maximal activation ($K_{0.5\ (CaM)}$), (Fig. 17A, Table VII). This suggests that the three substitutions within this loop in the amino terminal lobe have little effect on PDE activator properties. In contrast, CaM^{EKL} showed essentially no activation of NADK (Fig. 17B, Table VII). Further, CaM^{EKL} was a poor methyltransferase substrate and showed no detectable methylation (Fig. 18). Thus, the substitution of the methylation loop sequence at an analogous position in the amino terminal lobe was not adequate to confer

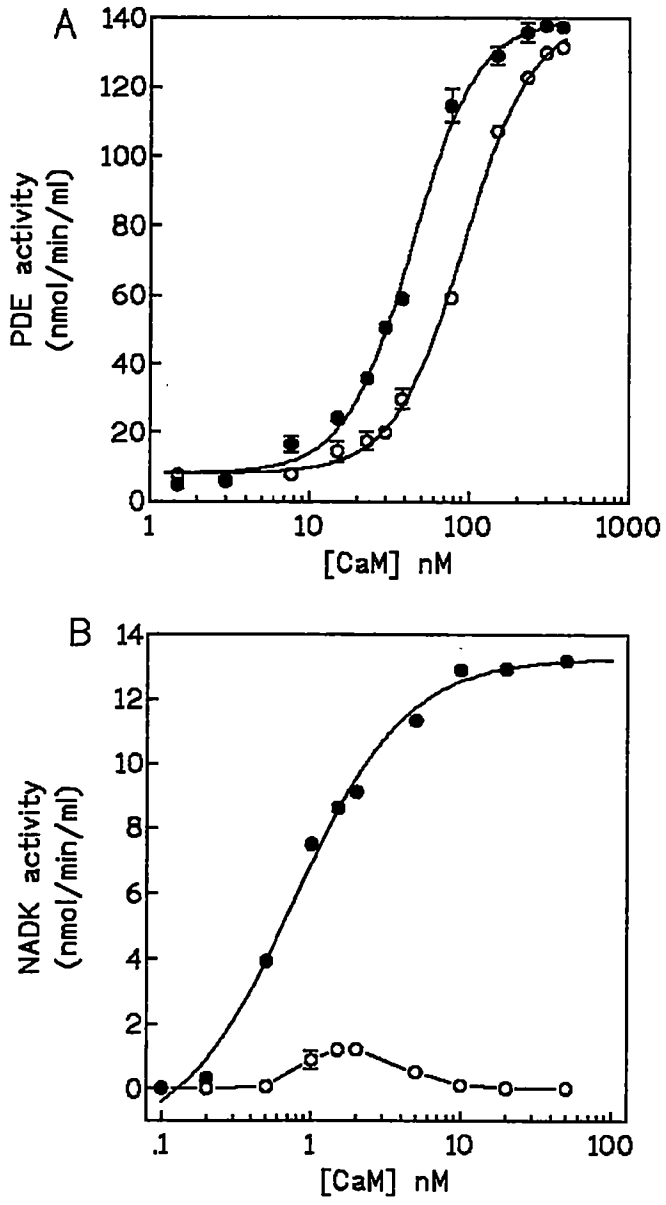

Figure 17. Enzyme activation of CaM^{EKL} Enzyme activation of VU-1 (●) or CaM^{EKL} (O) calmodulin. **A.** Activation of PDE; **B.** Activation of NAD kinase. All assays were done in 1 mM $CaCl_2$. Error bars show the S.E. and the absence of error bars indicates the error is smaller than the symbols.

Table VII. Activation parameters of calmodulin-dependent enzymes by mutant calmodulins in the loop-turn region of the amino-terminal lobe.

CaM	PDE % maximal rate[a]	$K_{0.5}^{(Cam)}$ [b]	NADK % maximal rate	$K_{0.5}^{(CaM)}$
VU-1	100	54 (±4.2)	100	1.8 (±.07)
CaM^{EKL}	100	91 (±7.8)	0	0
Q41E	97	85 (±9.0)	36	1.8 (±.06)
N42K	101	67 (±7.4)	80	0.8 (±.12)
P43L	101	66 (±8.8)	57	2.3 (±.06)

[a] % maximal rate: maximal activation of enzymes (PDE or NADK) by calmodulins standardized to VU-1 calmodulin (100%).

[b] $K_{0.5}^{(CaM)}$ Concentration of calmodulins (nM) giving half maximal activation. The S.E. value is shown in parentheses.

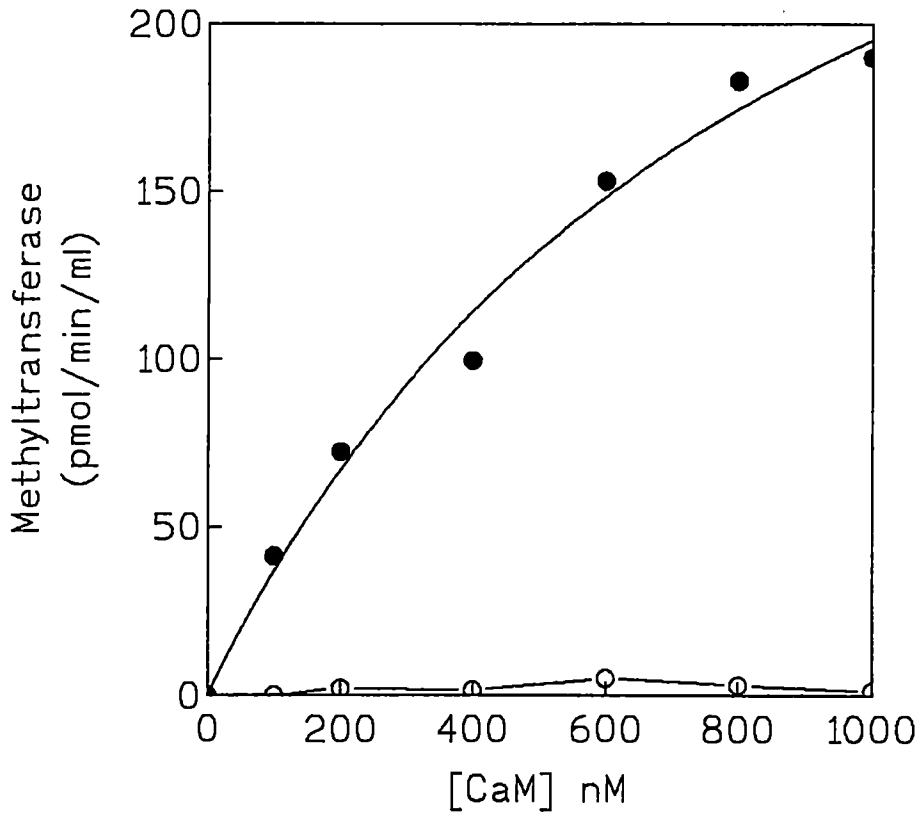

Figure 18. Methylation of CaM^{EKL} Methyltransferase kinetic comparisons of VU-1 (●) or CaM^{EKL} (O) calmodulins. Pseudo first order methyltransferase kinetics in constant saturating concentration of S-adenosylmethionine (12 μM) and calmodulin as the varied substrate. All assays were done in 1 mM $CaCl_2$. Error bars show the S.E. and the absence of error bars indicates the error is smaller than the symbols.

methyltransferase recognition, even though the two loops have a similar conformation (Fig. 16).

To investigate whether the loss of activation of NADK by CaM^{EKL} is the result of an inability of NADK to bind to the calmodulin, the ability of CaM^{EKL} to antagonize the activation of NADK by VU-1 calmodulin was tested (Fig. 19). CaM^{EKL} is indeed able to inhibit the activation of NADK by VU-1 calmodulin showing a K_i = 4 nM ± 0.25. Thus, CaM^{EKL} binds NADK, but this binding event is non-productive and does not lead to the activation of the enzyme. Since the activation of NAD kinase by wild type calmodulin has a similar affinity ($K_{0.5}$ = 2.6 nM, see Table VII), the findings suggest that the mutation does not affect the affinity of CaM^{EKL} for the enzyme.

Previous studies have shown that VU-3 (R-115) is a potent activator of NADK (Roberts *et al.*, 1986b, Roberts *et al.*, 1992). Thus, the aberrant NADK activator activity of CaM^{EKL} appears to be due to the substitution of EKL at residues 41-43 and not due to the presence of R-115. To further define which residue(s) are important for the activation of NADK, three calmodulin mutants with single amino acid substitutions (Q41E, N42K, P43L) in the loop

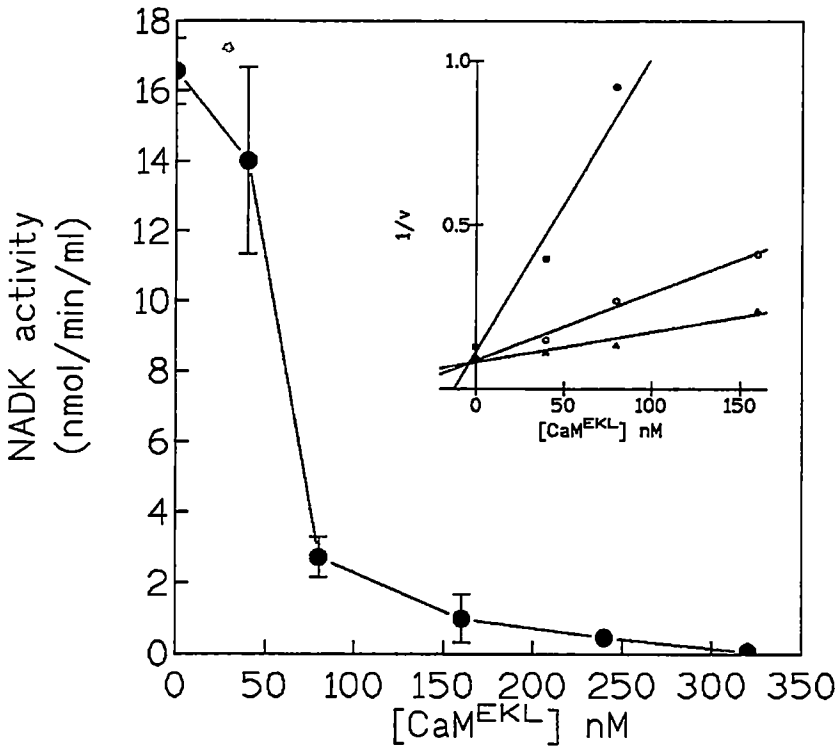

Figure 19. Interaction of CaM^{EKL} with NAD kinase A. The activation of NADK by 100 nM VU-1 CaM in the presence of increasing amounts of CaM^{EKL} is shown. The inset shows a Dixon plot of the activation of NAD kinase in the presence of fixed concentrations of VU-1: 1 nM (●), 5 nM (O), and 10 nM (▲) and increasing amounts of CaM^{EKL}. All assays were done in 1 mM $CaCl_2$. Error bars show the S.E. and the absence of error bars indicates the error is smaller than the symbols.

region were generated and analyzed (Fig. 20, Table VII). Of the three mutants, Q41E showed the largest effect, activating the enzyme to only 36% (Fig. 20, Table VII) of the level obtained by VU-1. P43L activates NAD kinase to 57% of the level of VU-1 calmodulin (Fig. 20, Table VII), and N42K showed the least effect on NADK activation (80% of wild type). The data show that the inability of the CaM^{EKL} to activate NADK is the cumulative effect of the three substitutions, and is not due to any single amino acid change.

Further evidence suggesting that the conformation of CaM^{EKL} binds to its targets similar to wild-type calmodulin comes from X-ray scattering measurements (Fig. 21). From the scattering data, the radius of gyration (R_g) was calculated for VU-1 and CaM^{EKL} in the presence of calcium, and calculated for CaM^{EKL} in the presence of calcium with a saturating amount of the MLCK-I peptide (derived from the calmodulin binding site of skeletal muscle MLCK, Blumenthal *et al.*, 1986). The R_g for Ca^{2+}-bound CaM^{EKL} (22.4 ± 0.4) and VU-1 CaM (21.3 ± 0.3) are identical within the standard error. The R_g value for CaM^{EKL} complexed to the M13 peptide

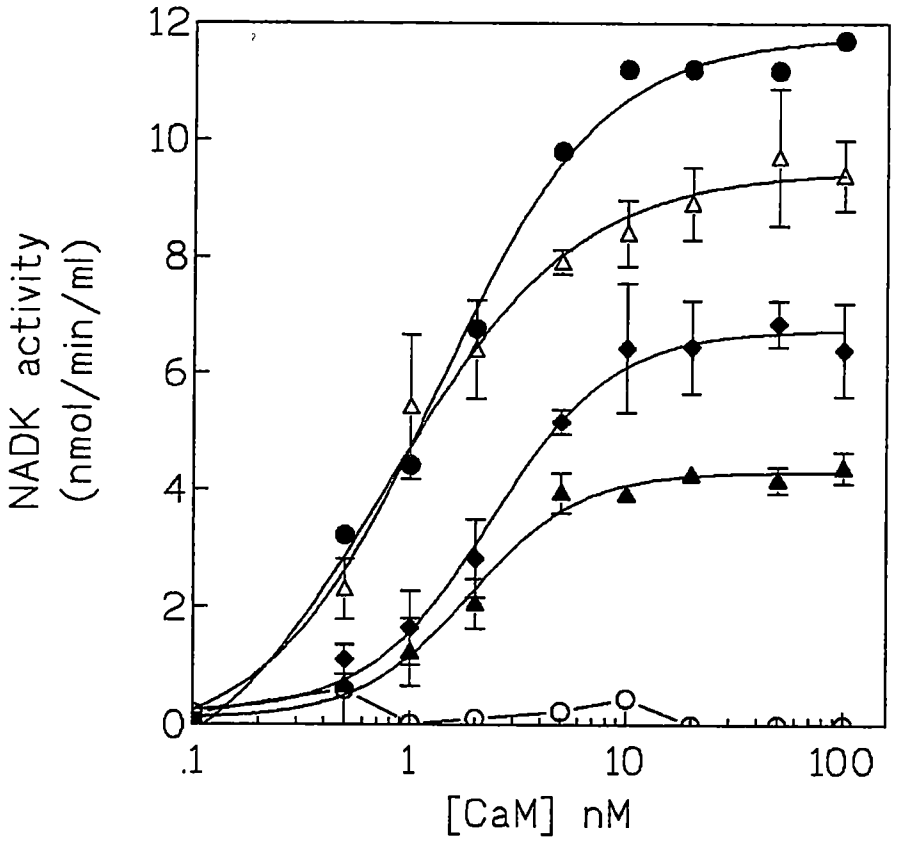

Figure 20. Interaction of Q41E, N42K, and P43L calmodulins with NAD kinase. Activation of NAD kinase by VU-1 (●), CaM^{EKL} (O), Q41E (▲), N42K (Δ), and (◆) P43L. All assays were done in 1 mM $CaCl_2$. Error bars show the S.E. and the absence of error bars indicates the error is smaller than the symbols.

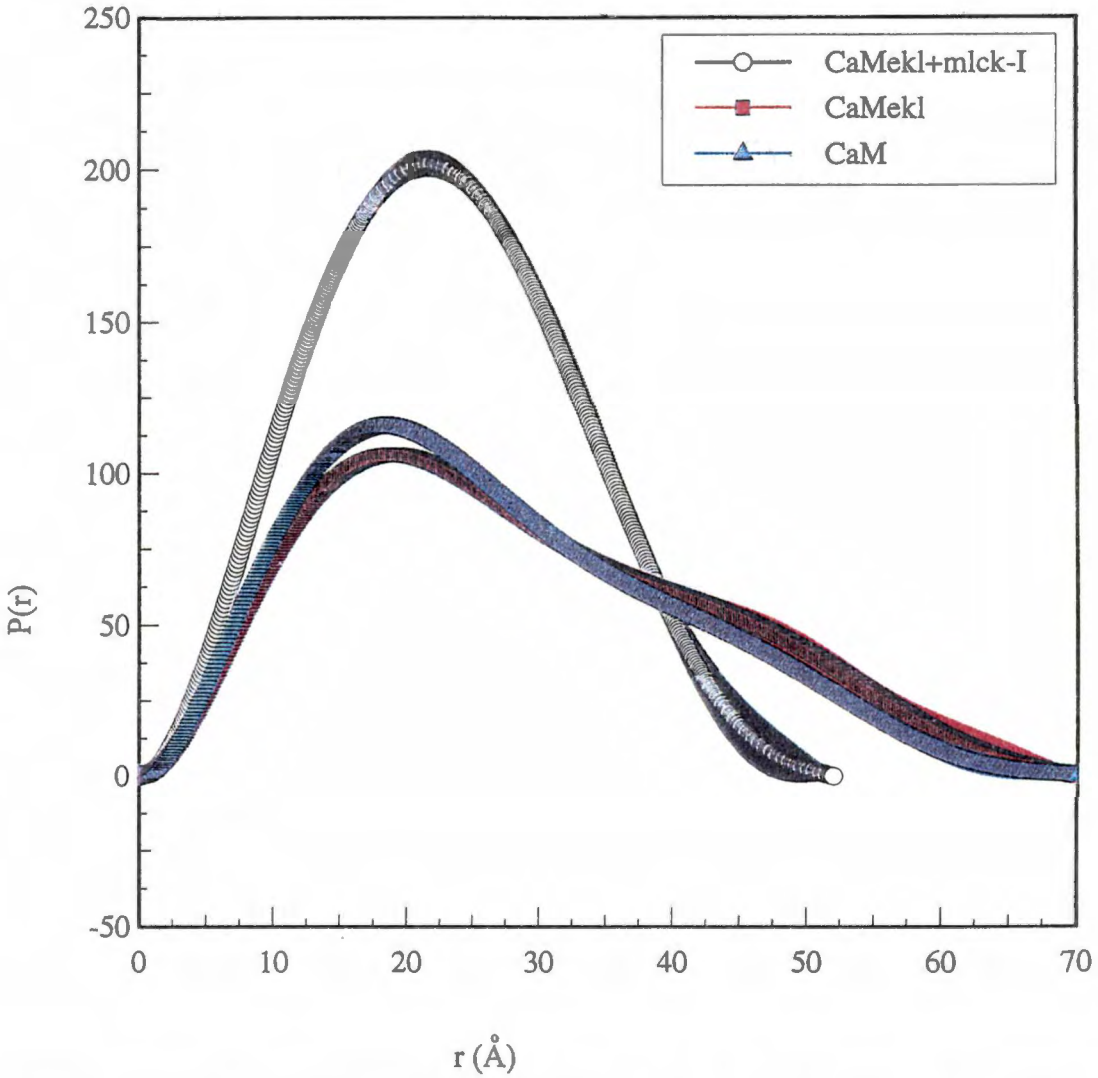

Figure 21. P(r) functions from X-ray scattering data for VU-1 CaM and CaM^{EKL}. P(r) functions for VU-1 CaM (red), CaM^{EKL}(blue) and CaM^{EKL} with peptide (clear) based on the CaM-binding sequence from skeletal muscle MLCK (MLCK-I). The length distribution, P(r), is the frequency of vectors connecting small-volume elements within the entire volume of the particle weighted according to their X-ray scattering power. X-ray data were collected on a small-angle X-ray scattering station at Los Alamos as previously described (Heidorn and Trewhella, 1987).

(17.5 ± 0.3) showed a significant change, suggesting that the structure has become more compact. Thus similar to previous measurements with wild type calmodulin and calmodulin-binding peptides (Krueger *et al.*, 1997), CaM^{EKL} showed a similar conformational change upon binding to a target peptide. Overall, the data from NAD kinase activation, inhibition and X-ray scattering strongly suggest that the affinity and conformation of CaM^{EKL} with targets is not altered compared to VU-1 calmodulin. However, a secondary interaction that is necessary for the activation of some target enzymes, such as NAD kinase appears to be lost.

Production and analysis of EF hand exchange mutants CaM^{1214} and CaM^{1232}.

The results of studies with mutations in the methylation loop and with CaM^{EKL} indicate that the sequence of the loop (residues 112-117) is important, but not sufficient for methylation. By taking advantage of the internal symmetry of calmodulin, a strategy involving the exchange of EF hands in the carboxyl-terminal lobe with the homologous EF-hands in the amino-terminal lobe was done to identify areas in addition to the loop region that may be required for methyltransferase recognition. CaM^{1214} and CaM^{1232} were constructed by generating a cassette containing

EF hand I or EF hand II by PCR, and replacing the coding regions for EF hands III or IV in VU-1 calmodulin (Fig. 22).

Based on previous structural work (Babu *et al.*, 1988; Chattopadhyaya *et al.*, 1992; Kuboniwa *et al.*, 1995; Zhang *et al.*, 1995) EF hands I and II are remarkably similar in backbone structure and amino acid sequence to EF hands III and IV respectively. However, the possibility exists that the complete substitution of whole EF hand structures within calmodulin could effect the folding and activity of the protein. To test this, the activation and calcium binding properties (as a function of calcium dependent activation) of CaM^{1214} and CaM^{1232} were examined. CaM^{1214} activated PDE to the same extent as VU-1 calmodulin (Fig. 23A, Table VIII), however the $K_{0.5(CaM)}$ for the activation is two-fold higher (Table VIII). CaM^{1232} activated PDE to only 52% (±2) of the level of VU-1 calmodulin. CaM^{1214} and CaM^{1232} also show a lower NADK activation, activating the enzyme to 66%(±4) and 79% (± 2) of the level obtained with VU-1 calmodulin (Fig. 23B, Table VIII).

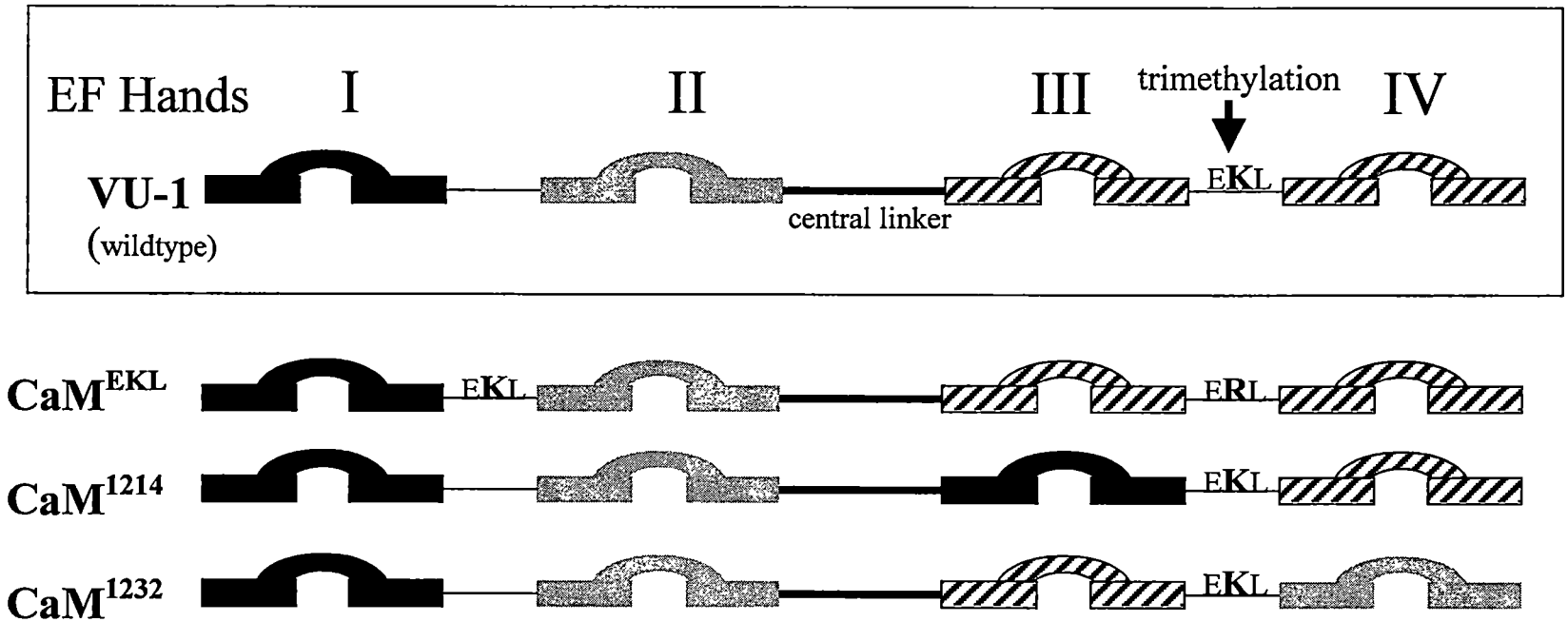

Figure 22. Domain organization of calmodulin and calmodulin mutants. Organization of the domain exchange calmodulin mutants are shown. **CaM^{EKL}** has an arginine at position 115 and and has the replacement of QNP 41-43 found in a loop between EF hand I (black) and EF hand II (gray) with the homologous methylation loop sequence EKL 114-116. **CaM^{1214}** contains the sequence of EF hand I (residues 13-39) replacing the sequence of EF hand III (residues 86-112). **CaM^{1232}** contains the sequence of EF hand II (residues 45-75) replacing the sequence of EF hand IV (residues 118-148).

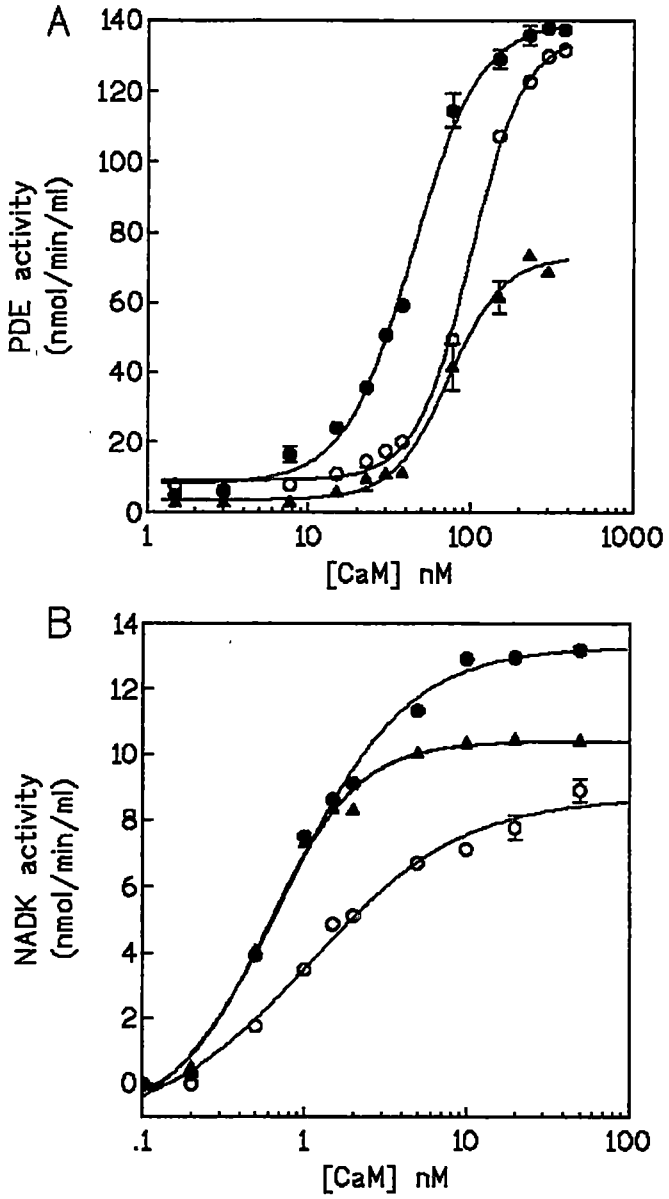

Figure 23. Enzyme activation of CaM^{1214} and CaM^{1232} The enzyme activator properties of VU-1 (●), CaM^{1214} (O), and CaM^{1232} (▲) are shown. Activation of **A.** PDE or **B.** NAD kinase in 1 mM $CaCl_2$ with varied calmodulin concentration. Error bars show the S.E. and the absence of error bars indicates the error is smaller than the symbols.

Table VIII. Activation parameters of calmodulin-dependent enzymes by EF hand domain exchange mutant calmodulins.

CaM	PDE % maximal rate[a]	$K_{0.5}^{(CaM)}$ [b]	NADK % maximal rate	$K_{0.5}^{(CaM)}$	$K_{0.5}^{(Ca2+)}$ [c]
VU-1	100	54 (±4.2)	100	1.8 (±.07)	96
CaM^{1214}	98	98 (±6.9)	66	1.1 (±.10)	120
CaM^{1232}	52	72 (±10.1)	79	0.7 (±.05)	148

[a] % maximal rate: maximal activation of enzymes (PDE or NADK) by calmodulins standardized to VU-1 calmodulin (100%).

[b] $K_{0.5}^{(CaM)}$ Concentration of calmodulins (nM) giving half maximal activation. The S.E. value is shown in parentheses.

[c] $K_{0.5}^{(Ca2+)}$ Concentration of calcium (nM) giving half maximal activation of enzyme NADK in the presence of a constant amount of calmodulin (0.1 μM).

The results show that the substitution of entire EF hands does slightly affect the level of activation. However, enzyme activation requires two functional, folded lobes of calmodulin (Ikura *et al*, 1992; Meador *et al.*, 1992), and the activation data strongly suggest that the replacement of EF hands III and IV with their homologous EF hands from the amino terminal lobe does not result in a drastic change in calmodulin structure/function. This is also supported by the calcium-dependence data (Fig. 24). NAD kinase activation by VU-1, CaM^{1232}, and CaM^{1214} showed a similar dependence on free calcium, with $K_{0.5\ (Ca^{2+})}$ values between 90-150 nM (Fig. 24, Table VIII). Calcium-binding to calmodulin involves positive cooperativity between EF hand pairs (reviewed in Klee *et al.*, 1988). From the fits of the data in Fig. 24, similar Hill co-efficients [n_{VU-1}= 3.6(± .7); n_{1214}=3.8 (± 1.3); n_{1232} =2.7 (± .5)] were determined. Thus, the substituted EF hands apparently fold and pack properly with the adjacent EF hand (III or IV) in the carboxyl-terminal lobe since calcium-binding properties remain relatively unchanged.

In contrast to the modest effects on calcium binding and enzyme activation, neither CaM^{1232} nor CaM^{1214} serve as a substrate for methylation by the calmodulin.

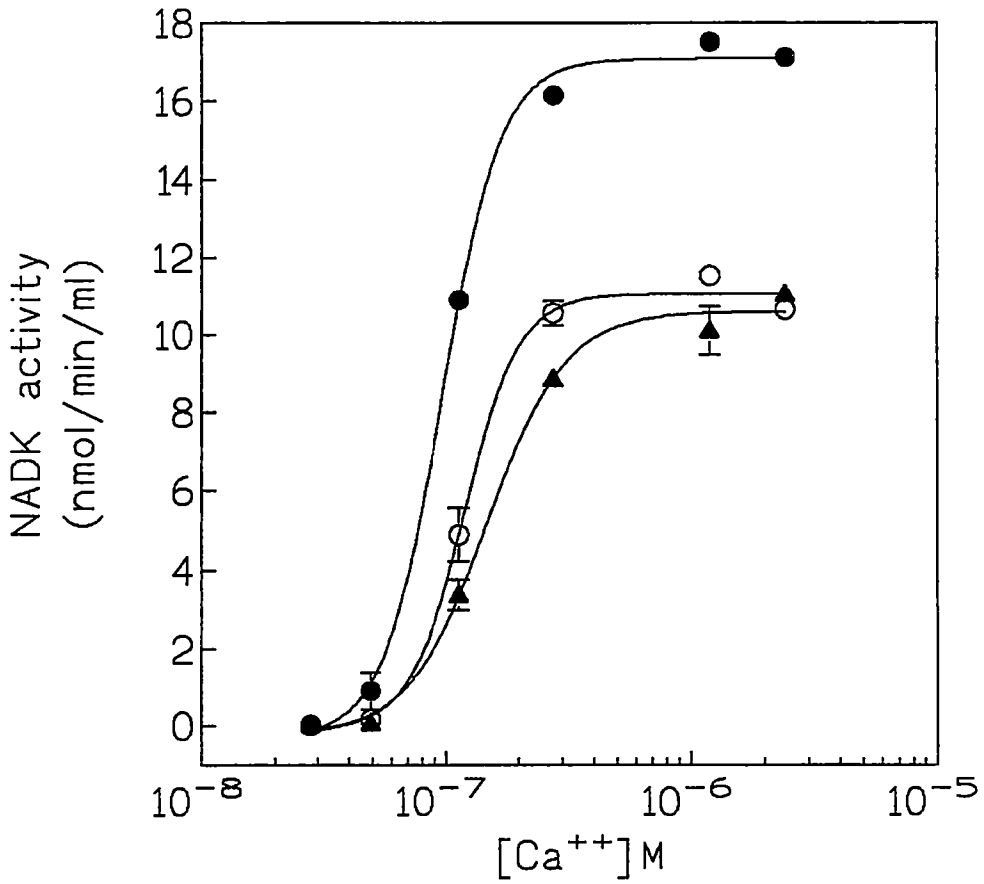

Figure 24. Calcium-dependent activation of NAD kinase by CaM^{1214} and CaM^{1232} The enzyme activator properties of VU-1 (●), CaM^{1214} (O), and CaM^{1232} (▲) are shown. Activation of NADK by 50 nM of each calmodulin with varied concentrations of free calcium by using the EGTA/Ca^{+2} buffering system described in the Materials and Methods. Error bars show the S.E. and the absence of error bars indicates the error is smaller than the symbols.

methyltransferase (Fig. 25). Together with the data for CaM^{EKL}, these findings indicate that amino acid residues unique to both EF hands III and IV are required for recognition by the calmodulin methyltransferase.

Production and analysis of sub-domain exchange mutations of calmodulin

Results from experiments with CaM^{1214} and CaM^{1232} showed that structural elements unique to both EF hands III and IV (and not found in homologous EF hands I and II) are required for methyltransferase recognition. EF hands are formed from a helix-loop-helix motif (Fig. 1). In an effort to identify the critical regions within EF hands III and IV necessary for methyltransferase recognition subdomain mutants were generated that contain substitutions of the helices or calcium binding loops of EF hands III and IV with the sequence from the homologous regions of EF hands I and II. Fig. 26 shows an alignment of the symmetry-related EF hands and the range of residues that were replaced in the subdomain mutants. A cassette-based mutagenesis approach that relies on internal restriction sites in the VU-1 gene (Roberts *et al.*, 1987) was used. Thus, the range of residues sometimes overlapped with other structural elements (e.g., CaM^{H8} has replacements in both

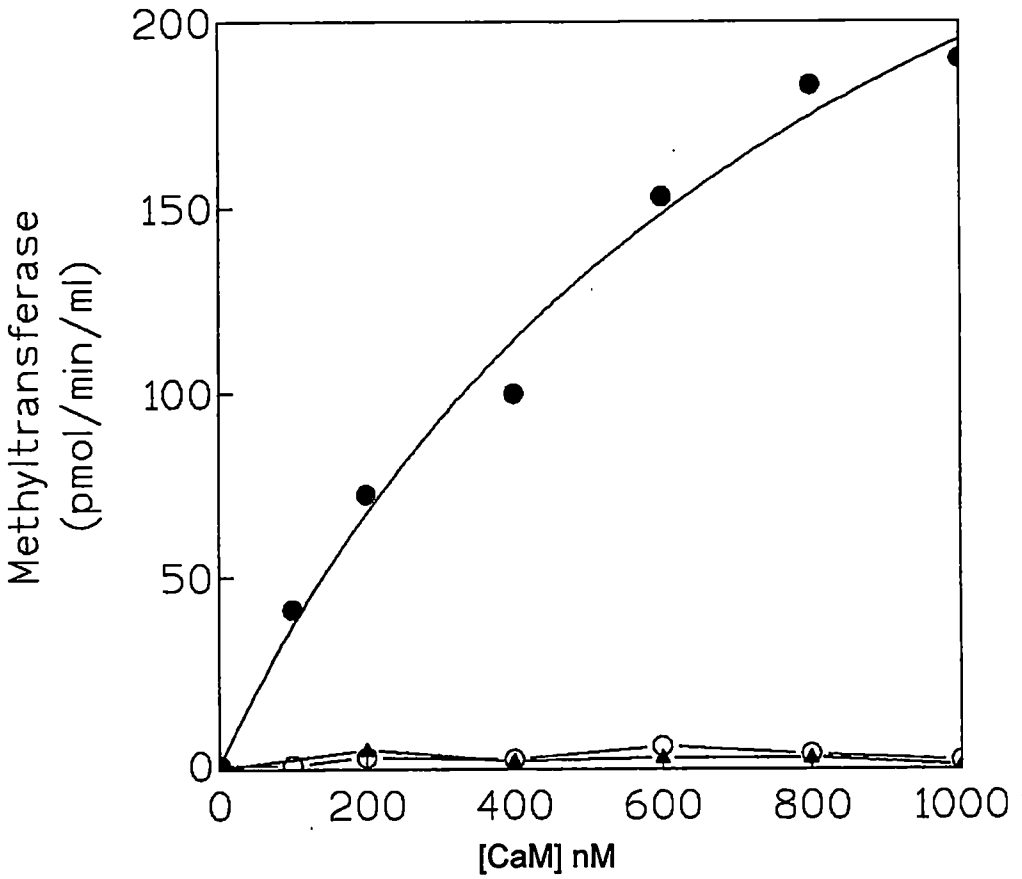

Figure 25. Methylation of CaM^{1214} and CaM^{1232}
Methyltransferase kinetic comparisons of VU-1 (●), CaM^{1214} (O), and CaM^{1232} (▲) are shown. Pseudo first order methyltransferase kinetics in constant saturating concentration of S-adenosylmethionine (12 μM) and calmodulin as the varied substrate in 1 mM $CaCl_2$. Error bars show the S.E. and the absence of error bars indicates the error is smaller than the symbols.

A.

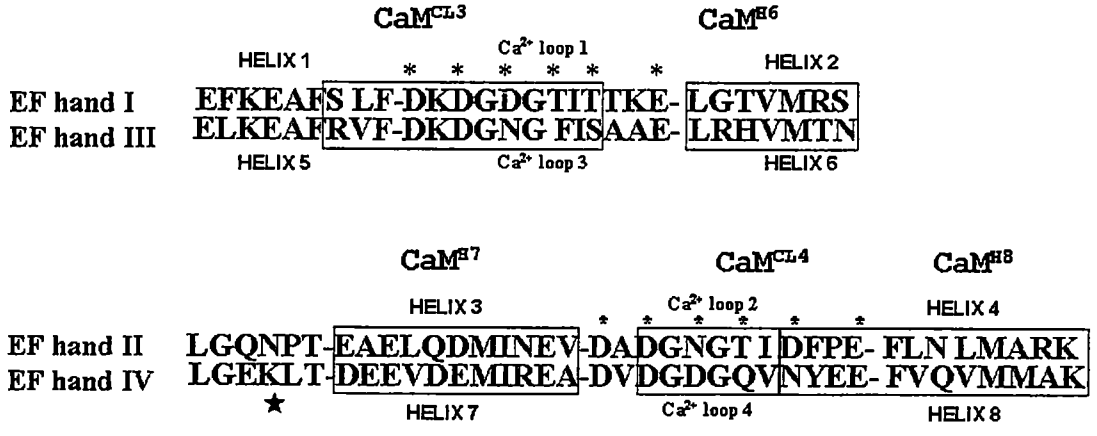

B.

Mutant	Residues replaced in N-terminus	Wild-type sequence	Residues substituted from C-terminus	Mutant sequence
CaM^{CL3}	90-101	RVF-DKDGNGFIS	17-28	SLF-DKDGDGTIT
CaM^{H6}	105-111	LRHVMTN	32-38	LGTVMRS
CaM^{H7}	118-128	DEEVDEMIREA	45-55	EAELQDMINEV
CaM^{CL4}	131-136	DGDGQV	58-63	DGNGTI
CaM^{H8}	137-148	NYEE-FVQVMMAK	64-75	DFPE-FLNLMARK

Figure 26. Organization of subdomain calmodulin mutants. A. Alignment of the amino acid sequence in the carboxyl-terminal lobe (EF hands III and IV) with the homologous sequence in the amino-terminal lobe (EF hands I and II) is shown. The boxed areas represent sequence in the carboxyl-terminal lobe that were replaced with the symmetry related sequence from the amino-terminal lobe for the generation of subdomain mutants: CaM^{CL3}, CaM^{H6}, CaM^{H7}, CaM^{CL4}, CaM^{H8}. **B.** The position and sequence of the residues replaced in wild type (VU-1), and the resulting sequence in the subdomain mutant calmodulins.

helix 8 as well as part of calcium binding loop 4). However, for the sake of simplicity, the mutants were named for the subdomain structural element that was most affected by the substitution (Fig. 26).

The enzyme activator properties of the subdomain mutants are summarized in Table IX. All subdomain mutants activated PDE similar to VU-1 (wildtype) calmodulin with mutants CaM^{H7} (89.6% ± 3) and CaM^{CA4} (81.3% ± 3) in EF hand IV showing a slight reduction in maximal activation (Table IX). Further, all subdomain mutants activated NADK similar to VU-1 calmodulin with the exception of CaM^{H6} which showed a reduction in maximal activation (66.3% ± 2) (Table IX). Interestingly, a similar decrease (66.0% ± 4) was observed with CaM^{1214}, a mutant calmodulin that has EF hand III (helix 5 - Ca^{2+} binding loop 3 - helix 6) replaced with EF hand I (helix 1 - Ca^{2+} binding loop 1 - helix 2). This suggests the decrease in maximal NAD kinase activation observed with CaM^{1214} is a result of the sequence substitution in helix 6.

Methyltransferase kinetics of subdomain mutant calmodulins

All subdomain mutants have been evaluated as substrates for the methyltransferase. During the analysis of the mutants it became clear that they showed different kinetic parameters depending on whether calcium was present or not. Therefore,

Table IX. Activation parameters of calmodulin-dependent enzymes by subdomain mutant calmodulins

CaM	PDE % maximal rate[a]	$K_{0.5}^{(CaM)}$ [b]	NADK % maximal rate	$K_{0.5}^{(CaM)}$
VU-1	100	58 (± 1.2)	100	2.6 (± .15)
CaM^{CL3}	106	70 (± 2.8)	103	1.9 (± .31)
CaM^{H6}	97.3	50 (± 2.2)	66.3	1.2 (± .40)
CaM^{H7}	89.6	68 (± 1.4)	95.0	1.5 (± .67)
CaM^{CL4}	81.3	59 (± 1.5)	97.2	2.3 (± .34)
CaM^{H8}	99.0	59 (± 1.6)	94.5	2.8 (± .23)

[a] % maximal rate: maximal activation of enzymes (PDE or NAD kinase) by calmodulins standardized to VU-1 calmodulin (100%).

[b] $K_{0.5}^{(CaM)}$ Concentration of calmodulins (nM) giving half maximal activation. The S.E. value is shown in parentheses.

the kinetics for each calmodulin mutant were determined separately both in the absence of calcium (i.e., presence of EDTA as a calcium chelator), and under saturating calcium conditions.

Methylation kinetics of apo-CaM

The two subdomain mutant calmodulins, CaM^{H6} and CaM^{H7}, with changes adjacent to the methylation loop, showed the most substantial affects on the rate of calmodulin methylation (Figs. 27 & 28). CaM^{H7} did not serve as a substrate for the methyltransferase at any concentration tested (Fig. 28, Table X). CaM^{H6} was a poor substrate for the methyltransferase, with the enzyme showing a k_{cat}/K_m ratio (0.238×10^4 s^{-1} M^{-1}) that is 20-fold lower than that observed with VU-1 (4.89×10^4 s^{-1} M^{-1}) (Fig. 27, Table X).

The other subdomain mutants exhibited a smaller effect on methyltransferase recognition (Table X). The CaM^{CL4} mutant showed a reduced V_{max} (17.0 nmol/min/mg) (Fig. 29, Table X) compared to VU-1 calmodulin (27.3 nmol/min/mg). Similarly, CaM^{H8} showed a reduction in V_{max} (19.7 nmol/min/mg) and a 3-fold increase in K_m (1350 nM ± 14.1)(Fig. 30, Table X). Thus, all three subdomain elements in EF hand IV affect methyltransferase recognition of apo-CaM, with the helix 7 to

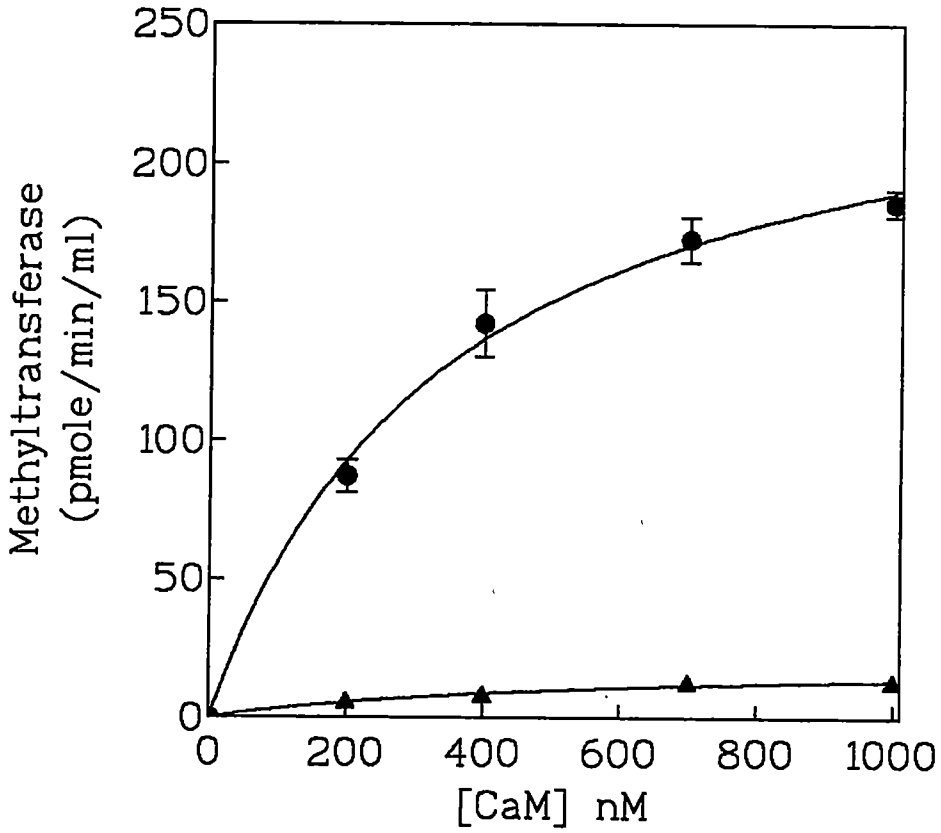

Figure 27. Methylation of apo-CaM^{H6} Methyltransferase kinetic comparisons of VU-1 (●) and CaM^{H6} (▲) are shown. Pseudo first order methyltransferase kinetics in constant saturating concentration of S-adenosylmethionine (12 μM) and calmodulin as the varied substrate in 1 mM EDTA. Error bars show the S.E. and the absence of error bars indicates the error is smaller than the symbols.

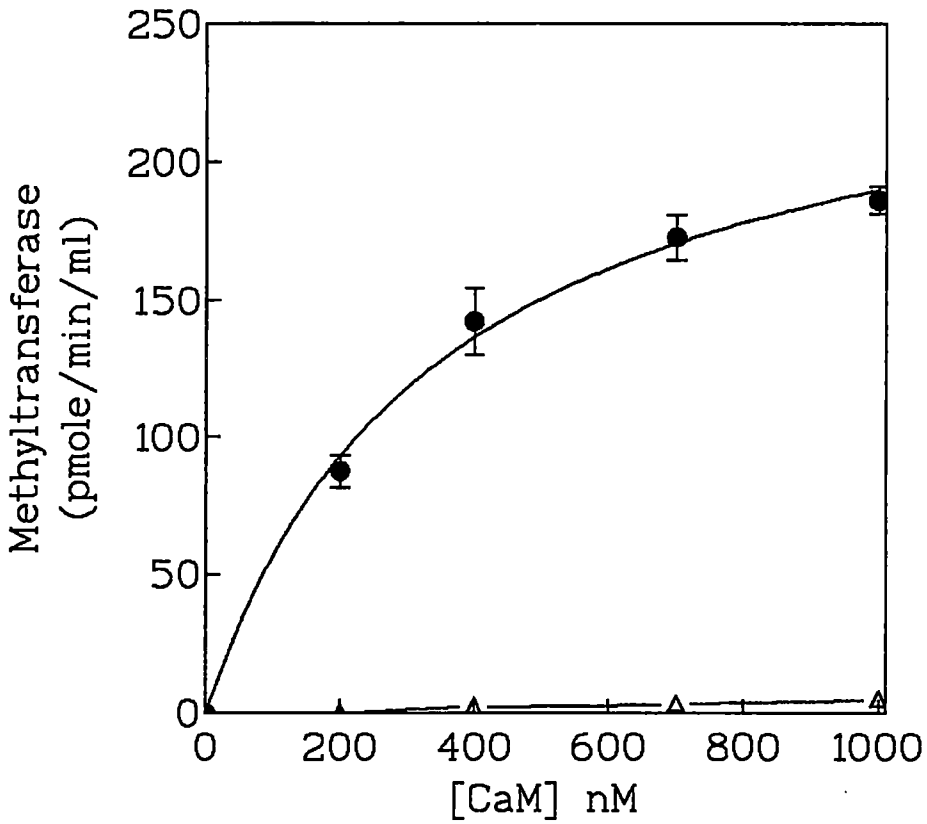

Figure 28. Methylation of apo-CaM^{H7} Methyltransferase kinetic comparisons of VU-1 (●) and CaM^{H7} (Δ) are shown. Pseudo first order methyltransferase kinetics in constant saturating concentration of S-adenosylmethionine (12 μM) and calmodulin as the varied substrate in 1 mM EDTA. Error bars show the S.E. and the absence of error bars indicates the error is smaller than the symbols.

Table X. Kinetic parameters[a] of the methylation of subdomain mutant calmodulins in the presence of EDTA.

CaM	K_m[b] (nM)	V_{max}[b] (nmol/min/mg)	k_{cat}[c] (s^{-1})	k_{cat}/K_m ($s^{-1} M^{-1}$)
VU-1	352 (±13.4)	27.3 (±1.4)	.0172	4.89×10^4
CaM^{CL3}	652 (±43.1)	33.3 (±2.2)	.0209	3.25×10^4
CaM^{H6}	505 (±9.34)	2.01 (±0.39)	.0012	0.238×10^4
CaM^{H7}	-------	0	0	0
CaM^{CL4}	117 (±4.13)	17.0 (±3.1)	.0107	9.14×10^4
CaM^{H8}	1350 (±14.1)	19.7 (±1.3)	.0124	0.918×10^4

[a] Assays were performed under standard conditions in the presence of 1 mM EDTA and 0.15 M KCl.

[b] Data for the calculation of K_m and V_{max} were derived from double reciprocal plots of $1/[CaM]$ vs $1/V_{max}$ under a constant saturating concentration of [AdoMet].

[c] k_{cat} was calculated using 38,000 as the molecular weight of the enzyme.

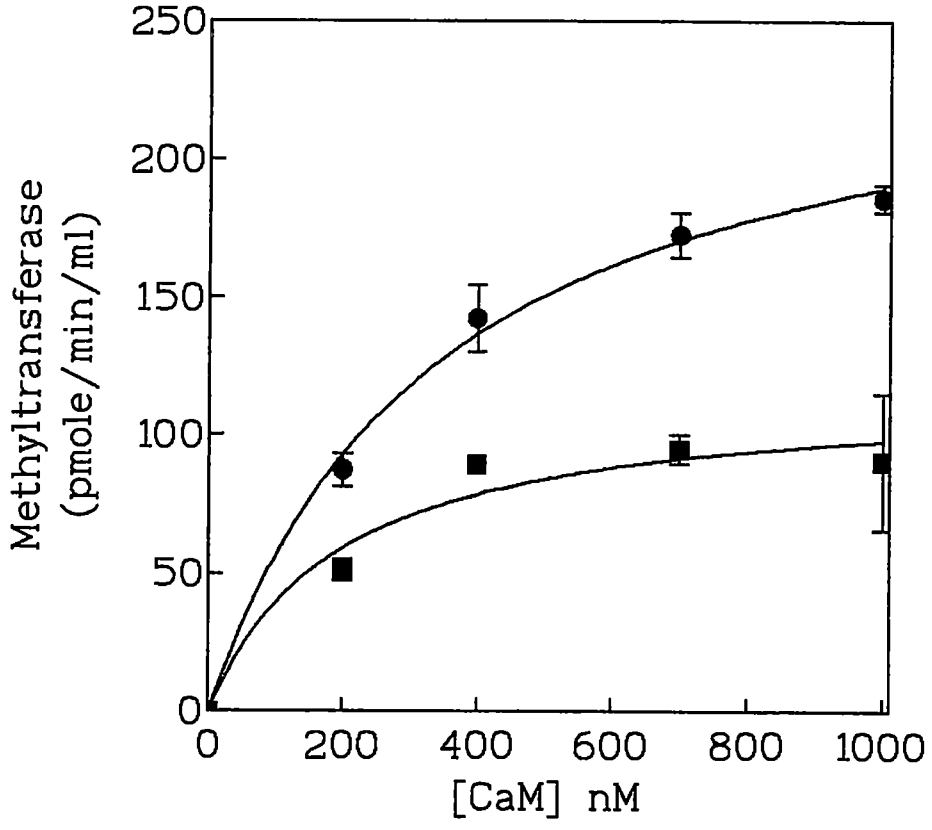

Figure 29. Methylation of apo-CaM^{CL4} Methyltransferase kinetic comparisons of VU-1 (●) and CaM^{CL4} (■) are shown. Pseudo first order methyltransferase kinetics in constant saturating concentration of S-adenosylmethionine (12 μM) and calmodulin as the varied substrate in 1 mM EDTA. Error bars show the S.E. and the absence of error bars indicates the error is smaller than the symbols.

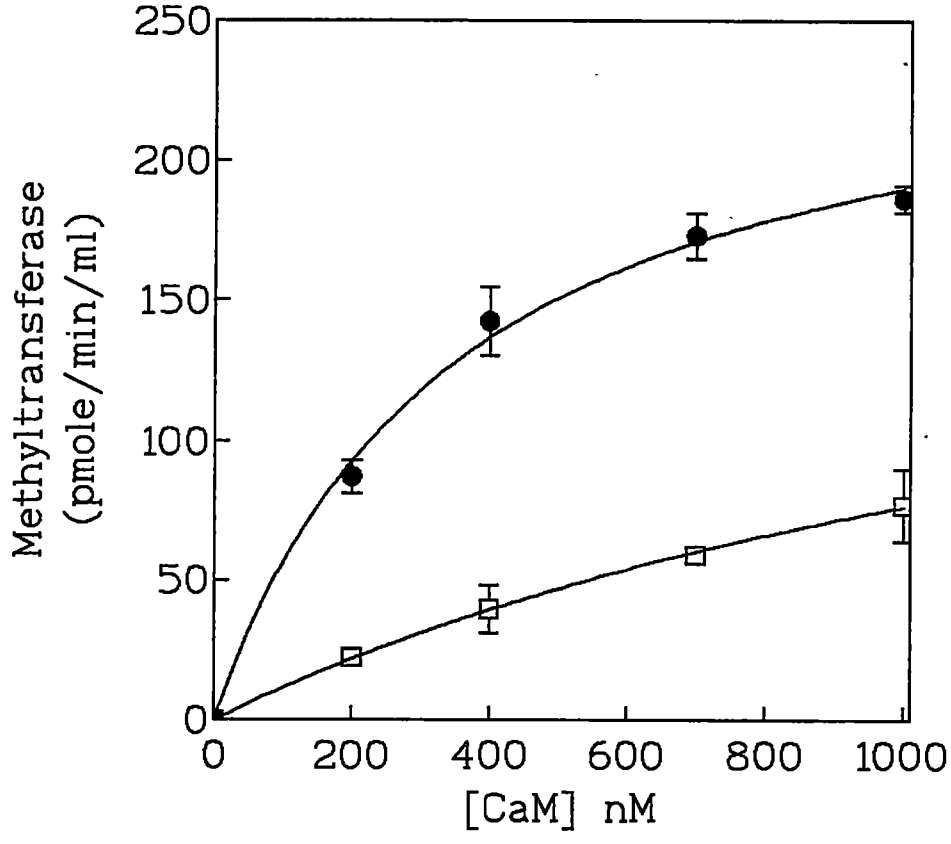

Figure 30. Methylation of apo-CaM^{H8} Methyltransferase kinetic comparisons of VU-1 (●) and CaM^{H8} (□) are shown. Pseudo first order methyltransferase kinetics in constant saturating concentration of S-adenosylmethionine (12 μM) and calmodulin as the varied substrate in 1 mM EDTA Error bars show the S.E. and the absence of error bars indicates the error is smaller than the symbols.

3 mutant CaM^{H7} (i.e., the α-helix adjacent to the methylation loop) showing the largest effect.

In contrast, the substitution of calcium-binding loop 3 showed the least affect on methyltransferase kinetics (Fig. 31, Table X), with CaM^{CL3} showing about a 2-fold increase in K_m (652 ± 43), but a k_{cat} value (.0209 s^{-1}) very similar to wildtype VU-1 CaM (.0172 s^{-1}) (Fig. 31, Table X). Thus, the inability of apo-CaM^{1214} to serve as a substrate for methylation stems from the substitution of helix 6 with helix 2 from EF hand I.

Methylation kinetics of Ca^{2+}-CaM

In the presence of calcium, all subdomain mutants with the exception of CaM^{H6} exhibit kinetic parameters similar to VU-1 CaM (Table XI). When CaM^{H6} is used as a substrate a decrease in V_{max} (7.25 nmol/min/mg) and a shift in K_m (475 nM ± 10) were observed compared to VU-1 (V_{max} = 28.9 nmol/min/mg, K_m=151 nM ± 15) (Fig. 32, Table XI). The methyltransferase still showed a large (13-fold) reduction in catalytic efficiency with CaM^{H6} (k_{cat}/K_m = .970 X 10^4 s^{-1} M^{-1}) compared to VU-1 (k_{cat}/K_m = 12.1 X 10^4 s^{-1} M^{-1}) (Table XI). However, in the presence of calcium, the other subdomain mutants show almost a normal interaction with the methyltransferase (Fig. 33, Table XI).

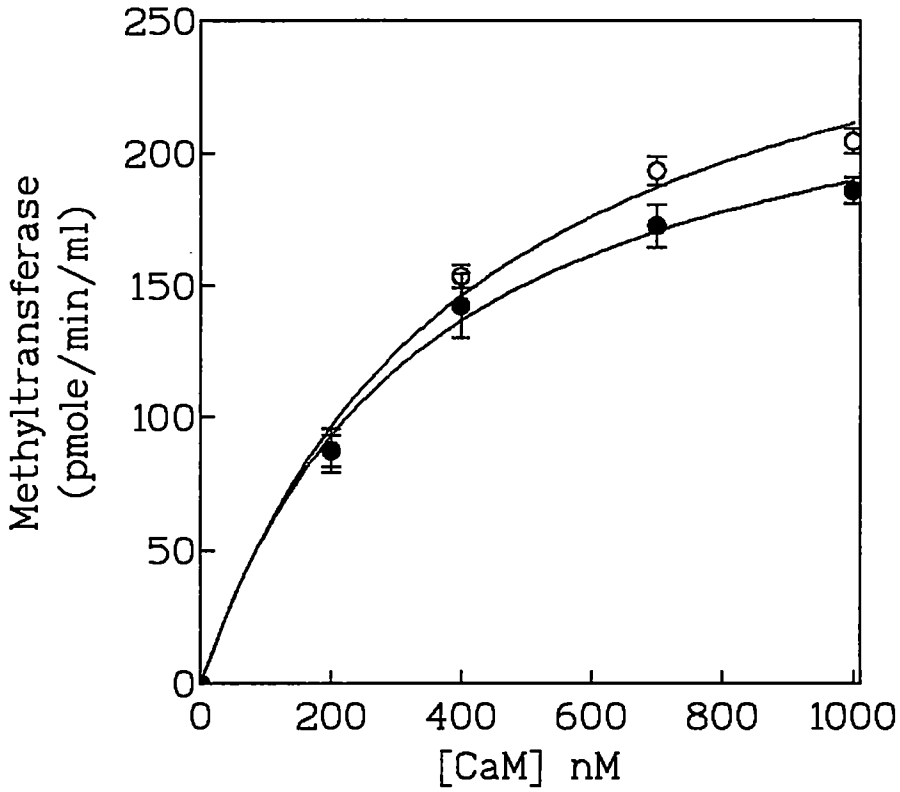

Figure 31. Methylation of apo-CaM^{CL3} Methyltransferase kinetic comparisons of VU-1 (●) and CaM^{CL3} (O) are shown. Pseudo first order methyltransferase kinetics in constant saturating concentration of S-adenosylmethionine (12 μM) and calmodulin as the varied substrate in 1 mM EDTA. Error bars show the S.E. and the absence of error bars indicates the error is smaller than the symbols.

Table XI. Kinetic parameters[a] of the methylation of subdomain mutant calmodulins in the presence of calcium

CaM	K_m[b] (nM)	V_{max}[b] (nmol/min/mg)	k_{cat}[c] (s^{-1})	k_{cat}/K_m (s^{-1} M^{-1})
VU-1	151 (±15.1)	28.9 (±0.89)	.0182	12.1 X 10^4
CaM^{CL3}	154 (±20.4)	29.2 (±1.1)	.0184	11.9 X 10^4
CaM^{H6}	475 (±9.73)	7.25 (±1.0)	.0046	.970 X 10^4
CaM^{H7}	262 (±70.4)	31.7 (±2.7)	.0200	7.63 X 10^4
CaM^{CL4}	153 (±13.4)	27.7 (±0.77)	.0175	11.4 X 10^4
CaM^{H8}	200 (±20.9)	28.7 (±1.7)	.0181	9.05 X 10^4

[a] Assays were performed under standard conditions in the presence of 1 mM calcium and 0.15 M KCl.

[b] Data for the calculation of K_m and V_{max} were derived from double reciprocal plots of $1/[CaM]$ vs $1/V_{max}$ under a constant saturating concentration of [AdoMet].

[c] k_{cat} was calculated using 38,000 as the molecular weight of the enzyme.

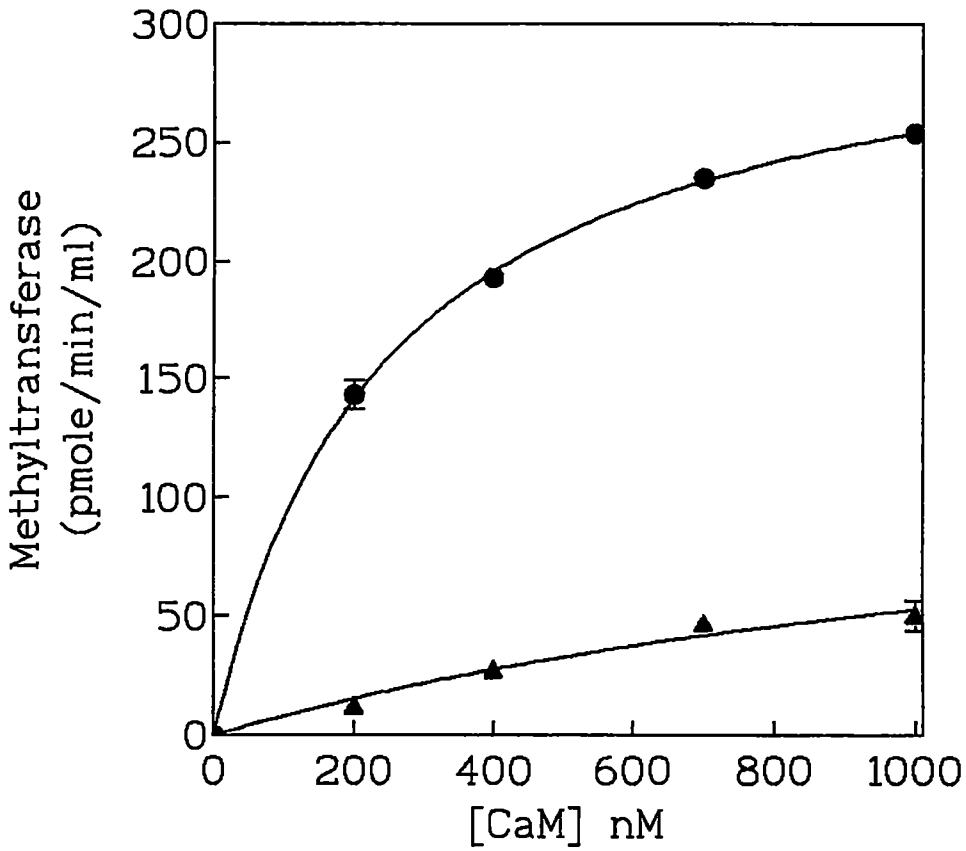

Figure 32. Methylation of Ca^{2+}-CaM^{H6} Methyltransferase kinetic comparisons of VU-1 (●) and CaM^{H6} (▲) are shown. Pseudo first order methyltransferase kinetics in a constant concentration of S-adenosylmethionine (12 μM) and calmodulin as the varied substrate in 1 mM $CaCl_2$. Error bars show the S.E. and the absence of error bars indicates the error is smaller than the symbols.

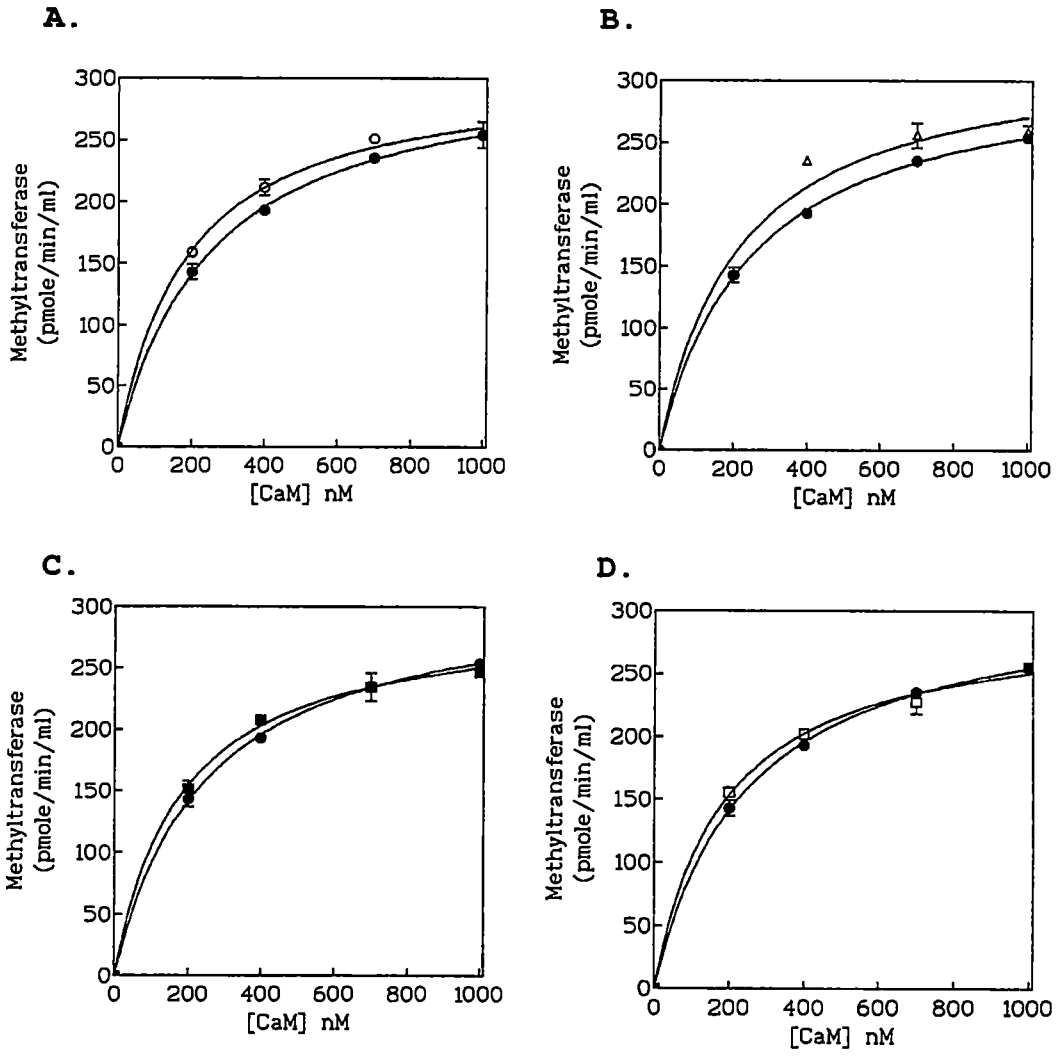

Figure 33. Methylation of Ca^{2+}-CaM^{CL3}, -CaM^{H7}, -CaM^{CL4}, and -CaM^{H8} Methyltransferase kinetic comparisons of VU-1 (●), CaM^{CL3} (O), CaM^{H7} (Δ), CaM^{CL4} (■), CaM^{H8} (□) are shown. Pseudo first order methyltransferase kinetics in a constant concentration of S-adenosylmethionine (12 μM) and calmodulin as the varied substrate in 1 mM $CaCl_2$. Error bars show the S.E. and the absence of error bars indicates the error is smaller than the symbols.

This is particularly striking with mutant CaM^{H7} which is not a substrate for the methyltransferse in the absence of calcium (Table X). Where calcium was present, the catalytic efficiency of the enzyme with CaM^{H7} (k_{cat}/K_m = 7.6 X 10^4 s^{-1} M^{-1}) was almost restored to the level of VU-1 CaM (k_{cat}/K_m = 12.1 X 10^4 s^{-1} M^{-1})(Fig. 33B, Table XI). Similarly, when either CaM^{CL4} or CaM^{H8} was used as a substrate in the presence of calcium, the catalytic efficiency (k_{cat}/K_m = 11.4 X 10^4 s^{-1} M^{-1}, and k_{cat}/K_m = 9.05 X 10^4 s^{-1} M^{-1}) increased to almost that of VU-1 (Fig. 33C & D, Table XI). Overall, the data suggest that, with the exception of CaM^{H6}, calcium binding restores the ability of the calmodulin mutants to be recognized by the methyltransferase. In the case of CaM^{H6}, a fundamental change occurs in calmodulin resulting in a loss of interaction between CaM and the methyltransferase regardless of whether calcium is present or not.

Site-specific substitutions of EF hands III and IV residues: effect on methyltransferase recognition.

The most substantial effects on methyltransferase activity were observed with subdomain mutants CaM^{H6} and CaM^{H7}. These two α-helices flank the methylation loop region and are present on the same face of the carboxyl-

terminal lobe as lysine-115 (Babu *et al.*, 1988). Together, these observations suggest that residues in both helix 6 and helix 7 are critical for methyltransferase activity. Mutagenesis involving single amino acid substitutions within these helices was carried out to attempt to identify specific residues important for methyltransferase recognition.

Residues in specific positions of helix 6 and 7 in the carboxyl-terminal lobe that differ from the amino-terminal lobe are shown in Fig 34. Based on the crystal structure (Babu *et al.*, 1988; Chattopadhyaya *et al.*, 1992) and NMR analysis (Kuboniwa *et al.*, 1995; Zhang *et al.*, 1995) most of these residues are exposed on the surface. Alanine scanning mutagenesis was performed to determine the effect of altering these surface charge residues on methyltransferase recognition.

Effect of point mutations in helix 6 (EF hand III)

The CaM^{H6} mutant has 4 residues substituted with residues from helix 2 (Fig. 34): R106, H107, T110, and N111 which are replaced with G106, T107, R110 and S111, respectively. N111 to S is likely not a significant substitution since this change is observed in naturally occurring calmodulins,

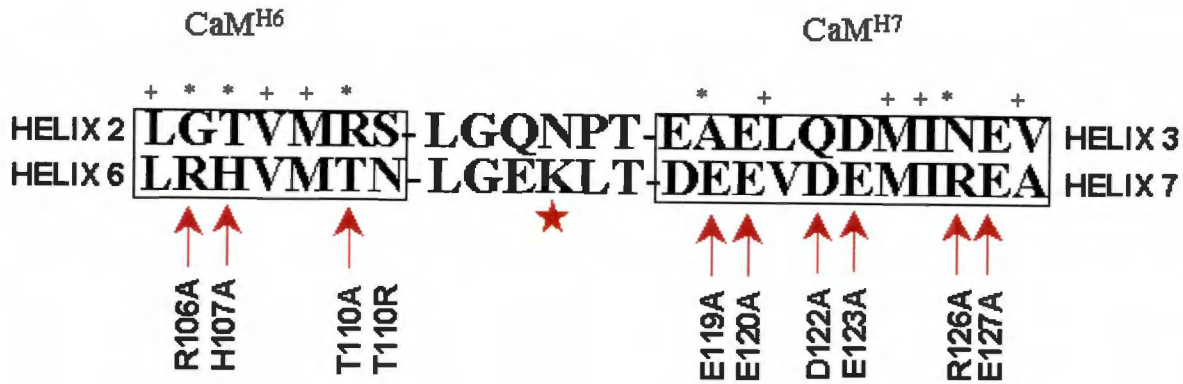

Figure 34. Sequence alignment of amino acid residues in the non-EF hand turns and adjacent α-helices of calmodulin. Helix 6 and helix 7 in the carboxyl-terminal lobe (bottom) aligned with their homologous residues in helix 2 and helix 3 in the amino-terminal lobe (top). The boxed areas indicate the sequences exchanged in either calmodulin mutant CaM^{H6} or CaM^{H7}. (*) indicates residues resulting in nonconservative substitutions, and (+) indicates residues on the hydrophobic faces of the helices. The arrows below the sequence alignment indicate residues that have been mutated, and the star indicates the site of methylation at K115.

such as *Dictyostelium* calmodulin (Marshak *et al.*, 1984) that are normal N-methyltransferase substrates (Rowe *et al.*, 1986). However, the other residues are highly conserved among calmodulin sequences. Calmodulin mutants R106A, H107A, double mutant R106A/H107A, T110A, and T110R were generated and their activator properties assessed (Table XII).

Similar to CaM^{H6}, the PDE activator properties of the mutants were not any different from VU-1. Interestingly, similar to the CaM^{1214} and CaM^{H6} mutations, certain point mutants in the helix 6 region also showed a significantly lower NAD kinase activation (Table XII). In particular, the substitutions at position 110 showed lower activation (Table XII, T110A = 65% ± 5.6; T110R = 83% ± 2.7).

However, in contrast to CaM^{H6} the point mutants showed only a modest effect on methyltransferase activity. In the absence of calcium, T110A (21.1 nmol/min/mg) and T110R (22.3 nmol/min/mg) gave only slightly lower activities compared to wild type VU-1 calmodulin (29.3 nmol/min/mg) when assayed at 3μM CaM concentrations (Table XIII). All other mutants in this region gave activities essentially identical to VU-1 calmodulin in their apo-state.

Table XII. Activation parameters of calmodulin-dependent enzymes by calmodulin mutants with substitutions in helix 6.

CaM	PDE % maximal rate[a]	$K_{0.5}^{(CaM)}$ [b]	NADK % maximal rate	$K_{0.5}^{(CaM)}$
VU-1	100	69 (± 1.1)	100	2.6 (± .15)
R106A	102	63 (± 1.2)	90	2.5 (± .14)
H107A	101	72 (± 1.1)	92	2.4 (± .28)
R106A/H107A	104	77 (± 1.2)	89	2.4 (± .02)
T110A	104	83 (± 1.4)	65	2.3 (± .26)
T110R	98	61 (± 1.0)	83	2.5 (± .10)

[a] % maximal rate: maximal activation of enzymes (PDE or NAD kinase) by calmodulins standardized to VU-1 calmodulin (100%).

[b] $K_{0.5}^{(CaM)}$ Concentration of calmodulins (nM) giving half maximal activation. The S.E. value is shown in parentheses.

Table XIII. Comparison of the methylation of calmodulins with single amino acid substitutions in helix 6 of EF hand III.

CaM	Activity[a] (nmol/min/mg) EDTA	Activity (nmol/min/mg) $CaCl_2$
VU-1	29.3 (±0.44)	28.8 (±1.7)
R106A	28.7 (±1.2)	28.4 (±1.6)
H107A	29.2 (±1.1)	29.2 (±1.6)
R106A/H107A	25.1 (±1.4)	27.9 (±1.8)
T110A	21.1 (±1.4)	24.4 (±0.73)
T110R	22.3 (±1.2)	29.0 (±2.7)

[a]Assays were performed in the presence of a standard amount of calmodulin (3μM) that is approximately 30 times the K_m for VU-1 calmodulin. Assays were performed under standard conditions (see materials and methods) in 0.15 M KCl, and either 1 mM EDTA or 1 mM $CaCl_2$. The S.E. value of three determinations is shown in parentheses.

In the presence of calcium all mutants serve as substrates for the methyltransferase with activities essentially identical to VU-1 (Table XIII). Overall, these results suggest that the reduced ability of CaM^{H6} to serve as a substrate for the methyltransferase is due to a combination of more than one amino acid substitution in helix 6. In addition, it shows that the removal or alteration of surface charge residues on helix 6 does not appear to affect interaction of either apo-CaM or Ca^{2+}-CaM with the enzyme.

Effect of mutations in helix 7 and Ca^{2+} binding loop 4 (EF hand IV):

The substitution of helix 3 for helix 7 in mutant CaM^{H7} cannot be methylated in its apo-form, however recognition is recovered in the presence of calcium. One possible interpretation of this observation is that there are key surface residues in helix 7 important for methyltransferase recognition of apo-CaM. However, upon binding calcium, additional residues (e.g. hydrophobic residues) become exposed that allow calmodulin to bind the methyltransferase. In support of this, Han *et al.* (1993) found fundamental differences between apo-CaM and Ca^{2+}-CaM as methyltransferase substrates. Helix 7 possesses a high

density of negatively charged residues (55% of all residues are glutamate or aspartate, Fig. 34) that might play an important role in methyltransferase recognition. To investigate further the role of these charged residues in the recognition of calmodulin by the methlytransferase a series of charge to alanine mutations were generated.

Adjacent to the non-EF hand turn in each lobe of calmodulin is a cluster of negatively charged residues (DEE/118-120 in the carboxyl-terminal lobe and EAE/45-47 in the amino-terminal lobe). The role of these clusters in calmodulin function was previously addressed by the generation of charge reversal mutations in which the conserved glutamates or aspartates were converted to positively charged lysine (Weber *et al.*, 1989; Shoemaker *et al.*, 1990). One of these mutants, VU-12 possesses a substitution of negatively charged residues DEE (118-120) with three lysines in helix 7 adjacent to the methylation loop. As shown in Fig. 35, VU-12 is a poor substrate for the methyltransferase. In the presence of calcium, the methyltransferase activity was 8-fold lower for VU-12 (3.6 nmol/min/mg) compared to VU-1 (28.8 nmol/min/mg), and in the absence of calcium it was 30-fold lower for VU-12 (0.93 nmol/min/mg) compared to VU-1 (29.0 nmol/min/mg).

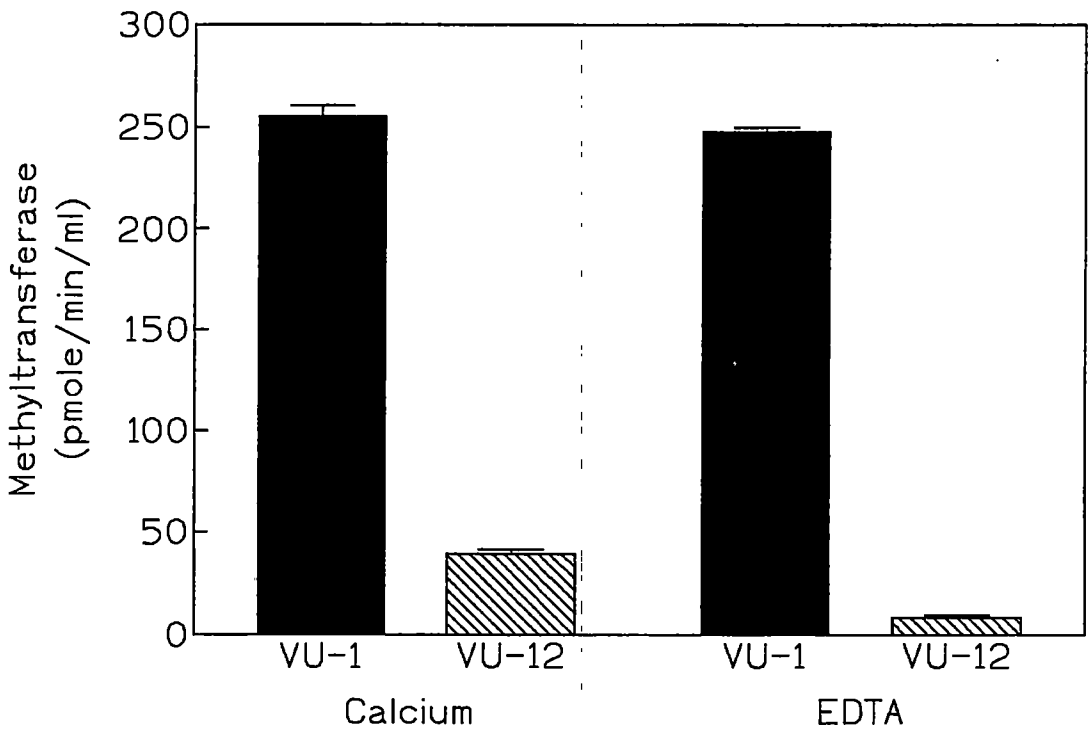

Figure 35. Methylation of VU-1 and VU-12. The enzyme was assayed under standard conditions in the presence of constant calmodulin concentrations (3 μM). Assays were performed in presence of 1 mM calcium or the absence of calcium (1 mM EDTA). Error bars show the S.E. of the mean from triplicate measurements

To further investigate the role of charged residues, E119, E120, D122, E123, R126, E127, and E139 were mutated to alanine. All mutants activated PDE in a manner indistinguishable from wildtype (Table XIV). Most mutants activated NAD kinase similar to VU-1 CaM, although a slight reduction in maximal activation was observed in mutants E127A (69% ± 2) and R126A (75% ± .6) compared to VU-1 (Table XIV).

The results of charge to alanine scanning mutants on the activity of the methyltransferase are shown in Table XV. Similar to the subdomain mutants, the largest differences were observed in their apo-forms. The most significant decrease in methyltransferase activity was observed with E120A (4.5 nmol/min/mg) to about 15% that of VU-1 (29.0 nmol/min/mg) (Table XV). A significant decrease in activity was observed with mutant calmodulin E127A to (13.3 nmol/min/mg) 46% that of VU-1(Table XV), and with mutants D122A (17.0 nmol/min/mg), R126A (16.7 nmol/min/mg), and E139A (16.3 nmol/mg/mg) to about 60% that of VU-1 (Table XV). The effect of these mutations on methyltransferase activity was less apparent in the presence of calcium, with only modest reductions observed in CaM mutants D122A, E127A, and E139A (Table XV).

Table XIV. Activation parameters of calmodulin-dependent enzymes by charge to alanine mutant calmodulins in EF hand IV.

CaM	PDE % maximal rate[a]	$K_{0.5}^{(CaM)}$ [b]	NADK % maximal rate	$K_{0.5}^{(CaM)}$
VU-1	100	69 (±1.1)	100	2.6 (± .15)
E119A	106	81 (±1.4)	98	2.1 (± .19)
D122A	100	63 (±1.2)	96	2.6 (± .10)
E123A	102	68 (±1.0)	103	3.1 (± .15)
R126A	99	60 (±1.2)	75	2.6 (± .03)
E127A	102	62 (±1.1)	69	2.6 (± .10)
E139A	104	68 (±1.5)	94	4.0 (± .36)

[a] % maximal rate: maximal activation of enzymes (PDE or NAD kinase) by calmodulins standardized to VU-1 calmodulin (100%).

[b] $K_{0.5}^{(CaM)}$ Concentration of calmodulins (nM) giving half maximal activation. The S.E. value is shown in parentheses.

Table XV. Methyltransferase activity with charge→alanine and VU-12 mutant calmodulins in EF hand IV.

CaM	Activity[a] (nmol/min/mg) EDTA	Activity (nmol/min/mg) $CaCl_2$
VU-1	29.0 (±0.15)	28.8 (±0.06)
VU-12	0.93 (±0.13)	3.60 (±0.29)
E119A	29.1 (±4.4)	28.9 (±0.03)
E120A	4.5 (± .62)	34.9 (±2.5)
D122A	17.0 (±1.5)	21.1 (±1.5)
E123A	28.7 (±2.3)	28.8 (±0.61)
R126A	16.7 (±1.3)	28.8 (±3.4)
E127A	13.3 (±1.9)	19.3 (±1.2)
E139A	16.3 (±1.5)	23.2 (±1.8)

[a]Assays were performed in the presence of a standard amount of calmodulin (3 μM) that is approximately 30 times the Km for VU-1 calmodulin. Assays were performed under standard conditions (see materials and methods) in 0.15 M KCl, and either 1 mM EDTA or 1 mM $CaCl_2$. The S.E. value of three determinations is shown in parentheses.

This recovery is similar to what is observed when CaM^{H7} is used as a substrate in the presence of calcium. The E to A mutations at 119 and 123 had a minimal effect on methylation of lysine 115. Overall, the data suggest that the conservation of residues 118,120,122,126, and 127 in helix 7 is important for optimal calmodulin methyltransferase recognition.

CHAPTER IV

DISCUSSION

Calmodulin is trimethylated at lysine 115 in most eukaryotic cells by a lysine N-methyltransferase that utilizes S-adenosyl methionine as a co-substrate. Previous studies have shown that a tryptic fragment containing residues 78-148 is sufficient for methyltransferase recognition and lysine-115 methylation with kinetic properties indistinguishable from intact calmodulin (Han *et al.*, 1993). Thus, the residues that comprise the recognition site for calmodulin methyltransferase are localized solely in the carboxyl-terminal lobe of the molecule. In the present study, as discussed below, specific residues within the methylation loop-turn sequence as well as within EF hands III and IV appear to be required for the specificity of the calmodulin methyltransferase.

Determinants for methylation in the methylation loop.

The loop region (LGEKLT/ residues 112-117) is highly conserved among calmodulins (Roberts *et al.*, 1986), and provides a 90° hairpin turn between EF hands III and IV. The turn is facilitated by G-113 (ϕ/ψ = 93°/10°,

Chattopadhyaya *et al.*, 1992), which explains the high conservation of a flexible glycine at this position.

In the calcium-saturated structure of calmodulin the loop conformation appears to be stabilized by three hydrogen bonds between the backbone amide nitrogens of G-113 and E-114 and the backbone carbonyl oxygens of M-109 and T-110 in helix 6 of EF hand III (Chattopadhyaya *et al.*, 1992). Further stabilization comes from the side chain of L-116 that is imbedded in the core of the carboxyl terminal lobe, forming hydrophobic interactions with residues on the hydrophobic faces of the helices from EF hands III and IV (Babu *et al.*, 1988). As a result, the backbone of the loop region in Ca^{2+}-CaM has a temperature factor which is lower than the more flexible regions of calmodulin (e.g., central linker and α-helices 1 and 8) although not as low as the calcium-ligated loops or internal α-helices (Chattopadhyaya *et al.*, 1992). In contrast, the methylation loop in apo-calmodulin appears to be more dynamic, showing greater flexibility (Zhang *et al.*, 1995; Malmendal *et al.*, 1999). In both structures, lysine 115 is solvent-exposed (Chattopadhyaya *et al.*, 1992; Babu *et al.*, 1985; 1988; Kuboniwa *et al.*, 1995; Zhang *et al.*, 1994; 1995), and does

not appear to form contacts with any other part of the calmodulin structure.

The methylation loop contains the unique site of methylation (K115), and is a logical place to start identifying residues important for methyltransferase binding and recognition. The present study shows that three residues are essential for methylation of lysine-115: glycine-113, glutamate-114, and leucine-116. The substitution of these residues results in little effect on calmodulin functional properties, but the ability of these mutants to serve as substrates for the methyltransferase is lost. This effect was observed regardless of the calcium concentration suggesting that both Ca^{2+}-CaM and apo-CaM are affected.

Based on the structural features of the loop region, some possible roles for these residues in methyltransferase interaction can be suggested. For example, the replacement of leucine-116 with the more polar threonine could affect the interaction of this residue with the hydrophobic core. This could alter packing interactions among the 14 hydrophobic side chains that make up the hydrophobic core of the carboxyl-terminal lobe. This in turn could alter the positioning of the methylation loop as well as other

structural features in adjacent α-helices. However, the activation properties of the mutant, which require the hydrophobic surface of the carboxyl-terminal lobe (Ikura *et al.*, 1992; Meador *et al.*, 1992; 1993), are not affected. Thus, any influence on the loop region is apparently subtle, selectively affecting methyltransferase binding. While it is clear that the side chain of leucine-116 is inserted into the core of the carboxyl-terminal lobe, it is important to consider that this residue also has substantial flexibility and mobility based on ^{15}N-relaxation measurements (Zhang *et al.*, 1995; Malmendal *et al.*, 1999; Evenas *et al.*, 1999). Thus, it is also possible that the conformation of leucine-116 might change upon binding the methyltransferase, and that it participates directly in the interaction with the enzyme.

The substitution of the negatively charged, solvent-exposed glutamate 114 with the uncharged alanine also abolishes lysine 115 methylation. In previous work (Han *et al.*, 1993), it was shown that high ionic strength blocks the interaction of calmodulin with the methyltransferase. Thus, it was proposed that electrostatic interactions might help stabilize the interaction of calmodulin with the methyltransferase. Thus, the removal of the negatively

charged, surface-exposed glutamate at position 114 may have eliminated a point of contact for the enzyme.

In addition to the residues flanking lysine-115, the invariant glycine at position 113 is necessary for methyltransferase recognition. As discussed above, this glycine is required to facilitate the turn between EF hands III and IV. The substitution of a serine likely alters the conformational flexibility of the loop. This loss of flexibility might prohibit the residues within the loop from adopting an orientation suitable for methyltransferase binding and catalysis. Another likely outcome of the serine substitution is that the hairpin turn between EF hand III and IV is no longer formed since serine cannot usually assume the ϕ/ψ angles necessary to generate the turn (Ramachandran and Sasisekharan, 1968). The packing of the helices (in particular helix 6 and 7) may be altered. However, this mutant activated PDE and NAD kinase normally, suggesting that any altered conformation of these α-helices is not severe enough to affect calmodulin activator function.

While the substitutions at 113, 114, and 116 were defective regardless of calcium binding, the leucine-112T mutation showed a selective effect on apo-CaM. In the

absence of calcium, the substitution of leucine-112 with a more polar threonine resulted in a 4.5-fold reduction in the catalytic efficiency of the methyltransferase. L112 is more buried in the apo-form of calmodulin (Fig. 36). A conversion to threonine might disrupt the packing of the hydrophobic core in apo-calmodulin. This is particularly important to consider since in the absence of calcium, calmodulin folding and stability are more labile (Martin and Bayley, 1986; Zhang et al., 1995; Kuboniwa et al., 1995). The mutation L112T could result in a change of organization in the residues (L116T, E114A, G113S) necessary for methyltransferase binding and catalysis that is restored in the presence of calcium.

Unlike the other substitutions within the methylation loop the substitution of alanine for threonine-117 did not significantly affect methyltransferase activity. Threonine 117 has a solvent exposed side chain (Babu *et al.*, 1988; Chattopadhyaya *et al.*, 1992), the conservation of which is apparently not required for methylation.

While residues L112, G113, E114, and L116 in the methylation loop (LGEKLT/112-117) appear to be important for methyltransferase recognition, it is clear from the findings with CaM^{EKL} that other structural determinants are

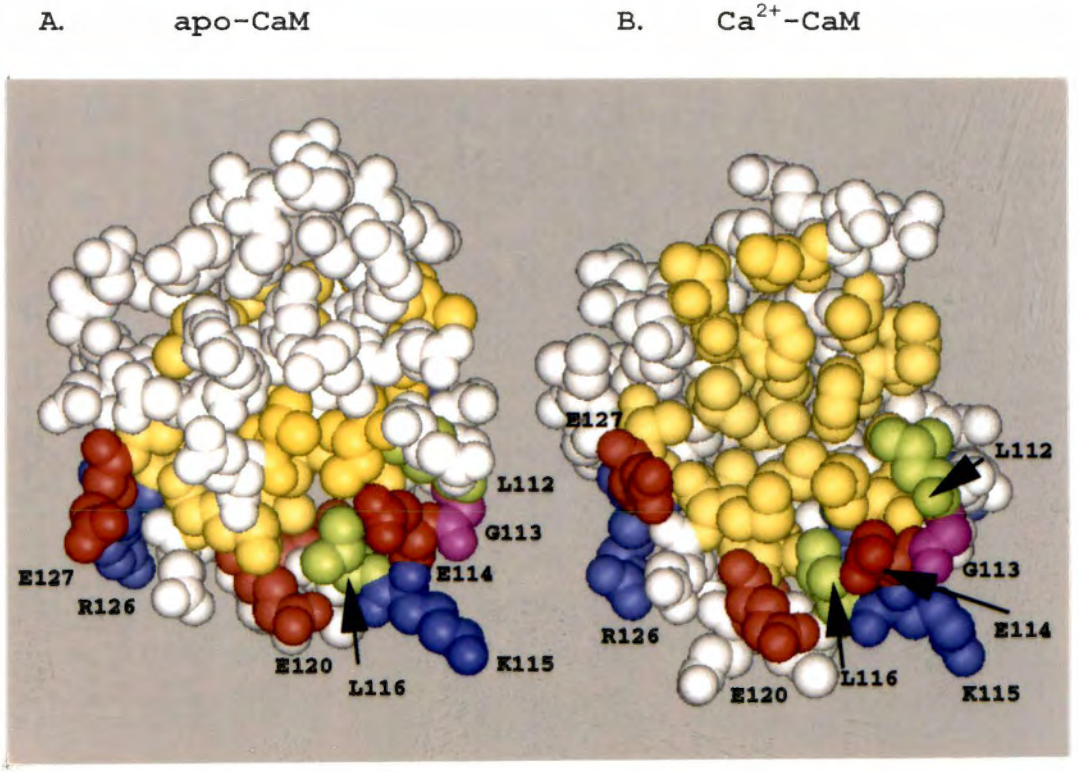

Figure 36. Comparison of the carboxyl-terminal lobe of apo-CaM and Ca^{2+}-CaM. The carboxy-terminal (residues 77-148) lobe from **A**.the NMR structure of apo-CaM (Kuboniwa *et al.*, 1995) and **B**.the X-ray crystal structure of Ca^{2+}-CaM (Babu *et al.*, 1988) are shown above. The hydrophobic residues (yellow) are more exposed after the binding of calcium. The methylation site (K115) and charged residues important for methylation are highlighted in red (negatively charged) and blue (positively charged). Hydrophobic residues in the methylation loop (L116 and L112) important for methyltransferase activity are colored in green. Glycine 113 (pink) allows the 90° turn in the loop-turn region.

also required. The CaM^{EKL} mutation resulted in the placement of the methylation loop sequence between EF hands I and II in the amino-terminal lobe in a conformation predicted to be identical to the methylation loop in the carboxyl-terminal lobe of native calmodulin (Fig. 16). The peptide backbone of EF hands I and II compared to EF hands III and IV shows a high degree of similarity in both the calcium saturated (rms deviation= 0.751 Å, Babu *et al.*, 1988) and apo (rms deviation = 2.00 Å, Kuboniwa *et al.*, 1995) states. Further, the loop/turn sequence (residues 39-45) shows an identical hydrogen bond network and interaction with the hydrophobic core as the methylation loop (Chattopadhyaya *et al.*, 1992). Thus, in CaM^{EKL} the methylation loop sequence is presumably placed within an environment that shares high similarity to its position in wild type calmodulin. The inability of the enzyme to methylate CaM^{EKL} strongly suggests that additional determinants outside of the loop region that are unique to EF hands III and IV are necessary for methyltransferase recognition.

Determinants for methylation in EF hands III and IV.

In mutants CaM^{1214} and CaM^{1232}, EF hands III and IV in the carboxyl-terminal lobe are replaced with EF hands I and II respectively. Neither of these mutants could serve as a

substrate for the calmodulin methyltransferase in either their calcium-saturated or apo-forms. EF hands I and II in the amino-terminal lobe fold and pack in a manner similar to EF hands III and IV in the carboxyl-terminal lobe. Both structures consist of an antiparallel four α-helix bundle with hydrophobic residues from the four helices (helix 1,2,3,&4 in the amino-terminal lobe and helix 5,6,7,and 8 in the carboxyl-terminal lobe) interacting to form a hydrophobic core (Chattopadhyaya *et al.*, 1992; Babu *et al.*, 1988). Each core is composed of 14 hydrophobic side chains originating from identical positions in each lobe. There are small differences between the structures of the two lobes, particularly in their apo-forms, but overall their similarity and structural symmetry is remarkable. Thus, the substitution of one EF hand with a symmetrically related EF hand is predicted to form the same packing interactions with its partner EF hand.

The current study shows CaM^{1214} and CaM^{1232} are functional, and still retain the ability to activate calmodulin-dependent NAD kinase and PDE (Cobb *et al.*, 1999). In addition calcium-dependent activation of NAD kinase indicates that the calcium-binding ability and cooperativity of CaM^{1214} and CaM^{1232} is similar to wild-type

VU-1 CaM. Similarly, a previous study by Persechini *et al.* (1996b) also showed that the substitution of homologous EF hands between the amino and carboxy terminal lobes produce folded, functional calmodulin proteins that bind four Ca^{2+} ions with high affinity, similar to wild-type calmodulin. Further, they showed that the exchange of EF hand I for III and EF hand II for IV resulted in calmodulins that could activate nitric oxide synthase, smooth muscle myosin light chain kinase, and skeletal muscle myosin light chain kinase (albeit to a lesser degree). This suggests that the substituted EF hand from the amino-terminal lobe interacts with the other EF hand in the carboxyl-terminal lobe yielding a folded, high affinity calcium binding pair (Kretsinger, 1980). Based on these observations, it is proposed that CaM^{1214} and CaM^{1232} are missing specific structural determinants that are required for methylation, but that the loss of methylation is not due to a gross misfolding of the mutant proteins.

To identify further the regions within both EF hands III and IV that are important for methyltransferase recognition, subdomain and single amino acid mutations were generated in the carboxyl-terminal lobe. EF hands are formed from a helix-loop-helix motif (Strynadka & James,

1989), and the subdomain mutants were designed to exchange a particular helix or calcium-binding loop from EF hand III or IV with sequence from the homologous positions in EF hand I and II.

Subdomain and point mutants in EF hand III

The replacement of EF hand I for EF hand III in CaM^{1214} results in the substitution of helix 1 (EFKEAFSLF) for helix 5 [ELKEAFRVF/(84-92)]. This region of EF hand III is almost completely conserved in CaM^{1214}, with the most notable change in sequence occurring at position 90 with an R to S substitution. To narrow down which structural changes in CaM^{1214} are responsible for the loss of its ability to be methylated, two subdomain mutants CaM^{CL3} and CaM^{H6} were generated. CaM^{CL3} possesses the exchange of the three residues at the end of helix 5 [RVF/(90-92)] with sequence from helix 1 [SLF/(17-19)]. In addition, the first nine residues of calcium binding loop 3 are replaced with sequence from calcium binding loop 1. The methyltransferase kinetics using CaM^{CL3} were not significantly different than VU-1 suggesting that the loss of methylation with CaM^{1214} is not due to substitutions in helix 5 or calcium binding loop 3.

In contrast to the results of CaM^{CL3}, the data with CaM^{H6} suggests that the exchange of helix 2 for helix 6 significantly contributes to the loss of methyltransferase recognition in CaM^{1214}. Helix 6 is located adjacent to the methylation loop (Babu *et al.*, 1988; Chattopadhyaya *et al.*, 1992; Kuboniwa *et al.*, 1995; Zhang *et al.*, 1995) and one possible interpretation is that there might be points of contact between this helix and the methyltransferase. This hypothesis was addressed by generating individual amino acid substitutions in helix 6, and examining their effects on methyltransferase recognition.

A comparison of the sequence in helix 6 of wild type calmodulin [LRHVMTN/(105-111)] with the substituted sequence in mutant CaM^{H6} [LGTVMRS] reveals no change in the hydrophobic residues that are involved in the packing of helix 6 with the other helices in the carboxy-terminal lobe. The possibility that key surface residues in helix 6 are important for calmodulin interaction with the methyltransferase was therefore addressed. Residues R106 and H107 were ideal candidates since electrostatic interactions have been proposed to be important for methyltransferase-calmodulin association (Han *et al.*, 1993). However, three calmodulin mutants R106A, H107A, and

the double mutant R106A/H107A showed that the removal of these charged residues caused little effect on methyltransferase activity. This suggests that neither R106 nor H107 are essential for methyltransferase binding and catalysis.

Another possible reason why methyltransferase activity is reduced in CaM^{H6} could be the introduction of a bulky charged arginine residue for threonine at position 110 in wild type calmodulin. However, the point mutant T110R was essentially identical to wild type calmodulin as a methylation substrate. Thus, the loss of methyltransferase activity in CaM^{H6} is not a result of an arginine introduced at position 110.

The only other mutation in helix 2 relative to helix 6 is the substitution of a serine for an asparagine at position 111. This conservative substitution is present in some naturally occurring calmodulins such as that found in *Dictyostelium discoideum* (Marshak *et al.*, 1984). Calmodulin isolated from *Dictyostelium* is not methylated *in vivo* (Marshak *et al.*, 1984) but is a good *in vitro* substrate for the methyltransferase (Rowe *et al.*, 1983; Rowe *et al.*, 1986). This suggests an N111S mutation would not significantly disrupt methyltransaferase recognition.

Overall, the data suggest that the loss of methylation in CaM^{H6} is not the result of a substitution in one specific amino acid, but that the conservation of the entire sequence in helix 6 is necessary for methyltransferase recognition. In the presence of calcium a superimposition of the backbone of helix 6 (residues 102-114) and helix 2 (residues 29-41) (Fig. 37A) shows a highly similar conformation with a rms deviation of 0.13 Å (Fig. 37B). Further, the crystal structure shows that helix 2 forms a packing structure with other α-helices in the amino-terminal lobe that is very similar to helix 6 in the carboxyl-terminal lobe (Babu *et al.*, 1988; Chattopadhyaya *et al.*, 1992; Zhang et al., 1995; Kuboniwa et al., 1995). Differences between the two helices are mostly in surface-exposed residues (Fig. 37), the side chains of which do not have any obvious stabilizing interactions with other residues in calmodulin (Babu *et al.*, 1988; Chattopadhyaya *et al.*, 1992).

In the absence of calcium there is a significant deviation between helix 2 and 6 (rms deviation = .72Å) with a kink at glutamate 31 in helix 2 that is missing from helix 6 (Fig. 38) (Zhang *et al.*, 1995; Kuboniwa *et al.*,

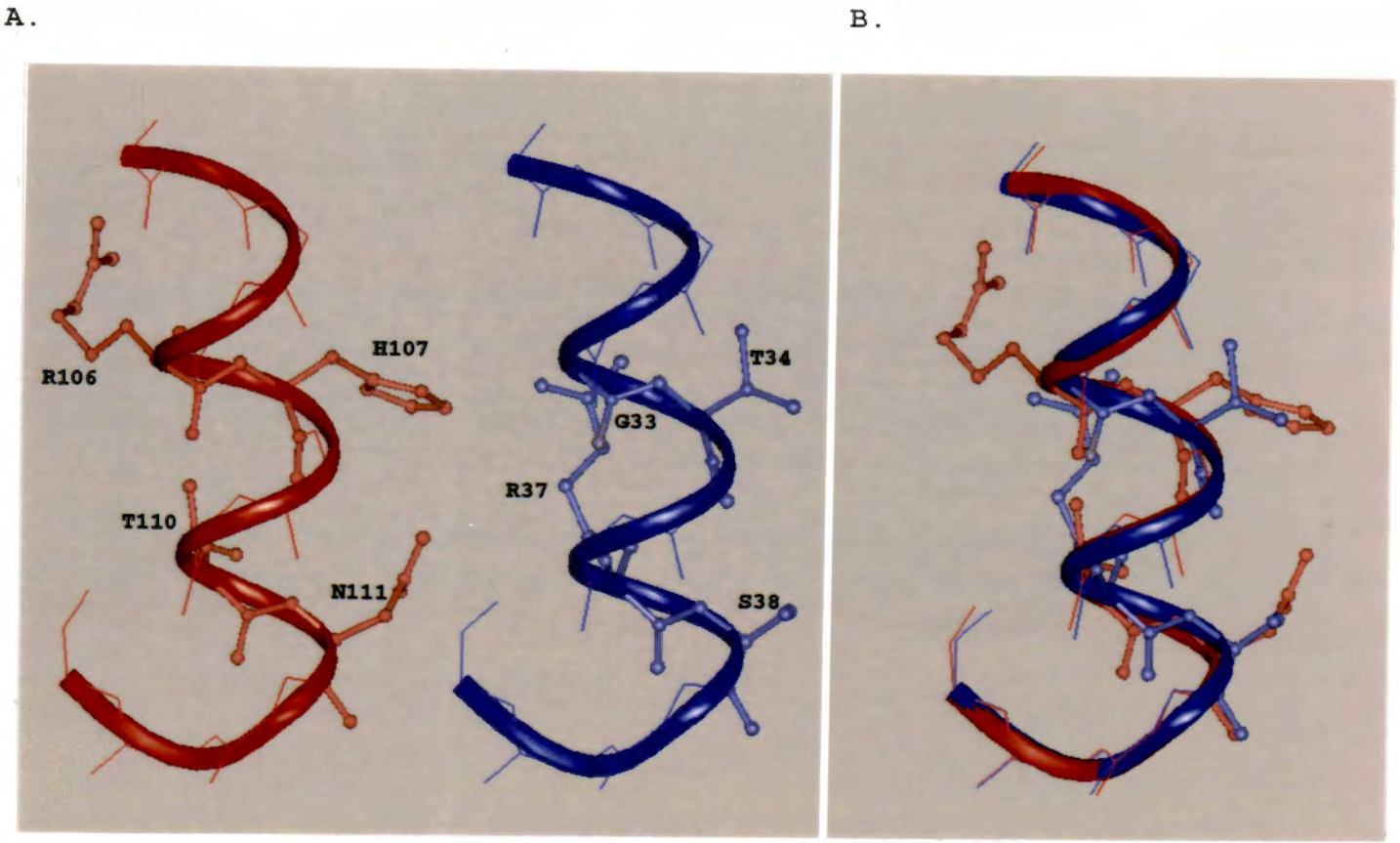

Figure 37. Comparison of the backbone structures of helix 2 and helix 6 in Ca^{2+}-calmodulin. The conformation of helix 6 (residues 102-114 shown in red) of the carboxy-terminal lobe and helix 2 (residues 29-41 shown in blue) of the amino-terminal as determined by the X-ray crystal structure of Ca^{2+}-CaM (Babu *et al.*, 1988) are shown apart (**A**) and superimposed (**B**). Side chains from residues that are not identical at symmetrical positions in the two helices are also shown. The two structures superimposed with a root-mean square difference of 0.13 Å. The images were generated using Silicon Graphics Indigo system and Insight II software.

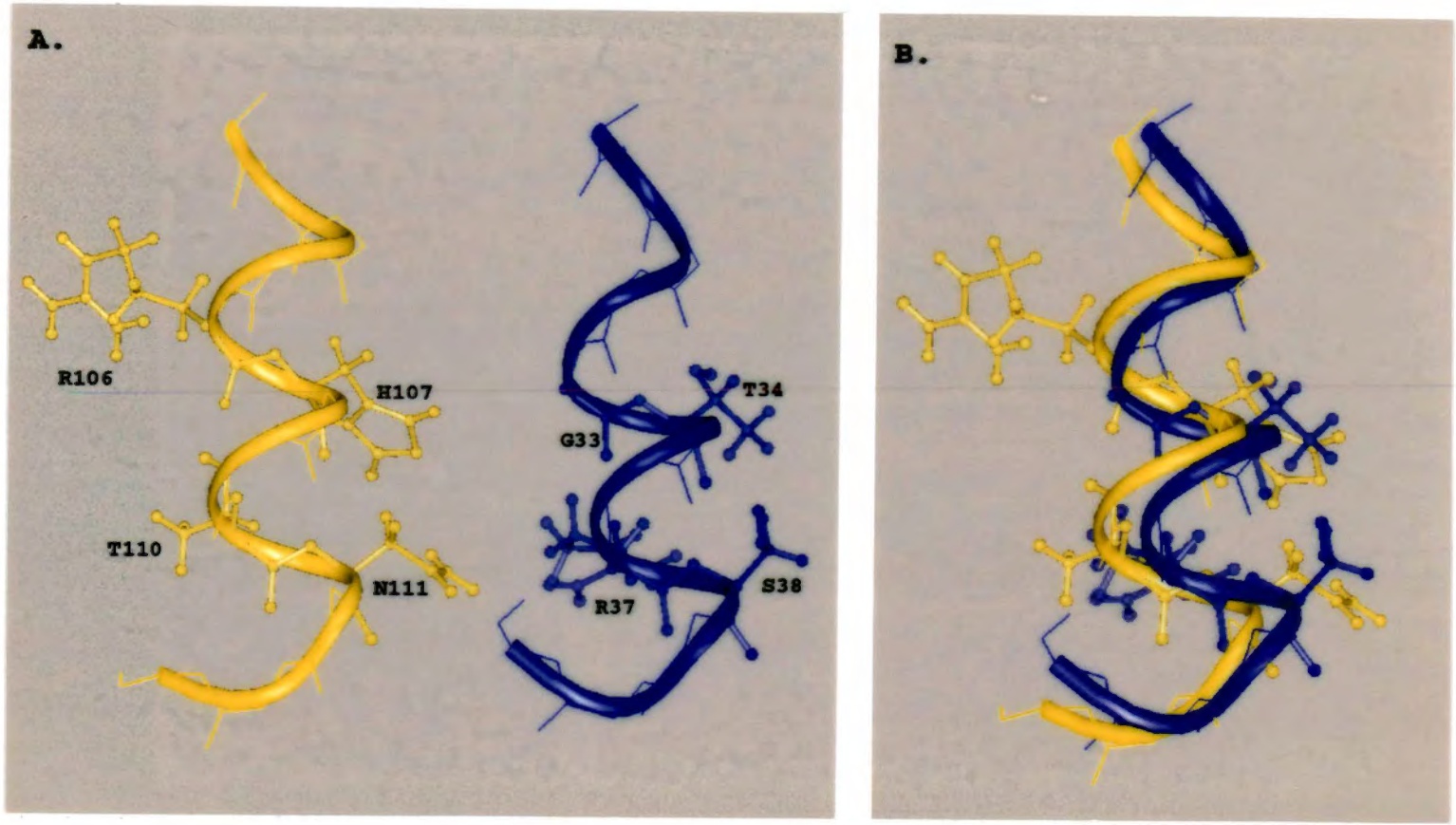

Figure 38. Comparison of the backbone structures of helix 2 and helix 6 in apo-calmodulin. The conformation of helix 6 (residues 102-114 shown in yellow) of the carboxy-terminal lobe and helix 2 (residues 29-41 shown in blue) of the amino-terminal as determined by the MNR structure of apo-CaM (Kuboniwa *et al.*, 1995) are shown apart (**A**) and superimposed (**B**). Side chains from residues that are not identical at symmetrical positions in the two helices are also shown. The two structures superimposed with a root-means square difference of 0.72 Å. The images were generated using Silicon Graphics Indigo system and Insight II software.

1995). However, since CaM^{H6} shows defective methylation in both Ca^{2+}- and apo-structures, this difference alone is inadequate to account for defects associated with CaM^{H6}.

Since the effects of single mutants in helix 6 are not additive, perhaps the substitution of the entire helix 6 with helix 2 in CaM^{H6} causes an unexpected change in the conformation that disrupts the methyltransferase binding site in both the apo- and calcium-bound states. However, such a change in conformation is likely to be subtle since the calcium-binding and enzyme activation properties of calmodulin mutants CaM^{1214} and CaM^{H6} are only modestly affected.

Subdomain and point mutants in EF hand IV

To attempt to narrow down the regions in EF hand IV that are necessary for calmodulin methylation, three subdomain mutants were generated CaM^{H7}, CaM^{CL4}, and CaM^{H8}. Unlike CaM^{H6}, all subdomain mutants in EF hand IV showed normal methylation kinetics in the calcium-saturated state but altered kinetics in the apo-state. The substitution of helix 3 for helix 7 (CaM^{H7}) showed the most significant result with essentially no methylation in the absence of calcium. Methyltransferase activity with apo-CaM^{CL4} or apo-

CaM^{H8} showed a k_{cat} that was reduced by approximately two-fold.

Since the apo-CaM^{H7} mutant showed the most significant effect on the methylation rate, and because helix 7 is found adjacent to lysine 115 on the same face of the carboxyl-terminal lobe, additional mutagenesis was performed to identify residues involved in methyltransferase recognition. In CaM^{H7}, the sequence in helix 7 [DEEVDEMIREA/(118-128)] is replaced with the sequence from helix 3 [EAELQDMINEV]. An examination of helix 7 shows that this region possesses an extremely high number of acidic side chains (6 out of 11 residues). These residues provide a surface-exposed patch of negative charge on the carboxyl-terminal lobe, adjacent to lysine-115 (Weber *et al.*, 1989, Fig. 39). As discussed above, ionic interactions have been proposed to be important in the interaction of apo-CaM with the calmodulin. methyltransferase (Han *et al.*, 1993) and with other apo-CaM target proteins such as neuromodulin and neurogranin (Van Hooff *et al.*, 1988; Baudier *et al.*, 1991; Urbauer *et al.*, 1995, Tsvetkov *et al.*, 1999).

The importance of a conserved charge cluster in helix 7 for methyltransferase recognition is evident from the

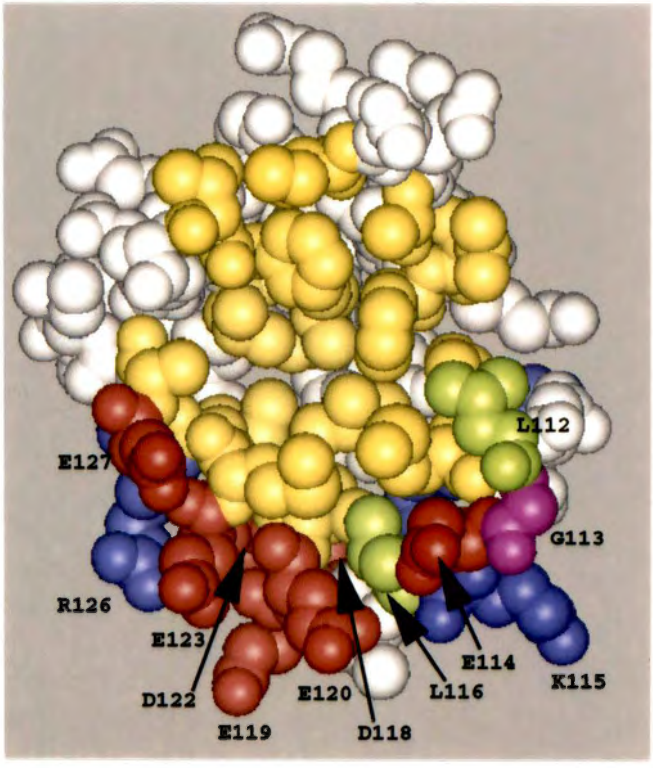

Figure 39. Space filling model of the carboxyl-terminal lobe of Ca^{2+}-CaM. X-ray crystal structure of the carboxyl-terminal (residues 77-148) lobe of Ca^{2+}-CaM (Babu *et al.*, 1988). The hydrophobic residues (yellow) are exposed after the binding of calcium. K115 and other charged residues in helix 7 and the methylation loop important for recognition are highlighted in red (negatively charged) and blue (positively charged). Hydrophobic residues in the methylation loop (L116 and L112) important for methyltransferase activity are colored in green. Glycine 113 (pink) allows the 90° turn in the loop-turn region.

results with VU-12 [DEE(118-120)/KKK]. This mutation results in a charge reversal in helix 7 adjacent to the methylation loop and neutralizes nearly half of the negative electrostatic potential surface on the carboxyl-terminal lobe (Weber *et al.*, 1989). VU-12 CaM was a poor substrate for the methyltransferase suggesting that this negative charge cluster adjacent to lysine 115 is important for the CaM/methyltransferase interaction. Also, in contrast to CaM^{H7}, methyltransferase activity remained low (8-fold reduction) when VU-12 was tested as a substrate in the presence of calcium. This suggests that the conservation of charge in residues 118-120 of helix 7 may be important for methyltransferase recognition even after calcium binds and the hydrophobic cleft of calmodulin opens.

In contrast to VU-12, E119A is methylated normally. This suggests that the loss of negatively charged E119 is not responsible for the poor kinetics observed with VU-12. In addition, E118 and E120 are more exposed on the surface of calmodulin (Babu *et al.*, 1988), and the large decrease in methylation observed with calmodulin mutant E120A suggests that the charge on this residue is important for methyltransferase recognition.

The alanine scanning mutagenesis of charged residues in helix 7 showed more subtle effects on methylation rates. As was the case with CaM^{H7}, the alanine scanning mutants showed higher methylation rates under conditions of saturating calcium. However, in their apo-states decreased methylation rates were observed with E120A (15%), D122A (50%), R126A (50%), and E127A (67%) compared to wild type VU-1 calmodulin. Overall, the data suggest that specific surface charge residues in helix 7 may contribute to the interaction of methyltransferase with apo-CaM. In addition, the complete loss of methyltransferase activity in apo-CaM^{H7} appears to be a cumulative effect involving the change in sequence of more than one conserved surface residue.

Methyltransferase recognition: apo- and Ca^{2+}-calmodulin

Based on the studies performed here the mutants fall into three classes: 1. Those that affect methylation of both Ca^{2+}-CaM and apo-CaM; 2. Those that affect methylation of apo-CaM only, and 3. Those that show no effect on methylation at all. With respect to residues that are important for the methylation of both apo and Ca^{2+}-CaM, the conservation of the methylation loop residues and the acidic cluster at 118-120 appear to be important for

enzyme recognition. An examination of this region in calmodulin shows that it is located on a ridge in the carboxyl-terminal lobe, and that the conformation of this part of the structure is the same in apo- and Ca^{2+}-CaM (Fig. 36) These residues may provide points of contact with the active site of the methyltransferase or, in certain cases, (e.g. G113) might enable a conformation that allows optimal binding.

Besides these mutations, other substitutions show a selective effect on the methylation of apo-CaM. The differences between apo-CaM and Ca^{2+}-CaM methylation are intriguing, and suggest that the site of interaction with the methyltransferase may change once calcium is bound. A different apo- or Ca^{2+}-CaM-methyltransferase interaction is supported by previous findings (Han *et al.*, 1993; Morino *et al.*, 1987; Pech *et al.*, 1994; Wright *et al.*, 1996) that show different kinetics for apo-CaM and Ca^{2+}-CaM methylation, and different sensitivities to ionic strength and ligand binding. For example, the methylation of apo-calmodulin shows sensitivity to increasing ionic strength and Ca^{2+}-CaM does not (Han *et al.*, 1993). Further, In the presence of calcium, ligands or peptides that bind the hydrophobic cleft block the interaction of the

methyltransferase with calmodulin (Han *et al.*, 1993). However, there is no effect of these reagents on the rate of apo-calmodulin methylation (Han *et al.*, 1993).

Two different conformations are adopted in calmodulin: 1. Closed (when hydrophobics are sequestered to interior of protein) or 2. Open (when hydrophobic side chains are exposed after the binding of calcium). In apo-CaM a closed conformation is assumed, and the carboxyl-terminal lobe consists of a tightly packed four α-helix bundle (Kuboniwa *et al.*, 1995; Zhang *et al.*, 1995). The two helices of each EF hand are in an antiparallel (128°-137°) orientation relative to one another. Figure 36 shows that apo-CaM has few exposed hydrophobic residues and many charged residues on the surface, predominantly in helix 7 (Kuboniwa *et al.*, 1995; Zhang *et al.*, 1995). Based on the substitutions of the charged residues in this region of calmodulin, electrostatic interactions between the methyltransferase and apo-CaM may help contribute to binding/orientation of the calmodulin substrate. This is similar to the proposed mechanism of apo-CaM binding to its target proteins such as neuromodulin (Chapman *et al.*, 1991) in which electrostatic interactions are predominant.

The binding of calcium induces a conformational change resulting in almost perpendicular interhelical angles (86°-101°) in the EF hands, adopting an "open state". This rearrangement results in the exposure of a pronounced hydrophobic pocket (see yellow surface in Fig. 36) on the surface of calmodulin that is reduced or absent in the apo-state (Kuboniwa *et al.*, 1995; reviewed in Ikura 1996).

How do these changes in structure lead to differential recognition of the two calmodulin forms? Examination of apo- and Ca^{2+}-CaM suggests that residues in the methylation loop and helix 7 that are essential for methylation do not change drastically after the binding of calcium (Fig. 36). However, the interhelical angles within each EF hand change significantly, exposing the hydrophobic core, with amino acids in the methylation loop and helix 7 forming a cluster of charge (predominantly negative) adjacent to the cleft (Figures 36 &39). The extensive hydrophobic surface on calmodulin, which is present after calcium binds, might provide additional interactions with the methyltransferase. This could explain why reagents, such as drugs and peptides, that interact selectively with the hydrophobic cleft might sterically block the binding of the methyltransferase to Ca^{2+}-CaM (Han *et al*, 1993).

While potential sites of interaction have been identified by the mutagenesis studies performed here, considerable work remains in defining the site in calmodulin for methyltransferase recognition. First, the data suggest that some of the subdomain/domain substitutions result in conformational changes that disrupt methyltransferase interactions. Structural analyses of these mutants may provide insight into how these changes disrupt the conformation surrounding the methylation site. Further, these analyses may provide information on similarities and differences in how the EF hands in calmodulin interact. It is interesting to note that while similarities exist between EF hands I/II and III/IV there are differences in structure (Zhang *et al.*, 1995; Kuboniwa *et al.*, 1995) as well as function (Minowa and Yagi, 1984; Linse *et al.*, 1991; Elshorst *et al.*, 1999). Finally, these mutants could aid in the analysis of other apo-CaM-interacting proteins (e.g. neuromodulin, IQ domain proteins) and may help identify the sequence in CaM necessary for interaction. Further, it is essential that the methyltransferase be characterized structurally. While this enzyme has been purified (Han *et al.*, 1993) virtually nothing in known regarding its catalytic mechanism and

structural features that confer specific calmodulin binding.

Determinants for activation of NAD kinase

In addition, the present study sheds new light on residues important for the activation of NADK. CaM^{EKL} does not activate NADK but is a potent antagonist of activation by wild type calmodulin, suggesting binding but not activation of the enzyme. Calmodulins with antagonist or partial agonist activities with other calmodulin-dependent enzymes have been generated via chemical modification of calmodulin with norchlorpromazine (Newton *et al.*, 1983), the production of troponin C/calmodulin chimeras (George *et al.*, 1990; Van Berkum & Means 1991; George *et al.*, 1993; Su *et al.*, 1994; Su *et al.*, 1995), by EF hand duplication within calmodulin (Persechini *et al.*, 1996a; Persechini *et al.*, 1996b), and by truncation of specific hydrophobic residues, particularly within the amino terminal lobe (Chin *et al.*, 1997).

From these observations, it has been proposed that calmodulin activation of enzymes follows a two step mechanism :

step 1: $[Ca^{2+}]_4\text{-CaM} + \text{enzyme}_{inact} \quad [Ca^{2+}]_4\text{-CaM}^{\bullet} - \text{enzyme}_{inact}$

step 2: $[Ca^{2+}]_4\text{-CaM}^{\bullet} + \text{enzyme}_{inact} \quad [Ca^{2+}]_4\text{-CaM}^{*} - \text{enzyme}_{act}$

This model, originally proposed by Blumenthal and Stull (1982) for smooth muscle MLCK, suggests that two separate interactions are required for enzyme activation. First, a high affinity interaction between the hydrophobic surface of the carboxyl- and/or the amino terminal lobe of calmodulin with key hydrophobic side chains of the calmodulin- binding peptide takes place (Figs. 5 & 40). This results in the amino- and carboxyl-terminal lobes of calmodulin converging, forming a hydrophobic channel that surrounds the peptide (Fig. 40) (Meador *et al.*, 1992; Ikura *et al.*, 1992; reviewed in Ikura *et al.*, 1996).

The formation of this high affinity complex ($[Ca^{2+}]_4$-$CaM^{\bullet}$ - $enzyme_{inact}$) is followed by additional specific interactions between calmodulin and the enzyme that lead to an active complex ($[Ca^{2+}]_4$-CaM^{*}- $enzyme_{act}$). The nature of these interactions is not yet defined but is proposed to involve several short range contacts between calmodulin and the enzyme (Chin *et al.*, 1997). Based on mutagenesis, two sets of interactions leading to activation are proposed (discussed in Chin *et al.*, 1997; summarized in Table XVI). One set of interactions are nonpolar in nature and involve specific residues in the hydrophobic cleft, particularly in

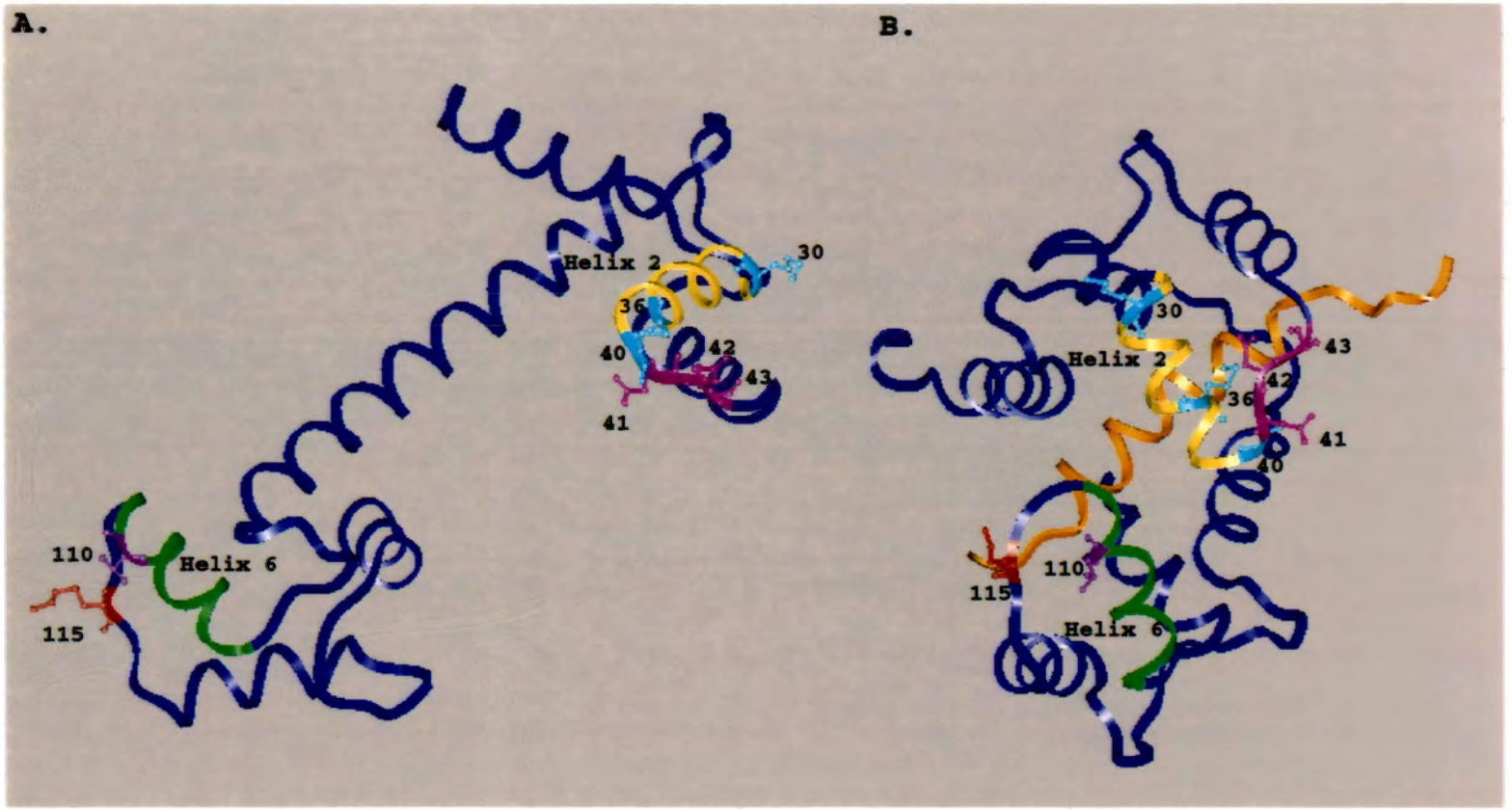

Figure 40. Structure of helices 2 and 6 and the loop-turn regions in calmodulin highlighting residues important for the activation of NAD kinase. **A.** X-ray crystal structure of Ca^{2+}-calmodulin (Babu *et al.*, 1998); **B.** NMR structure of the peptide (shown in orange and comprising the CaM binding domain of smMLCK) bound form of Ca^{2+}-calmodulin (Ikura *et al.*, 1992). Helix 2 (yellow) in the amino-terminal lobe and helix 6 (green) in the carboxyl-terminal lobe come together upon binding petide, forming the "latch domain". Specific residues in CaM important for the activation of NAD kinase are shown: K30, M36, and G40 in helix 2 (light blue, Lee *et al.*, 1997); Q41, N42, and P43 in the loop-turn region (pink, Cobb *et al.*, 1999); T110 in helix 6 (purple, current study); and K115 in the mehtylation loop-turn region (red, Roberts et al., 1986; 1992).

Table XVI. Residues implicated for the activation of calmodulin-dependent enzymes

Enzyme	Residues	Location	Ref.
Nitric Oxide Synthase	T34, S38	Helix 2	a
	L112	Helix 6	a
Myosin LC kinase (sm)	E14	Helix 1	b
	T34, S38, L32	Helix 2	b,g
	T110, L112	Helix 6	c
	K115	Methylation loop	c
	M51, V55	Helix3	g
	M71	Helix4	g
NAD kinase	K30, M36, G40	Helix 2	d
	Q41, N42, P43	Loop	e
	T110	Helix 6	current study
	K115	Methylation loop	f

a. Su *et al.*, 1995; b. VanBerkum and Means, 1991; c. Su *et al.*, 1994; d. Lee *et al.*, 1997; e. Cobb *et al.*, 1999; f. Roberts *et al.*, 1986; 1992; g. Chin *et al.*, 1997.

the amino terminal lobe (Chin *et al.*, 1996; 1997). Presumably, these additional interactions are required for removal of the auto-inhibitory region (Kemp *et al.*, 1996) from the catalytic cleft of calmodulin-dependent enzymes (Chin *et al.*, 1996). However, a second set of interactions (George *et al.*, 1990; VanBerkum and Means, 1991; George *et al.*, 1993; Su *et al.*, 1994; 1995; Klee *et al.*, 1998; and Cobb *et al.*, 1999) map to the hydrophilic surface-exposed regions that do not occur at the calmodulin-peptide interface. Many of these map to an area known as the "latch domain". This region is formed upon peptide binding (Figs. 40 & 41) by helix 2 of EF hand I interacting with helix 6 of EF hand III, linking the two lobes of calmodulin in a "latch" (Meador *et al.*, 1992).

Besides the identification of residues involved in "activation" of NADK, these mutagenesis studies show that each enzyme has a differential sensitivity to mutations (summarized Table XVI). A clear example of this in the present work is the finding that mutations that abolish NAD kinase activation showed no effect on PDE activation. As discussed in the introduction, the available structures for calmodulin bound to peptides of various target proteins showed considerable diversity

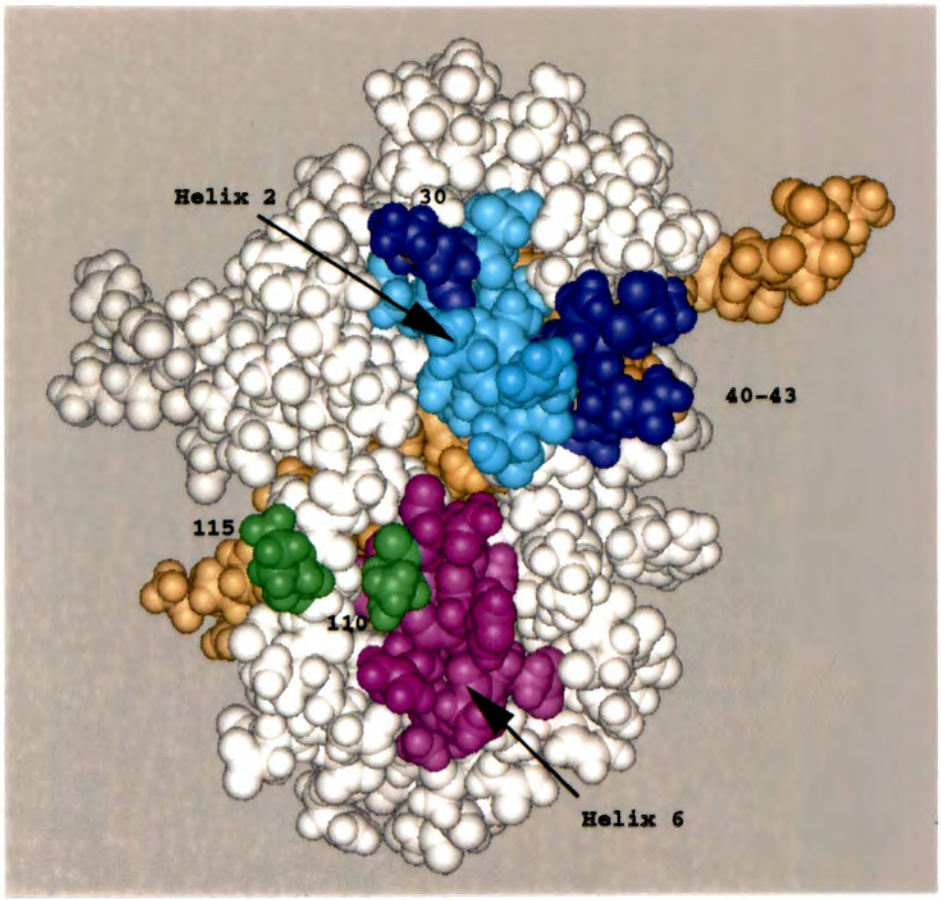

Figure 41. Structure of Ca^{2+}-peptide-bound calmodulin showing the latch domain and adjacent regions important for NAD kinase activation. Space filling model of the NMR structure of the peptide (shown in orange and comprising the CaM binding domain of smMLCK) bound form of Ca^{2+}-calmodulin (Ikura *et al.*, 1992). Helix 2 (light blue) in the amino-terminal lobe and helix 6 (pink) in the carboxyl-terminal lobe come together upon binding peptide, forming the "latch domain". Residues in CaM important for the activation of NAD kinase are primarily located on the same face of the molecule as the "latch" and are shown: in dark blue (K30, GQNP/40-43 of the amino terminal lobe) and green (T110 and K115 of the carboxyl terminal lobe).

(Ikura *et al.*, 1992; Meador *et al.*, 1992; 1993; Osawa et al., 1999, Elshorst et al., 1999), and it follows that the latch residues required for activation may be different.

Along these lines from the present study, as well as earlier work, it is clear that NAD kinase is distinct from other calmodulin-target proteins in terms of interactions that control activation. Some of these residues appear to be on the latch surface. For example, by using a chimeric approach with soybean calmodulin (SCaM-1) and a calmodulin-like protein (SCaM-4), residues within helix 2 in EF hand I were implicated as being important for activation of the NAD kinase (Lee *et al.*, 1997). In particular, mutations in residues K30E, M36I, and G40D were found to be disruptive, indicating that these positions in CaM are important for maximal activation of NAD kinase (Lee *et al.*, 1997). Similar to our work with CaM^{EKL}, these substitutions showed an additive effect, suggesting that multiple interactions between the enzyme and calmodulin result in activation.

The present study shows that additional residues in the loop/turn region between EF hands I and II adjacent to helix 2 also play a critical role in activation. The substitutions of QNP (residues 41-43) to EKL in CaM^{EKL} are predicted to assume the same backbone structure (Fig.16),

suggesting that the defect is likely not due to a disruption of calmodulin conformation in this region. Since these residues are localized close to the latch domain (Fig. 41), it is possible that they form part of the structure that is required for activation of NAD kinase upon calmodulin binding. Among the residues in the QNP triad, Q41E appears to exert the greatest effect on activity, suggesting that the introduction of a negative charge for the conserved amide at position 41 affects NADK activation. Additionally, the replacement of the conserved, relatively rigid proline-43 residue with leucine, a larger branched hydrophobic residue, also shows a significant decrease in activation. Evidence for the importance of residue 43 in calmodulin function also comes from genetic studies of *Drosophila melanogaster* in which a point mutation of P-43 to L in calmodulin results in enhanced lethality and abnormal behavioral characteristics (Nelson *et al.*, 1997). Since these substitutions do not seem to affect the overall backbone structure of the loop-turn region in Ca^{2+}-CaM (Babu *et al.*, 1988; Chattopadhyaya *et al.*, 1992), the defect is likely related to an inability to assume an activation-competent structure after binding to NAD kinase.

As described in the introduction, the use of mutant calmodulins (e.g. VU-3) that selectively hyperactivate NAD kinase in transgeneic plants has been instructive in the analysis of its function *in vivo* in plant defense responses (Harding et al., 1997; Harding and Roberts, 1998). Based on the current study CaM^{EKL} may be useful as a potential antagonist of NADK for similar *in vivo* studies

Besides the findings with CaM^{EKL}/helix 2 mutants, residues in helix 6 and in the methylation loop may also be involved in enzyme activation. In previous work it was shown that the activation of NAD kinase was drastically reduced by methylation of lysine-115 (Fig. 41) while binding was relatively unaffected (Roberts *et al.*, 1986; Roberts unpublished). However, the present work shows that the substitution of other residues surrounding lysine 115, including the conserved glycine-113, showed no ill effects on NAD kinase activation. The L116T and T117A mutations actually showed a slight increase on NAD kinase activation. Thus, in the methylation loop (residues 112-117), only the modification of lysine-115 appears to inhibit NADK activation.

There are a few features of this particular target-enzyme interaction that are unique. First, trimethylation

of lysine-115 does not influence the activation of other calmodulin-dependent enzymes (Roberts *et al.*, 1984; 1985; 1986b; Putkey *et al.*, 1986). Second, the substitution of lysine-115 with other amino acids has no effect on NAD kinase activation (Roberts *et al.*, 1986; 1990). A substitution of a threonine for lysine-115 was shown to reduce the activation of MLCK (Su *et al.*, 1994). This suggests that position 115 also influences this CaM-dependent enzyme, but in a different manner. Finally, unlike the other substitutions in the latch domain, this post-translational modification is naturally occurring and is regulated *in vivo* (Oh and Roberts, 1990; Oh *et al.*, 1992). Thus, this switch from agonist to partial agonist/antagonist may be a mechanism for selective regulation of NAD kinase.

Although the effect is not as pronounced, CaM^{H6} and CaM^{1214} also showed a lower activation of NAD kinase. Based on site-specific mutations, this defect appears to be the result of substitution of T110 (Fig. 41). This result complements previous work (Su *et al.*, 1994) that showed substitution of position 110 resulted in a reduced activation of MLCK with little effect on binding.

Figures 40 and 41 show a model highlighting the location of residues that have been shown to affect NAD kinase activation but not binding. Based on the proposed collapsed structure of calmodulin with the calmodulin-binding site peptide, it appears as if these residues are present on the surface of the "latch" (helices 2 & 6) as well as on the two symmetrical non EF hand turns adjacent to these helices (Figs. 40 & 41). These residues are proposed to interact with as yet undetermined regions with NAD kinase resulting in activation. As a further note, the peptide shown in Figures 40 and 41 is derived from smooth muscle MLCK. We do not yet have a structure for the NAD kinase peptide nor its structure in complex with calmodulin. Such a structure would enable a clearer picture of these residues in complex with NAD kinase.

Based on this study and previous work, it is clear that the activation of calmodulin-dependent enzymes proceeds by more than a simple one step removal of an "autoinhibitor" from the catalytic cleft of the enzyme (Kemp *et al*, 1996). Additional, undefined interactions are required to achieve activation. The nature of these interactions is vague since the crystal structure of a calmodulin/calmodulin-dependent enzyme activation complex

has yet to be solved. However, support for the proposal that activation involves a change in structure of the complex comes from X-ray and neutron scattering experiments of calmodulin in complex with MLCK with and without substrates (Krueger *et al.*, 1997; 1998).

Scattering data is dependent on the geometric shape of the molecule, and measurements are extremely sensitive to conformational changes (Trewhella 1997). Small-angle scattering is most powerful when used as a complementary tool with other structural techniques such as NMR and X-ray crystallography that provide key structural information. When combined with high-resolution structural data small-angle scattering can be key to understanding biomolecular mechanisms (Trewhella 1997).

Trewhella and colleagues have investigated the interaction of Ca^{2+}-CaM with a catalytic fragment of MLCK (Krueger *et al.*, 1997; 1998). Based on these studies, a model was proposed showing that upon binding substrates (i.e., active conformation of the kinase) the orientation of calmodulin relative to the MLCK changes, lending support to an additional interaction between bound calmodulin and the enzyme in the active state (Krueger *et al.*, 1998). Once inhibition is released by CaM, the kinase can bind and

close about the substrate in order to bring together the chemical constituents required for catalysis. Accompanying closure of the catalytic cleft within the MLCK is a movement of the CaM and MLCK centers-of-mass toward each other. In addition, the orientation of calmodulin relative to MLCK changes so that its N-terminal sequence interacts with the kinase surface (Krueger *et al.*, 1998).

In the current study X-ray scattering experiments have been used to show that in solution the shape and structure of CaM^{EKL} is identical to wild type calmodulin in the absence of peptide. This provides further support that the replacement of QNP (41-43) for EKL (114-116) does not affect the overall structure of calmodulin or the initial binding of calmodulin to target enzymes.

Future work to determine how calmodulin activates NAD kinase should include further analysis of the enzyme, and calmodulins interaction with the enzyme. NAD kinase needs to be cloned, and the CaM-binding site in NAD kinase needs to be identified. In addition, the interaction of calmodulin with this binding site needs to be determined, and compared with other CaM-peptide models. Ultimately, to identify residues important for NAD kinase activation, the structure of NAD kinase in complex with wild type CaM and

with antagonistic CaM (i.e. CaM^{EKL}) needs to be compared. Further study of CaM^{EKL}, and other calmodulins that form non-productive complexes with target enzymes, will hopefully yield insight into the nature of "activation" vs "antagonist" interactions.

LIST OF REFERENCES

LIST OF REFERENCES

Aletta, J., Cimato, T., and Ettinger, M. (1998) *Trends Biochem. Sci.* **23**, 89-91.

Alexander, K.A., Cimler, B.M., Meier, K.E., and Storm, D.R. (1987) *J. Biol. Chem.* **262**, 6108-6113.

Allen , B.G. and Walsh, M.P. (1994) *Trends Biochem. Sci.* **19**, 362-368.

Apel, E.D., Byford, M.F., Au, D., Walsh, K.A., and Storm, D.R. (1990) *Biochemistry* **29**, 2330-2335.

Apel, E.D., and Storm, D.R. (1992) *Perspect. Dev. Neurobiol.* **1**, 3-11.

Aswad, D.W. (1984) *J. Biol. Chem.* **259**, 10714-10721

Aswad, D.H. and Johnson, B. (1987) *Trends Biochem. Sci.* **12**, 155-158.

Babu , Y.S., Sack, J.S., Greenhough, T.J., Bugg, C.E., Means, A.R., and Cook, W.J. (1985) *Nature* **312**, 37-40.

Babu, Y.S., Bugg, C.E., and Cook, W.J. (1988) *J. Mol. Biol.* **204**, 191-204.

Bahler, M., Kroschewski, R., Stoffler, H.E, and Behrmann, T. (1994) *J. Cell Biol.* **126**, 375-389.

Barbato, G., Ikura, M., Kay, L.E., Pastor, R.W., and Bax, A. (1992) *Biochemistry* **31**, 5269-5278.

Baudier, J., Deloume, J.C., Dorsselaer, A.V., Black, D., and Matthes, H.W.D. (1991) *J. Biol. Chem.* **266**, 229-237

Baum, G., Chen Y., Arazi, T., Takatsuji, H., and Fromm, H. (1993) *J. Biol. Chem.* **268**, 19610-19617.

Beavo, J.A. (1995) *Physiological Reviews* **75**, 725-748.

Bennett, M.K. and Kennendy, M.B. (1987) *Proc. Natl. Acad. Sci. USA.* **84**, 1794-1800.

Berridge, M.J. (1993) *Nature* **361**, 315-325.

Blumenthal, D.K., and Stull, J.T. (1982) *Biochemistry* **21**, 2386-2391.

Blumenthal, D.K., Takio, K., Edelman, A.M., Charbonneau, H., Titani, K., Walsh, K.A., and Krebs, E.G. (1985) *Proc Natl Acad Sci USA.* **82**,3187-3191.

Bradford, M.M.(1976) *Anal. Biochem.* **72** 248-254.

Brushia R.J., and Walsh, D.A. (1999) *Front Biosci* **4**, D618-D641.

Carafoli, E. (1987) *Annu. Rev. Biochem.* **56**, 395-433.

Chattopadhyaya, R., Meador, W.E., Means, A.R., and Quiocho, F.A. (1992) *J. Mol. Biol.* **228**, 1177-1192.

Cheney, R.E., and Mooseker, M.S. (1992) *Curr. Opin. Cell Biol.* **4**, 27-35.

Cheung, W.Y. (1970) *Biochem. Biophys. Res. Commun.* **38**, 533-538.

Chin, D. and Means, A.R. (1996) *J. Biol. Chem.* **271**, 30465-30471.

Chin, D., Sloan, D., Quiocho, F.A., and Means, A.R. (1997) *J. Biol. Chem.* **272**, 5510-5513.

Clapham, D.E. and Sneyd, J. (1995) *in Advances in Second Messenger and Phosphoprotein Research* **30**, 1-24.

Clarke, S. (1985) *Ann. Rev. Biochem* **54**, 479-506.

Clarke, S. (1993) *Curr. Opin. Cell Biol.* **5**,977-983.

Cobb, J.A., Han, C.H., Wills, D.M., and Roberts, D.M. (1999) *Biochem. J.* **340**, 417-424.

Cohen, P., and Klee, C.B. (1988) *Molecular Aspects of Cellular Regulation.* Vol **5.**: *Calmodulin* (Cohen, P. & Klee, C.B. eds.) Elsevier, Amsterdam.

Cohen, P. (1988) in *Molecular Aspects of Cellular Regulation.* Vol. 5: *Calmodulin* (Cohen, P. & Klee, C.B. eds.) pp 123-144, Elsevier, Amsterdam.

Cox, J.A. (1988) *Biochem. J.* **249**,621-629.

Crouch, T.H. and Klee, C.B. (1980) *Biochemistry* **19**, 3692-3698.

Dasgupta, M., Honeycutt, T., and Blumenthal, D.K. (1989) *J. Biol. Chem.* **264**, 17156-17163.

da Silva, A.C.R. and Reinach, F.C. (1991) *Trends Biochem. Sci.* **16**, 53-57.

Davis, T.N., Ureda, M.S., Masiarz, F.R. and Thorner, J. (1986) *Cell* **47**, 423-431.

Dupont, G. and Goldbeter, A. (1998) *Bioessays* **8**, 607-610.

Durban, E., Nochumson, S., Kim, S., Paik, W.K., and Chan, S.K. (1978) *J. Biol. Chem.* **253**, 1427-1433.

Elshorst, B., Hennig, M., Forsterling, H., Diener, A., Maurer, M., Schulte, P., Schwalbe, H., Griesinger, C., Krebs, J., Schmid, H., Vorherr, T., and Carafoli, E. (1999) *Biochemistry* **38**, 12320-12332.

Enslen, H., Sun, P., Bricky, D., Soderling, S.H., Klamo, E., and Soderling, T.R. (1994) *J. Biol. Chem.* **269**, 15520-15527.

Enenas, J., Forsen, S., Malmendal, A., and Akke, M. (1999) *J. Mol. Biol.* **289**, 603-617.

Finn, B.E., Evenas, J., Drakenberg, T., Waltho, J.P., Thulin, E., and Forsen, S. (1995) *Nature Struct. Biol.* **2**, 777-783.

Friedberg, F. (1990) *Protein Seq. Data Anal.* **3**, 335-337.

Fukami, Y., Nakamura, A., and Takeharu, K (1986) *Proc. Natl. Acad. Sci USA* **83**, 4190-4193.

Gagon, C., Kelly, S., Manganiello, V., Vaughan, M., Odya, C., Strittmatter, W., Hoffman, A., and Hirata, F. (1981) *Nature* **291**, 515-517.

Gallagher, P.J., Herring, B.P., and Stull, J.T. (1997) *J Muscle Res Cell Motil.* **18**,1-16.

Gange, S.M., Tsuda, S., Li, M., Smillie, L.B., and Sykes, B.D. (1995) *Nature Struct. Biol.* **2**, 784-788.

George, S.E., VanBerkum, M., Ono, T., Cook, R., Hanley, R., Putkey, J., and Means, A.R. (1990) *J. Biol. Chem.* **265**, 9228-9235.

George, S.E., Su, Z., Fan, D., and Means, A.R. (1993) *J. Biol. Chem.* **268**, 25213-25220.

Gopalakrishna, R. and Anderson, W.B. (1982) *Biochem. Biophys. Res. Commun.* **104**, 830-836.

Gregori, L., Marriot, D., West, C.M., and Chau, V. (1985) *J. Biol. Chem.* **260**, 5232-5235.

Gregori, L., Marriot, D., Putkey, J.A., Means, A.R. and Chau, V. (1987) *J. Biol. Chem.* **262**, 2562-2567.

Grover, A.K., and Khan, I. (1992) *Cell Calcium* **13**, 9-17.

Grynkiewicz, G., Poenie, M., and Tsien, R.Y. (1985) *J. Biol. Chem.* **260**, 3440-3450.

Guerini, D., Krebs, J., and Carafoli, E. (1984) *J. Biol. Chem.* **259**, 15172-15177.

Han, C.H., Richardson, J., Oh, S.H., and Roberts, D.M. (1993) *Biochemistry* **32**, 13974-13980.

Han, C.H and Roberts, D.M. (1997) *Eur. J.Biochem.* **244**, 904-912.

Harding, S., Oh, S.H., and Roberts, D.M. (1997) *EMBO J.* **16**, 1137-1144.

Harding, S.A. and Roberts, D.M. (1998) *Planta* **206**, 253-258.

Heidorn, D.B. and Trewhella, J. (1988) *Biochemistry* **27**, 909-915.

Hergenhahn, H.G., Kegel, G., and Sedlmeier, D. (1984) *Biochim. Biophys. Acta.* **787**, 196-203.

Higuchi, S., Tamura, J., Giri, P.R., Polli, J.W. and Kincaid, R.L. (1991) *J. Biol. Chem* **266**, 18104-18112.

Houdusse, A., and Cohen, C. (1995) *Proc. Natl. Acad. Sci. USA* **92**, 10644-10647.

Ikura, M., Spera, S., Barbato, G., Kay, L.E., Krinks, M., and Bax, A. (1991) *Biochemistry* **30**, 9216-9228.

Ikura, M., Clore, G.M., Gronenborn, A., Zhu, G., Klee, C., and Bax, A. (1992) *Science* **256**, 632-638.

Ikura, M. (1996) *Trends Biochem. Sci.* **21**, 14-17.

Jackson, R.L., Dedman, J.R., Schreiber, W.E., Bhatnagar, P.K., Knapp, R.D., and Means, A.R. (1977) *Biochem Biophys Res Commun* **77**, 723-729.

Jones, D.A., Glod, J., Wilson-Shaw, D., Hahn, W.E. and Sikela, J.M. (1991) *FEBS Lett.* **289**, 105-109.

Jurado, L.A., Chockalingam, P.S., and Jarrett, H.W. (1999) *Physiol. Rev.* **79**, 661-682.

Kagan, R. and Clarke, S. (1994) *Arch. Biochem. Biophy.* **310**, 417-427.

Kakiuchi,S., and R. Yamazaki. (1970) *Biochem. Biophys. Res. Commun.* **41**, 1104-1110.

Kataoka, M., Head, J.F., Vorherr, T., Krebs, J. and Carafoli, E. (1991) *Biochemistry.* **30**, 6247-6251.

Kawasaki, H., Nakayama, S., and Kretsinger, R. (1998) *Biometals* **11**, 277-295.

Kemp, B.E., and Stull, J.T. (1990) in *Peptides and Protein Phosphorylation*. Kemp, B.E. ed. CRC Press, Boca Raton, pp. 115-133.

Kemp, B.E., and Pearson, R.B. (1991) *Biochim. Biophys. Acta* **1094**, 67-76.

Kemp, B.E., Barden, J.A., Kobe, B., House, C., and Parker, M.W. (1996) *Adv. Pharmacol.* **36**, 221-249.

Kilhoffer, M.C., Cemaille, J.G., and Gerard, D. (1981) *Biochemistry* **20**, 4407-4414.

Kleene, S.J., Toews, M.L., and Adler, J.(1997) *J.Biol.Chem.* **252**, 3214-3218.

Klee , C.B. and Vanaman, T.C. (1982) *Adv. Protein Chem.* **35**, 213-321.

Klee, C.B. (1988) in *Molecular Aspects of Cellular Regulation*. Vol. 5: *Calmodulin* (Cohen, P. & Klee, C.B. eds.) pp. 35-53, Elsevier, Amsterdam.

Klee, C.B., Ren, H., and Wang, X. (1998) *J. Biol. Chem.* **273**,13367-13370.

Klein, R.R. and Houtz, R.L. (1995) *Plant Mol. Biol.* **27**, 249-261.

Kobe, B., Heierhorst, J., and Kemp, B.E. (1997) *Adv. Second Messenger Phosphoprotein Res.* **31**, 29-40.

Kretsinger, R.H. and Nockolds, C.E. (1973) *J. Biol. Chem.* **248**, 3313-3326.

Kretsinger, R.H. (1977) *Calcium-Binding Proteins and Calcium Function*. 63.

Kretsinger, R.H. (1980) *Crit. Rev. Biochem.* **8**, 119-174.

Kretsinger, R.H., Rudnick, S.E. and Weismann, L.J. (1986) *J. Inorg. Biochem.* **28**, 289-302.

Krueger, J.K., Olah, G.A., Rokop, S.E., Zhi, G., Stull, J.T., and Trewhella, J.(1997)*Biochemistry* **36**, 6017-6023.

Krueger, J.K., Zhi, G., Stull, J.T., and Trewhella, J.(1998)*Biochemistry* **37**, 13997-14004.

Kuboniwa, H., Tjandra, N., Grzesiek, S., Ren, H., Klee, C.B., and Bax, A. (1995) *Nat. Struct. Biol.* **2**, 768-776.

Laemmli, U.K. (1970) *Nature* **227**, 680-685.

LaBadie, J.H., Dunn, W.A., and Aronson, N.N.(1976). *Biochem. J.* **160**, 85-95.

Lee, S.H., Seo, H.Y., Kim, J.C., Heo, W.D., Chung, W.S., Lee, K.J., Kim, M.C., Cheong, Y.H., Choi, J.Y., Lim, C.O., and Cho, M.J. (1997) *J. Biol. Chem.* **272**, 9252-9259.

Linse, S., Helmerson, A., and Forsen, S. (1991) *J. Biol. Chem.* **266**, 8050-8054.

Linse, S., Brodin, P., Drakenberg, T., Thulin, E., and Sellers, P. (1987) *Biochemistry* **26**, 6723-6735.

Lukas, T.J., Burgess, W.H., Prendergrast, F.G., Lau, W., and Watterson, D.M. (1986) *Biochemistry* **25**, 1458-1464.

Lukas, T.J., Craig, T.A., Roberts, D.M., Watterson, D.M., Haiech, J., and Prendergast. F.G. (1987) *Health and Disease* (Carafoli, E., Imesin, G., Means, A.R., Norman, A.W., Siegel, F.L., Suttie, J.W., & Vanaman, T.C., eds.) 533-543, Academic Press.

Lukas, T.J., Friedman, M.W., Kung, C., and Watterson, D.M. (1989) *Proc. Natl. Acad. Sci. USA* **86**, 7331-7335.

Malmendal, A., Evenas, J., Forsen, S., and Akke, M. (1999) *J. Mol. Biol.* **293**, 883-899.

Marshak, D.R., Clarke, M., Roberts, D.M., and Watterson, D.M. (1984) *Biochemistry*. **23**, 2891-2899.

Martin, S.R. and Bayley, P.M. (1986) *Biochem. J.* **238**, 485-490.

Martin, S.R., Linse, J.J., Bailey, P.M. and Forsen, S. (1986) *Eur. J. Biochem.* **161**, 595-601.

Masters, B.S., McMillan, K., Sheta, E.A., Nishmura, J.S., Roman, L.J., and Martasek, P. (1996) *FASEB J.* **10**, 522-528.

Meador, W., Means, A.R., and Quiocho, F.A. (1992) *Science* **257**, 1251-1255.

Meador, W., Means, A.R., and Quiocho, F.A. (1993) *Science* **263**, 1718-1721.

Means, A.R., Tash, J.S., and Chafouleas, J.G. (1982) *Physiol. Rev.* **62**, 1-39.

Minowa, O. and Yagi, K. (1984) *J. Biochem.* **96**, 1175-1182.

Moews, P.C., and Kretsinger, R.H. (1975) *J. Mol. Biol.* **91**, 201-207.

Molla, A., Kilhoffer, M.C., Ferraz, C., Audemard, E., Walsh, M.P., and Demaille, J.G. (1981) *J. Biol. Chem.* **256**, 15-18.

Moncrief, N.D., Kretsinger, R.H., and Goodman, M. (1990) *J. Mol. Evol.* **30**, 522-562.

Montell, C. and Rubin, G.M. (1988) *Cell* **52**, 757-772.

Morino, H., Kawamoto, T., Miyake, M., and Kakimoto, Y. (1987) *J. Neurochem.* **48**, 1201-1208.

Morishima, I. and Bodnaryk, R.P. (1985) *Comp. Biochem. Physiol.* **80B**, 419-423.

Murtaugh, T.J., Wright, L.S., and Siegel, F.L.(1986) *J. Neurochem* **47**, 164-172.

Nairn, A.C. and Greengard, P. (1987) *J. Biol Chem.* **262**, 7273-7281.

Nairn, A.C., Hemmings, H.C. Jr., and Greengard, P. (1985) *Annu. Rev. Biochem.* **54**, 931-976.

Najbauer, J. and Aswad, D. (1990) *J. Biol. Chem* **265**, 12717-12721.

Najbauer, J., Johnson, B.A., Young, A.L. and Aswad, D. (1993) *J. Biol. Chem* **268**, 10501-10509.

Najbauer, J., Orpiszewski, J., and Aswad, D. (1996) *Biochemistry* **35**, 5183-5190.

Nakayama, S. and Kretsinger, R.H. (1994) *Annu. Rev. Biophys. Biomol. Struct.* **23**, 473-507.

Nelson, H.B., Heiman, R.G., Bolduc, C., Kovalick, G.E., Whitley, P., Stern, M., and Beckingham, K. (1997) *Genetics* **147**, 1783-1798.

Newton, D.L., Burke, T.R. Jr, Rice, K.C., and Klee, C.B. (1983) *Biochemistry* **22**, 5472-5476.

Niewmierzycka, A. and Clarke, S. (1999) *J. Biol. Chem.* **274**, 814-824.

Ogawa, H. and Fujioka, M.(1982) *J. Biol. Chem.* **257**, 3447-3452.

Oh, S.H., and Roberts, D.M. (1990) *Plant Physiol.* **93**, 880-887.

Oh, S.H., Steiner, H.Y., Dougall, D.K., and Roberts, D.M. (1992) *Arch. Biochem. Biophys.* **297**, 28-34.

Oh, S.H. (1992) Ph.D. Dissertation, The University of Tennessee, Knoxville.

Olah, G. and Trewhella, J. (1994) *Biochemistry* **33**, 12800-12806.

Osawa, M., Swindells, M., Tanikawa, J., Kurihara, H., Orita, M., Shibanuma, T., Furuya, T., and Ikura, M. (1998) *J. Mol. Biol.* **276**, 165-176.

Osawa, M., Tokumitsu, H., Swindells, M., Kurihara, H., Orita, M., Shibanuma, T., Furuya, T., and Ikura, M. (1999) *Nat. Struct. Biol.* **6**, 819-824.

Paik, W.K., and Kim, S. (1970) *J. Biol. Chem.* **245**, 6010-6015.

Paik, W.K., and Kim, S. (1980) *Protein Methylation*, John Wiley and Sons, New York Press.

Paik, W.K., and Kim, S. (1985) *In The Enzymology of Posttranslational Modification of Proteins*. **2**, 187-228. Academic Press, London.

Paik, W.K., and Kim, S. (1990) *Protein Methylation*, CRC Press, Boca Raton, Florida.

Park, K.S., Frost, B., Tuck, M., Ho, L., Kim, S., and Paik, W.K. (1987) *J. Biol. Chem* **262**, 702-708

Patel, S., Morris, S.A., Adkins, C.E., O'Beirne, G., and Taylor, C.W. (1997) *Proc. Natl. Acad. Sci.* USA **94**, 11627-11632.

Pattanayek, R., Newcomer, M.E., and Wagner, C. (1998) *Protein Sci.* **7**, 1326-1331.

Pech, L.L., and Nelson, D.L. (1994) *Biochim. Biophys. Acta* **1199**, 183-194.

Persechini, A., and Kretsinger, R.H. (1988) *J. Biol Chem.* **263**, 12175-12178.

[a]Persechini, A., Stemmer, P., and Ohashi, I. (1996) *J. Biol Chem.* **271**, 32217-32225.

[b]Persechini, A., Gansz, K.J., and Paresi, R.J. (1996) *Biochemistry* **35**, 224-228.

Picciotto, M.R., Czernik, A.J., and Nairn, A.C. (1993) *J. Biol. Chem.* **268**, 26512-26521.

Putkey, J.A., Draetta, G.F., Slaughter, G.R., Klee, C.B., Cohen, P., Stull, J.L., and Means, A.R. (1986) *J. Biol. Chem.* **261**, 9896-9903.

Ramachandran, G.N. and Sasisekharan, V. (1968) *Adv. Protein Chem.* **23**, 283-437.

Riechers, D.E. and Timko, M.P. (1999) *Plant Mol Biol.* **41**, 387-401.

Roads, A.R., and Friedberg, F. (1997) *FASEB J.* **11**, 331-340.

Roberts, D.M., Burgess, W.H., and Watterson, D.M. (1984) *Plant Physiol.* **75**, 796-798.

Roberts, D.M., Crea, R., Malecha, M., Alvarado-Urbina, G., Chiarello, R.H., and Watterson, D.M. (1985) *Biochemistry* **24**, 5090-5098.

[a]Roberts , D.M., Lukas,T.J., and Watterson, D.M. (1986) *Crit. Rev. Plant Sci.* **4**, 311-339.

[b]Roberts, D.M., Rowe, P.M. Siegel, F.L., Lukas, T.J., and Watterson, D.M. (1986) *J. Biol. Chem.* **261**, 1491-1494.

Roberts, D.M., Zimmer, W.E., and Watterson, D.M. (1987) *Methods Enzymol.* **139**, 290-303.

Roberts, D.M., Besl, L., Oh, S.H., Masterson, R.V., Schell, J., and Stacey, G. (1992) *Proc. Natl. Acad. Sci. USA.* **89**, 8394-8398.

Roberts, D.M., and Harmon, A.C. (1992) *Annu. Rev. Plant Physiol. Mol. Biol.* **43**, 375-414.

Rowe, P.M., Murtaugh, T.J., Bazari, W.L., Clarke, M., and Siegel, F.L. (1983) *Anal. Biochem.* **133**,394-400.

Rowe, P.M., Wright, L.S., and Siegel, F.L. (1986) *J. Biol Chem.* **261**, 7060-7069.

Sambrook, J., Fritsch, E.F., and Maniatis, T. (1989) *Molecular Cloning: A laboratory Manual*, Cold Spring Harbor Laboratory, Cold Spring Harbor, N.Y.

Selhub, J. (1999) *Annu Rev Nutr.* **19**, 217-246.

Schaefer, W.H., Lukas, T.J., Blair, I.A., Schultz, J.E., and Watterson, D.M. (1987) *J Biol Chem.* **262**, 1025-1029.

Schleicher, M., Lukas, T.J., and Watterson, D.M. (1984) *Arch. Biochem. Biophys.* **229**, 33-42.

Sharma, R.K., Wang, T.H., Wirch, E., and Wang, J.H. (1981) *J. Biol. Chem.* **255**, 5916-5923.

Shattuck, R.L., and Storm, D.R. (1988) in *Molecular Aspects of Cellular Regulation*. Vol. 5: *Calmodulin* (Cohen , P. & Klee, C.B. eds.) pp. 249-264, Elsevier, Amsterdam.

Shou, C., Farnsworth, C.L., Neel, B.G. and Feig, L.A. (1992) *Nature* **358**, 351-354.

Siegel, F.L., Vincent, P.L., Neal, T.L., Wright, L.S., Heth, A.A., and Rowe, P.M. (1990) in *Protein Methylation* (Paik, W.K., and Kim, S., Eds.) pp. 33-58, CRC Press, Boca Raton, Florida.

Sitaramayya, A., Wright, L.S., and Siegel, F.L.(1980) *J. Biol. Chem* **255**, 8894-8900.

Skeleton, N.J.(1994) *Nat. Struct. Biol.* **1**, 239-245.

Smith, P.K., Krohn, R.I., Hermanson, G.T., Mallia, A.K., Gartner, F.H., Provenzano, M.D., Fujimoto, E.K., Goeke, N.M., Olson, B.J., and Klenk, D.C. (1985) *Anal Biochem* **150**, 76-85.

Soderling,T.R. (1990) *J. Biol. Chem.* **265**, 1823-1826.

Soderling,T.R. (1999) *Trends Biochem. Sci.* **24**, 232-236.

Springer, M., Goy, M., and Adler, J.(1979) *Nature* **280**, 279-284.

Strynadka, N.C., and James, M.N.G. (1989) *Annu. Rev. Biochem.* **58**, 951-998.

Stull, J.T., Kamm K.E., Krueger J.K., Lin, P., Luby-Phelps, K., and Zhi, G. (1997) *Adv Second Messenger Phosphoprotein Res.* **31**, 141-150.

Su, Z., Fan, D., and George, S. (1994) *J. Biol. Chem.* **269**, 16761-16765.

Su, Z., Blazing, M., Fan, D., and George, S. (1995) *J. Biol. Chem.* **270**, 29117-29122.

Takeda, T., and Yamamoto, M. (1987) *Proc. Natl. Acad. Sci. USA.* **84**, 3580-3584.

Takeda, T., Imai, Y., and Yamamoto, M. (1989) *Proc. Natl. Acad. Sci. USA.* **86**, 9737-9741.

Tanaka, T., Ames, JB, Harvey T.S., Stryer, L., and Ikura, M. (1995) *Nature* **376**,444-447

Tanokura, M. and Yamada, K. (1983) *J. Biochem.* **94**, 607-609.

Tanokura, M. and Yamada, K. (1984) *J. Biochem.* **95**, 634-649.

Tesmer, J.J. and Sprang, S.R. (1998) *Curr. Opin. Struct. Biol.* **6**, 713-719.

Toda, H., Yazawa, M., and Yagi, K. (1992) *Eur. J. Biochem.* **205**, 653-660.

Tokumitsu, H., Enslen, H., and Soderling, T.R. (1995) *J. Biol. Chem.* **270**, 19320-19324.

Trewhella, J., Blumenthal, D.K., Rokop, S.E., and Seeger, P.A. (1990) *Biochemistry* **29**, 9316-9321.

Trewhella, J. (1994) in Structural Biology: The State of the Art (Sarma, R.H., and Sarma, M.H., eds.) Adenine Press, Guilderland, N.Y.

Urbauer, J.L., Short, J.H., Dow, L.K., and Wand, A.J. (1995) *Biochemistry* **34**,8099-8109.

Van Der Werf, P., and Koshland, D.E., Jr. (1977). *J. Biol. Chem.* **252**, 2793-2795.

VanBerkum, M., and Means, A. (1991) *J. Biol. Chem.* **266**, 21488-21495.

Van Hooff, C.O.M., De Graan, P.N.E., Oestreicher, A.B., and W.H. Gispen. (1988) *J. Neurosci.* **8**,1789-1795.

Watterson, D.M., Sharief, F., and Vanaman, T.C. (1980) *J. Biol. Chem.* **255**, 962-975.

Woodring P.J. and Garrison, J.C. (1997) *J. Biol. Chem.* **272**, 30447-30454.

Wylie, D.C. and Vanaman, T.C.(1988) in *Molecular Aspects of Cellular Regulation*. Vol. 5: *Calmodulin* (Cohen , P. & Klee, C.B. eds.) pp 1-15, Elsevier, Amsterdam.

Wright, L.S., Bertice, P.J., and Siegel, F.L. (1996) *J. Biol. Chem.* **271**, 12737-12743.

Yang, H., Reedy, M.M., Burke, C.L., and Strasburg, G.M. *Biochemistry* **33**, 518-525, 1994.

Yazawa, M., Ikura, M., Hikichi, K., Ying, L., and Yagi, K. (1987) *J. Biol. Chem.* **262**, 10951-10954.

Ying, Z., Janney, N., and Houtz, R.L. (1996) *Plant Mol. Biol.* **32**, 663-671.

Ying, Z., Mulligan, R.M., Janney, N., and Houtz, R.L. (1999) *J Biol Chem* **274**, 36750-36756.

Zhang, M., Huque, E., and Vogel, H.J. (1994) *J. Biol. Chem.* **269**, 5099-5105.

Zhang, M., Tanaka, T. and Ikura, M. (1995) *Nat. Struct. Biol.* **2**, 758-767.

Zhang, M. and Yuan, T. (1998) *Biochem. Cell. Biol.* **76**, 313-323.

Ziegenhagen, R., Goldberg, M., Rakutt, W.D., and Jennissen, H.P. (1990) *FEBS Lett.* **271**, 71-75.

VITA

Jennifer Ann Cobb was born on March 31, 1970 in Carbondale, Illinois. She moved to Huntsville, Alabama in 1984 and graduated from Huntsville High School in 1988. She attended the University of Utah and received a Bachelors of Science degree in 1992, with a major in psychology. After graduating she worked for a consulting firm in Washington D.C. before returning for graduate studies in 1995. In August 1995 she entered the graduate program in Biochemistry at the University of Tennessee. She joined the laboratory of Dr. Daniel M. Roberts and received the Ph.D. degree in Biochemistry and Cellular and Molecular Biology in 2000.